INITIATION AND TERMINATION OF A HYBRID ATRP SYSTEM

INITIATION AND TERMINATION OF A HYBRID ATOM TRANSFER RADICAL POLYMERIZATION SYSTEM

By

MARK J. MACHADO, B.Eng

A Thesis

Submitted to the School of Graduate Studies

in the Partial Fulfilment of the Requirements

for the Degree

Master of Applied Science

McMaster University

MASTER OF APPLIED SCIENCE (2008) McMaster University

(Chemical Engineering) Hamilton, Ontario

TITLE: Initiation and Termination of a Hybrid Atom Transfer Radical Polymerization System

AUTHOR: Mark J. Machado (McMaster University)

SUPERVISORS: Dr. Shiping Zhu & Dr. Santiago Faucher

NUMBER OF PAGES: xiii, 102

ABSTRACT

Atom transfer radical polymerization (ATRP) is a controlled/living polymerization process used to synthesize polymers with controlled molecular weight and narrow polymer distributions. Control of these key parameters allows for the fabrication of well-defined macromolecular structures, a necessary tool for the synthesis of advanced materials. Since its discovery in 1995, ATRP has received considerable interest and widespread adoption from the academic community. Unfortunately, it faces several complex challenges which have hindered its full scale commercialization, mainly its high catalyst loadings to obtain fast reaction kinetics.

One of the premises of this research project was to augment the slow reaction rates of ATRP while using extremely low catalyst concentrations. A hybrid ATRP system was employed which encompassed the fast reaction kinetics associated with conventional free radical processes, with the attractive control features of ATRP. When high free radical initiator concentrations in the range of 0.1 M to 0.2 M were used in concert with ATRP, fast reaction rates were realized, while maintaining a polymerization with living characteristics. Conversions of 81% (0.117M) and 91% (0.234M) were achieved within 2 hours as compared to typical ATRPs where achieving such conversions would take up to 24 hours.

For those same free radical initiator loadings (0.117M and 0.234M) the reaction demonstrated living characteristics with molecular weight growing in a linear fashion with respect to increasing monomer conversion. Despite the high free radical initiator concentration, the polymer distribution remained relatively narrow, not exceeding a

polydispersity of 1.30. Chain extension experiments from a synthesized macroinitiator were successful which demonstrated the living characteristics of the hybrid ATRP process.

The aforementioned polymerizations were conducted with various copper concentrations. Catalyst concentrations as low as 16 ppm (0.234mM) were found to be effective, i.e. one catalyst mediated the growth of over 100 polymer chains, and thus saving post polymerization purification. Moreover, the expensive ligand cost could be cut dramatically through a nearly 100 time reduction in the ligand concentration for these polymerizations.

A hybrid ATRP system was used as a unique method to determine termination rate coefficients of MMA at 70°C as a function of both conversion and chain length. A three dimensional composite map was developed to elucidate the coupling effects of both conversion and chain length on the termination rate coefficient over a total range of data which can be used for modelling systems of this nature.

ACKNOWLEDGEMENTS

Firstly I would like to express my deepest gratitude to Professor Shiping Zhu for his unrelenting support, guidance, patience and insight. The enthusiasm and dedication he shows on a daily basis to his students is truly remarkable. It was a true pleasure to work under his supervision.

To my co-supervisor Dr. Santiago Faucher, I thank you so much for taking me under your wing and teaching me how to fly. The confidence you showed in me, allowed me to reach my potential.

To all my group members during my tenure here, namely Dr. Santiago Faucher, Dr.Wei Feng, Dr. Hualong Pan, Ping Liu, Rachel Gong, Jerry Chen, Shane Gao, Mary Jin, Sara Alibeik, Helen Gu, Mohammad Haj Abed, Jason Doggart and Thomas Kowpak. As well as my close friends, in particular Kyla Sask, I thank you for your assistance and support.

I am also thankful to Rahul Gandhi for his help with all my Matlab questions.

I would also like to express my sincere gratitude to the faculty, office and technical staff from Department of Chemical Engineering. In particular, I would like to thank Paul Gatt, Doug Keller, Justyna Derkach, Lynn Falkiner, Kathy Goodram, Andrea Vickers, James Lei, Dr.Kostanski and Dr. Sheardown,

I am grateful for the financial support provided by the Department of Chemical Engineering and from the Ontario Graduate Scholarship (OGS).

Finally I am most grateful to my parents for instilling me with such a strong sense of work ethic, and dedication. I am forever thankful for your endless love, support and encouragement you have showed me throughout my life.

TABLE OF CONTENTS

Abstract iii

Acknowledgements v

List of Figures x

List of Schemes xii

List of Tables xiii

Chapter 1 Introduction

1.1 Polymers 1

1.2 Conventional Free Radical Polymerization 2

1.2.1 Diffusion Controlled Termination 3

1.2.1.1 Conversion-Dependent Termination 5

1.2.1.2 Chain-Length-Dependent Termination 5

1.2.2 Determination of the Termination Rate Coefficient k_t 7

1.3 Controlled/Living Polymerization 11

1.3.1 Living Ionic Polymerization 11

1.3.2 Controlled/Living Radical Polymerization 12

1.3.2.1 Nitroxide Mediated Polymerization(NMP) 15

1.3.2.2 Reversible Addition Fragmentation Chain Transfer (RAFT) 18

1.3.2.3 Atom transfer radical polymerization (ATRP) 21

1.3.2.3.1 Reverse Atom Transfer Radical Polymerization (RATRP) 24

1.3.2.3.2 Simultaneous Reverse and Normal Initiation (SR&NI) 27

1.3.2.3.3 Initiators for Continuous Activator Regeneration (ICAR) ATRP 28

1.3.2.3.4 Activator Generated Electron Transfer (AGET) ATRP 29
1.3.2.3.5 Activator Regenerated Electron Transfer (ARGET) ATRP 30

1.4 Comparison of NMP, ATRP, and RAFT 31

1.5. Challenges of ATRP 34

1.6 Objective and Outline of This Thesis 38

Chapter 2 Experimental Materials and Methodology 40

2.1 Materials 40

2.2 Experimental Procedures 41

2.2.1 Polymerization Procedures 41

2.2.1.1 Synthesis of Poly (methyl methacrylate) Macroinitiator 42

2.2.1.2 PMMA Chain Extension 42

2.2.2 Characterization 43

2.3 Procedure for k_t Determination 43

2.3.1 Estimate k_t from NMR Measurements 43

2.4 Rate Enhanced ATRP in the Presence of High Free Radical Initiator Experiments 45

2.4.1 Analysis of Living Regions under GPC Curves 45

2.5 Modelling ATRP Process with a Second Radical Source 47

2.5.1 Mass Balance Equations 47

2.5.2 Method of Moments 48

2.5.3 Matlab Program: ATRP with a Second Radical Source 50

Chapter 3 Results and Discussion 51

3.1. Enhancing reaction kinetics in ATRP at low catalyst concentrations 51

3.1.1. Simulated Experimental Results for a Rate Enhanced ATRP at Low Catalyst Concentrations 52

3.1.2 Experimental Reaction Kinetics 58

3.1.3 Experimental Molecular Weight Results 60

3.1.4 Analysis of GPC Curves 62

3.1.5 Chain Extension from PMMA Macroinitiator 70

3.1.6 Effect of Catalyst Concentration 74

3.2 Determination of k_t via NMR Technique 78

Chapter 4 Conclusions and Recommendations 87

4.1 Conclusions 87

4.2 Recommendations and Future Work 88

Appendix A Matlab Program: Analysis of GPC Curves 90

Appendix B Matlab Program: ATRP with a 2nd Radical Source 92

References 94

LIST OF FIGURES

Chapter 1

Figure 1.1: Relative monomer concentrations as a function of time for a single pulse. 9

Figure 1.2: Examples of the macromolecular structures and architectures that can be produced by controlled/living polymerization 14

Figure 1.3: General structures of RAFT Agents 19

Chapter 2

Figure 2.1: Chemical structures of the reagents and solvent used in the experiments 40

Figure 2.2: Gel Permeation Chromatography (GPC) Plot 46

Chapter 3

Figure 3.1: Simulated Monomer Conversion vs. Time and First Order Rate Plot for the ATRP of MMA with Varying Free Radical Initiator Concentrations 53

Figure 3.2: Simulated Number Average Molecular Weight and PDI vs. Conversion at various Free Radical Initiator 55

Figure 3.3: Simulated Monomer Conversion vs. Time and First Order Rate Plot for the ATRP of MMA with Varying Catalyst Concentrations 56

Figure 3.4: Simulated Number Average Molecular Weight and PDI vs. Conversion at various Catalyst Concentrations 57

Figure 3.5: Monomer conversion vs. time and first order rate plot for the ATRP of MMA with varying free radical initiator concentrations 60

Figure 3.6. PMMA Molecular weight and polydispersity as a function of conversion for varying free radical initiator concentrations 62

Figure 3.7. Gel Permeation Chromatography (GPC) Plot at 45% monomer conversion 64

Figure 3.8. Gel Permeation Chromatography (GPC) Plot at 76% monomer Conversion 65

Figure 3.9: Gel Permeation Chromatography (GPC) Plot at 21% monomer Conversion 66

Figure 3.10: Gel Permeation Chromatography (GPC) Plot at 92% monomer Conversion 67

Figure 3.11: Percentage of living region as function of monomer conversion for the ATRP of MMA with varying free radical initiator concentrations 68

Figure 3.12: Kinetic Chain Length and Conversion vs. Time: ATRP of MMA 70

Figure 3.13: Gel Permeation Chromatography (GPC) data showing the molecular weight evolution from the PMMA chain extension 71

Figure 3.14. Gel Permeation Chromatography (GPC) Plot at 41 % monomer Conversion 72

Figure 3.15 Gel Permeation Chromatography (GPC) Plot at 63% monomer Conversion 73

Figure 3.16: Image of post polymerization PMMA samples at different catalyst concentrations 76

Figure 3.17: Conversion vs. Time plot for the ATRP of MMA in the presence of free radical initiator 79

Figure 3.18: Theoretical Degree of Polymerization vs. Conversion plot for the ATRP of MMA in the presence of free radical initiator 80

Figure 3.19: Log k_t vs. log chain length plot for the ATRP of MMA in the presence of free radical initiator 82

Figure 3.20: Log k_t vs. log chain length plot for the ATRP of MMA in the presence of free radical initiator with raw experimental data 83

Figure 3.21: Log k_t vs. Conversion plot for the ATRP of MMA in the presence of free radical initiator with raw experimental data 84

Figure 3.22. Three-dimensional plot of the termination rate coefficients for MMA at 70°C 85

LIST OF SCHEMES

Chapter 1

Scheme 1.1: Elementary Reactions for Free Radical Polymerization 2

Scheme 1.2: Schematic demonstrating the molecular process involved in bimolecular termination 4

Scheme 1.3: Reversible activation/deactivation in CLRP 13

Scheme 1.4: Unimolecular initiation process for a nitroxide mediated polymerization 16

Scheme 1.5: Bimolecular initiation process for NMP 16

Scheme 1.6: Schematic of the RAFT Mechanism 20

Scheme 1.7: Schematic of the ATRP Mechanism 22

Scheme 1.8: Schematic of the Reverse ATRP mechanism 25

Scheme 1.9: Illustration Depicting the Formation of Block Copolymers 27

Scheme 1.10: Schematic of the Simultaneous reverse and normal initiation (SR&NI) Mechanism 28

Scheme 1.11: Schematic of the ICAR ATRP Mechanism 29

Scheme 1.12: Illustration Depicting the Formation of pure block copolymers 30

Scheme 1.13: Schematic of the ARGET ATRP Mechanism 31

LIST OF TABLES

Chapter 1

Table 1.1a: List of the ATRPs of MMA at Various Catalyst Concentrations 36

Table 1.1b: List of the ATRPs of MMA at Various Catalyst Concentrations 37

Chapter 3

Table 3.1: Parameters and Initial Conditions for the ATRP of MMA in Solution 52

Table 3.2: Effect of increased initiator concentration on ATRP with a 2^{nd} Radical Source 59

Table 3.3: Effect of Metal Salt Concentration on an ATRP with a 2^{nd} Radical Source 75

CHAPTER 1

INTRODUCTION

1.1. Polymers

Polymers have become an increasingly significant sector in the world economy. In 2004, the U.S. alone produced nearly 39 x 10^6 metric tons of plastic, 4 x10^6 metric tons of synthetic fibers and 5 x 10^6 metric tons of paints and coatings.[1] Of these materials produced, nearly half are estimated to be synthesized via a free radical polymerization route.[2] Free radical chemistry is responsible for the production of a vast array of polymeric materials, including, low density polyethylene (LDPE) at high pressures. The production of poly (vinyl chloride) (PVC) in particular contribute to nearly 20% of the total plastic production figure above.[1] Moreover, products derived from styrenic, acrylic, and fluro based polymers were also great in demand, which is no surprise since these materials are used in many applications ranging from adhesives and coatings to paper making and packaging. However, the major drawback of free radical polymerization is its inability to control significant reaction variables that are necessary to prepare well-defined macromolecular structures with controlled molecular weight and polydispersity. Living radical polymerization techniques such as atom transfer radical polymerization (ATRP) have been developed to fill this void and hold great industrially potential.

1.2. Conventional Free Radical Polymerization

For the past fifty years, conventional free radical polymerization (FRP) has been the most commonly used method for the synthesis of commercially available polymers. Its commercial success can be largely attributed to its versatility to a wide range of monomers, polymerization processes, and reaction conditions, as well as its tolerance to impurities. Radical polymerizations can be described by a set of elementary reactions as shown in Scheme 1.1. The three primary reactions in free radical polymerization are initiation, propagation and termination.

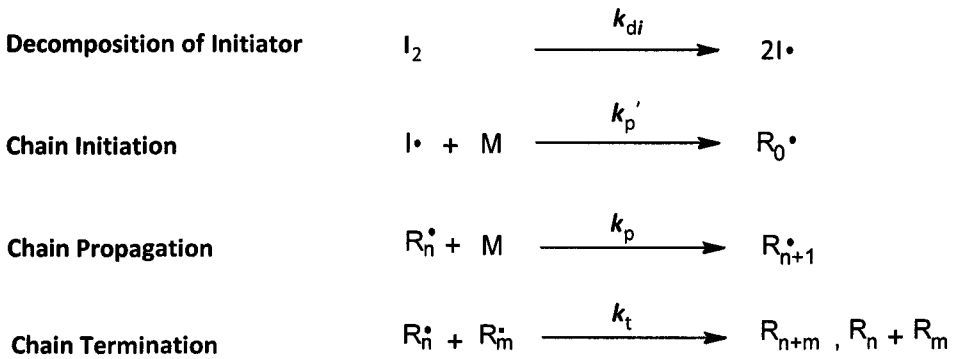

Scheme 1.1: Reaction scheme for free radical polymerization

The initiator (I_2) typically undergoes thermal or photochemical decomposition reaction to form primary radicals ($I\cdot$). The primary radicals that leave the solvent cage unreacted and go on to begin the polymerization can be quantified by the initiator efficiency, denoted f, which ranges from 0 to 1. A value of $f=1$ indicates that every single primary radical has left the solvent cage and gone to initiate the polymerization. The rate of initiation is described by Equation 1.1 where k_{di} is the initiator decomposition rate coefficient.

$$R_I = \frac{d[I\cdot]}{dt} = 2fk_{di}[I_2] \quad (1.1)$$

The radicals that do escape the solvent cage can partake in a propagation reaction with a monomer to generate an active macroradical capable of undergoing a subsequent addition reaction with other monomer molecules. The rate of propagation is defined by Equation 1.2, where k_p is the propagation rate coefficient that is unique for each monomer and dependent on temperature as well as the viscosity of the reaction medium.

$$R_p = -\frac{d[M]}{dt} = k_p[M][R\cdot] \quad (1.2)$$

Termination is also a possible reaction route and, it occurs when one radical center meets another. Free radicals can terminate by one of two mechanisms, disproportionation or coupling. Termination via coupling, also referred to as combination is the result of two macroradicals ($R_n\cdot$ and $R_m\cdot$) coming together and forming a stable bond (R_{n+m}). In contrast, disproportionation occurs when a hydrogen atom from one of the chain ends is abstracted yielding two dead polymer chains (R_n and R_m).

1.2.1. Diffusion Controlled Termination

The termination mechanism described above seems straightforward, but is greatly complicated by polymer diffusion limitations. Bimolecular termination is a reaction occurring between two macroradicals thus it is more susceptible to diffusion control as opposed to propagation and initiation.

There are three definable steps in the bimolecular termination process and they are shown in Scheme 1.2 below.

1. Translational diffusion: it involves the movement of individual macroradical coils towards each other through the reaction medium.

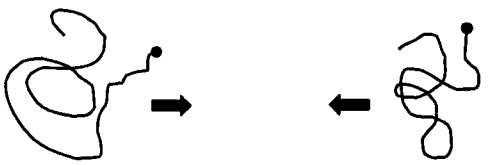

2. Segmental diffusion: the radical centers of the polymer chains reorient themselves in a position which could enable a reaction to take place.

3. Chemical reaction: when the two radicals overcome the chemical barrier and react to form a dead polymer chain.

Scheme 1.2: Schematic demonstrating the molecular process involved in bimolecular termination

In a sequence of reactions the slowest step will always be the rate determining step. The third step here is the most rapid; therefore segmental and translational diffusion determine the overall reaction rate.

The rate of termination is described below in Equation 1.3 and is second order with respect to the radical concentration. The termination rate coefficient k_t is dependent on a number of factors including temperature, pressure, monomer conversion, the reaction media as well as molecular weight. Many of these factors are a function of the polymer diffusion processes described above.

$$R_T = \frac{d[R\cdot]}{dt} = -2k_t[R\cdot]^2 \quad (1.3)$$

1.2.1.1. Conversion-Dependent Termination

The polymer concentration has a considerable influence on the termination rate coefficient. Intuitively, increasing conversion of monomer to polymer would increase the viscosity of the medium and consequently affect the mobility of the growing polymer chains. At low monomer conversions, polymer coils can move freely in the reaction medium making translational diffusion fast and segmental diffusion the rate determining step in this conversion regime. At high conversions however, when the entanglement of polymer chains becomes more influential, a significant decrease in the translational diffusion coefficients of individual polymer coils occurs and thus the reaction becomes diffusion controlled.

1.2.1.2. Chain-Length-Dependent Termination

There is also a significant chain length dependency on k_t. Several theories exist for describing the diffusion of polymer chains in dilute and semi-dilute regimes including DeGennes, and Vrentas & Duda's free volume theory however, more simplistic

correlations exist. For instance, the average value for the termination rate coefficient $\langle k_t \rangle$ is usually expressed in a power law form as defined by Equation 1.4[3], where i_x is the average degree of polymerization and α is a parameter which quantifies its influence. The slope of a log k_t versus log i_x plot yields $-\alpha$ and an intercept of k_t^0. In this form α is usually an average value representative of chain lengths typically exceeding 100 units.

$$\langle k_t \rangle = k_t^{\,0} \cdot i_x^{\,-\alpha} \qquad (1.4)$$

In this long chain regime α values of 0.075,[4] as well as values ranging from 0.14 -0.20 [5, 6] have been reported for bulk polymerizations of MMA. The long chain α value has also been predicted using scaling theory[7], and is believed to be a result of entropic shielding of chain reactive centers during a collision of terminating radical coils. Short chain radicals ($i<100$) however, are not polymeric coils and thus termination is dominated by center of mass diffusion, consequently α values ranging from 0.50-0.65 have been reported for MMA.[8] Therefore, more accurate depictions of the reacting system can be obtained however, through the use of a "2 α" model where values for α correspond to a short (α_s) when $i < 100$ and a long chain(α_L) regime (Equation 1.5).[9]

$$\begin{aligned} &\text{for } i_x < i_{SL},\ k_t^{i,j} = k_t^{1,1} \cdot i_x^{\,-\alpha s} \\ &\textit{for } i_x \geq i_{SL},\ k_t^{i,j} = k_t^{1,1} \cdot i_{SL}^{\,\alpha L - \alpha S}\, i_x^{\,-\alpha L} \end{aligned} \qquad (1.5)$$

The term i_{SL} represents the cross over chain length from the short to the long chain regime. The complicated nature of the termination step has made it difficult to accurately determine some of the rate parameters.

1.2.2. Determination of the Termination Rate Coefficient k_t

The need for accurate rate coefficients is of considerable interest commercially for free radical polymerization systems, especially with the recent renaissance of living radical polymerizations. There are still no benchmark values for k_t for even the most commonly studied monomers. The reason for this is that a great deal of the work done in this area was completed in an era (pre 1987) when k_p could not be accurately measured thus making the k_t values determined not very reliable. Now, using pulsed laser polymerizations (PLP- SEC) as the benchmark technique recommended by IUPAC, k_p can be determined accurately for a wide range of monomers under many reaction conditions.[10] Measuring k_t directly on the other hand has been a cumbersome task because it is dependent on so many interrelated variables that change throughout the course of the polymerization. There are over 20 prominent methods employed to determine k_t which range in complexity and effectiveness. Some of the most promising methods use kinetic measurements to determine k_t.

Electron paramagnetic resonance (EPR) is a unique method as it can directly measure the radical concentration as opposed to other methods which obtain it from indirect measurements. This method is particularly effective when the conversion vs. time data is obtained simultaneously throughout the course of a reaction. Fourier transform-near infrared (FT-NIR) spectroscopy has been combined with EPR in a successful manner to obtain k_t as a function of conversion.[11] Electron paramagnetic resonance has also been used to measure the absolute radical concentration for UV initiated polymerizations of MMA at 25°C. The UV light is switched on and off, during the period of darkness (R_I =

0), so that it is possible to solve directly for k_t at various conversions. A high concentration of initiator was required however, to acquire strong EPR signal with high signal to noise ratio[12]. EPR has been used extensively but has limitations which have prevented it from being a benchmark technique. Firstly, it requires considerable expertise in order to obtain reliably consistent values. As well, measurements of the radical concentration are typically carried out at unconventional reaction conditions in order to obtain a more favourable signal to noise ratio. Most importantly, for many monomers the radical concentration at low conversions is too low to measure rendering this method ineffective for some applications.

Pulsed laser polymerization is another method used to determine k_t and, has been used extensively since the 1980s when the technique was originally developed. At this time, however, the corresponding values for k_p were not accurately measured, therefore they yielded results that were inconsistent and not reliable. Work conducted since then by Buback and Olaf have re-examined the method, performing it with various monomers, including acrylate [13] and methacrylate [14] systems. This method entails the use of a photoinitiator and monomer solution that is exposed to a high energy laser pulse to generate free radicals instantaneously on the timescale of termination. The instantaneous generation of radicals at t = 0 is advantageous because all the radicals formed have roughly the same length. The simplified relationship depicting the radical concentration as a function of time is shown below in Equation 1.6.

$$\frac{d[R]}{dt} = R_i - 2k_t[R]^2 \qquad (1.6)$$

The rate of initiation (R_i) in the absence of a laser pulse is zero. The termination rate constant can then be determined in association with time resolved monomer conversion time data (Figure 1.1) using the following expression (Equation 1.7), where $[R\cdot]_{LP}$ is the maximum free radical concentration immediately reached after laser pulse, and t is the time of an individual pulse.[3] When $[R\cdot]_{LP}$ and k_p are known, k_t can be determined directly.

$$\frac{[M]}{[M]_0} = (2k_t[R\cdot]_{LP}t + 1)^{-k_p/2k_t} \qquad (1.7)$$

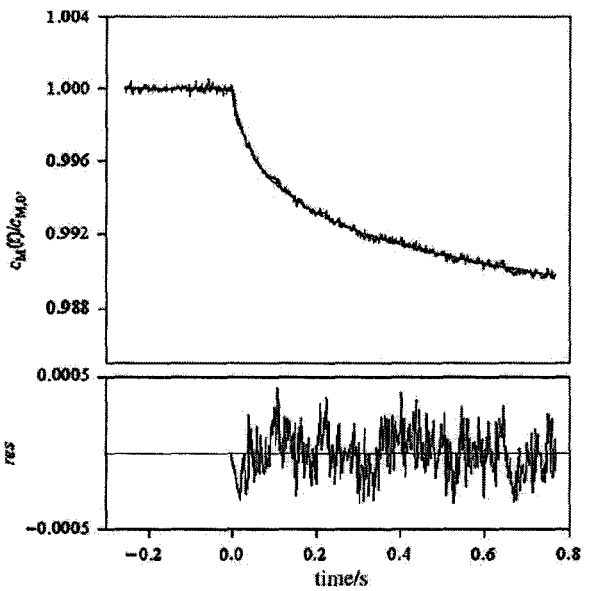

Figure 1.1: Relative monomer concentrations as a function of time for a single pulse. The difference between the measured and the expected values is plotted as the residuals[15]

Perhaps the most promising method for the determination of k_t has been recently explored by Barner-Kowollik et al.[16] This method is particularly of great interest since the termination rate coefficient can be obtained while incorporating the coupling effects of conversion and chain length dependencies. This novel technique, involves the use of a

living radical polymerization technique known as reversible addition fragmentation chain transfer (RAFT). In this method RAFT polymerizations are carried out in a differential scanning calorimeter (DSC) and the rate of polymerization is monitored online as a function of time. The data obtained from the DSC measurements can then be used to compute the values for the termination rate coefficient using Equation 1.8.

$$k_t = \frac{2fk_d[I]_0 e^{-k_d t} - \dfrac{d\left(\dfrac{R_p(t)}{k_p([M]_0 - \int_0^t R_p(t)dt)}\right)}{dt}}{2\left(\dfrac{R_p(t)}{k_p([M]_0 - \int_0^t R_p(t)dt)}\right)^2} \qquad (1.8)$$

The purpose of using a RAFT polymerization is that the terminating radicals are considered to be approximately the same length since living radical polymerization systems follow a Poisson distribution in theory. The time axis therefore can then be easily converted to reflect the evolution of chain length over the course of the polymerization using Equation 1.9. The chain length is denoted as i(t) and the initial concentration of the RAFT agent is represented by $[RAFT]_0$.

$$i(t) = \frac{\int_0^t R_p(t)}{[RAFT]_0} \qquad (1.9)$$

Consequently, this method can determine the termination rate coefficient as a function of both conversion and chain length. This is of considerable interest because

most methods to date are based on broad chain length distributions determining an average k_t from $k_t^{i,j}$ values where i, and j are radicals of different chain lengths. By utilizing this system the accurate determination of $k_t^{i,i}$ for a vast array of polymers can be ascertained. For example, this method has been successfully employed with styrene[16], methyl acrylate[17, 18] and methyl methacrylate[9, 19, 20].

The only limitation of this technique is that it requires knowledge of the propagation rate constant, and all of the initiation parameters, but overall these are typically are available in the literature. A key question is whether the values obtained using this method can be easily translated to FRP or more importantly other living radical polymerization systems such as nitroxide mediated polymerization (NMP) and atom transfer radical polymerization (ATRP) where the mechanism is slightly different.

1.3. Controlled/Living Polymerization

1.3.1. Living Ionic Polymerization

Living ionic polymerization has been studied in great detail since its discovery in 1956 by Micheal Szwarc.[21] Ionic polymerization can be used to produce polymers with very narrow molecular weight distributions, and controlled molecular weight. Conversely, ionic polymerization is severely limited due to the very strict reaction conditions required (i.e. very low temperatures) for the polymerization of some acrylates and methacrylates. Moreover, the types of monomers that can be successfully employed in living ionic polymerizations are greatly limited. This technique is also very sensitive to moisture and other protonic chemicals, thus requiring extensive purification. Therefore, living ionic

polymerizations are difficult to implement industrially, typically limited only to small batch scale processes.

1.3.2. Controlled/Living Radical Polymerization

The ability to produce new and enhanced polymeric products with improved material properties is of considerable interest from both an industrial and academic perspective. The industrial success of free radical polymerization may have suggested that it could be employed to produce these new specialized polymeric products. However, free radical polymerization, lacks the ability to synthesize polymers with tailored molecular weights, narrow polydispersity and specific macromolecular architectures which is necessary to produce these new advanced polymeric materials. In fact, the only viable technique that can yield polymers with significantly controlled macromolecular structures is living polymerization. Szwarc defined a living polymerization as a chain growth process free of termination or chain transfer.[21] Therefore, the living end enables polymer chains to further grow upon the addition of monomer, so block copolymers and other macromolecular architectures can be easily produced. A living polymerization however does not necessarily generate polymers with controlled molecular weight and narrow polydispersities. In order to satisfy these criteria, the initiator should be consumed at the very beginning so that all of the polymer chains can grow over roughly the same time period under the same reaction conditions. In addition, the deactivation of propagating radicals should be fast in order to minimize bimolecular termination.

From a mechanistic standpoint controlled/living radical polymerization and conventional free radical polymerization are nearly identical since they both undergo initiation, propagation and termination. They differ however, in the fact that living radical polymerizations undergo an additional activation/deactivation process as shown in Scheme 1.3.

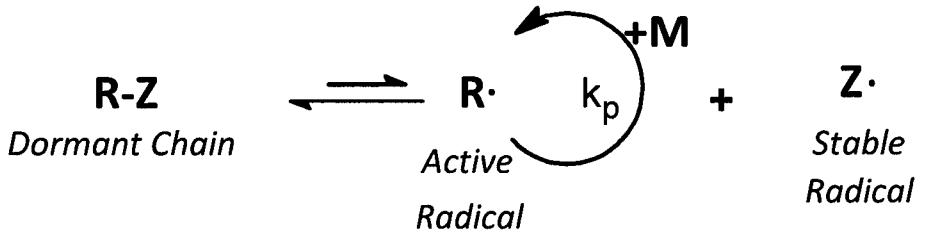

Scheme 1.3: Reversible activation/deactivation in CLRP

The dormant chain (initiator) can be activated by some added reagent, or undergo homolytic cleavage to form an active radical (R·) and stable free radical (Z·). The active radical can perform an addition reaction through propagation with a monomer or be subsequently deactivated again to become a dormant chain (R-Z). In living systems, the lifetime of propagating radicals can be extended to timescales of hours compared to conventional free radical polymerizations systems where active radical chains experience very short lifetimes of <1s. The reason for the prolonged lifetime of propagating radicals is because of the high probability of the deactivation of growing polymer chains via the dynamic equilibrium process demonstrated in Scheme 1.3. In fact, the time interval between activation and deactivation of propagating radicals is on the order of 0.1-10 ms which is much faster than the timescale of termination of roughly a second. The repeated cycle of activation and deactivation of the dormant polymer enables the polymerization to

retain its living characteristics. Consequently, controlled/living radical polymerizations can effectively control the topology, composition and functionality of polymeric structures (Figure 1.2).

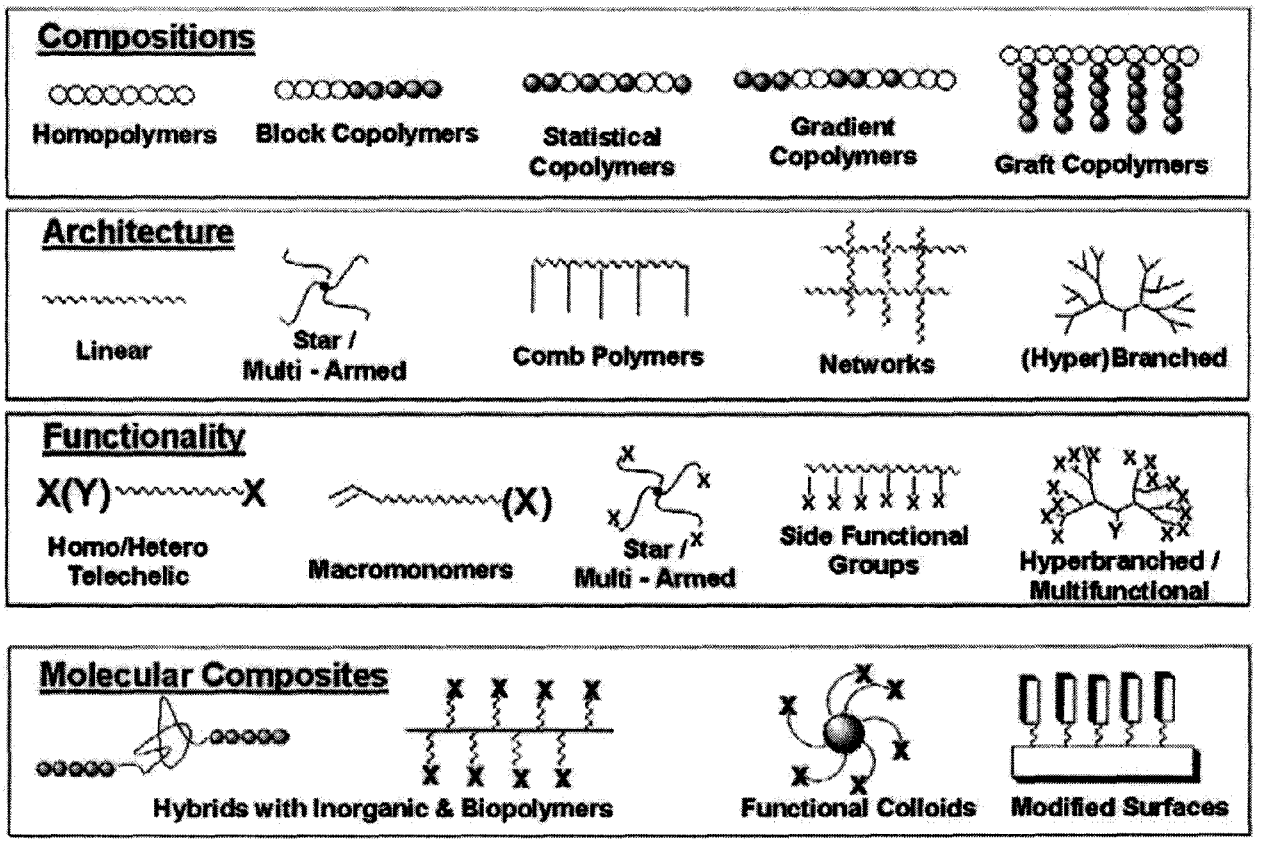

Figure 1.2: Examples of the macromolecular structures and architectures that can be produced by controlled/living polymerization[2]

The past 20 years has seen a renaissance in the area of controlled living polymerizations with the discovery of nitroxide mediated polymerization (NMP), reversible fragmentation chain transfer (RAFT) and atom transfer radical polymerization (ATRP) [22, 23].

1.3.2.1. Nitroxide Mediated Polymerization

There are several stable free radicals that have been used as the deactivating species in stable free radical polymerization (SFRP). When stable free radical polymerizations are conducted with nitroxides they are referred to as nitroxide mediated polymerization (NMP). One of the most extensively studied nitroxides is 2,2,6,6-tetramethyl-1-piperidinoxyl (TEMPO) and its derivatives. The first nitroxide mediated polymerization was performed by Georges, where low polydisperity (1.20) polystyrene and styrene-based copolymers were produced with TEMPO at high temperatures (130°C) in bulk.[24] There are two distinct methods that are typically employed with NMP. The first method, described in Scheme 1.4, involves the thermal cleavage of an alkoxyamine (initiator) which results in the formation of an active radical and TEMPO the stable radical. The second method requires the addition of a conventional free radical initiator (BPO in Scheme 1.5), as well as the stable free radical (TEMPO) as shown in Scheme 1.5. A unimolecular initiator approach is more effective because it allows for better control of the target molecular weight since an initially set concentration of initiator is administered, thus allowing all the chains to grow uniformly from time zero.

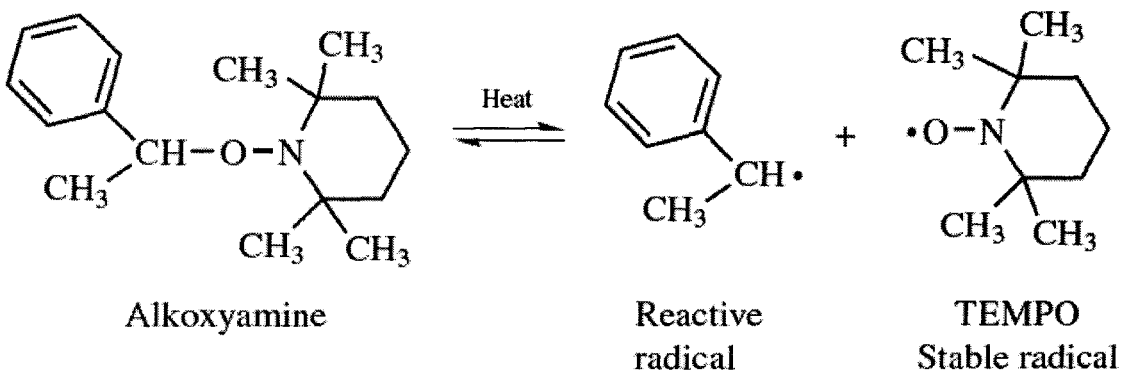

Scheme 1.4: Unimolecular initiation process for a nitroxide mediated polymerization [25]

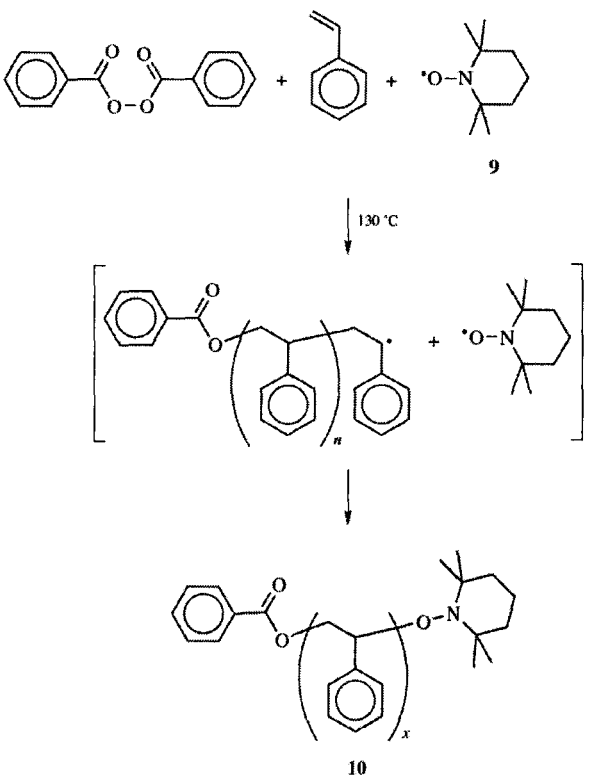

Scheme 1.5: Bimolecular initiation process for NMP [3]

In both methods (Schemes 1.4 & 1.5) the nitroxide radical reacts rapidly with the active radical centers to effectively deactivate and decrease its concentration of propagating radicals to suppress bimolecular termination.

Many of the first generation of these alkoxyamines were derivatives of TEMPO with cyclic chemical structures and were proven successful for many styrenic type monomers. These cyclic alkoxyamines however, were found to yield uncontrolled polymerizations of butyl acrylate. Therefore, sterically hindered cyclic as well as non-cyclic alkoxyamine were synthesized, many with phosphonate chemistry and were found to effectively mediate the polymerization of both styrene, and acrylate type monomers. When the appropriate alkoxyamines are utilized, complex molecular architectures can be synthesized to produce block copolymers, as well as star [26, 27], hyperbranched and dendritic polymers [28]. NMP has also been used to graft polymer brushes from surfaces.[29]

The design of new alkoxyamines is still a high priority for researchers in this area since methacrylate and vinyl acetate based polymers are still difficult to produce, although some successful polymerizations have been conducted with MMA recently.[30] Another challenge for NMP is improving the commercial availability of these alkoxyamines which is essential to improving research capabilities and industrial feasibility for this system. Nitroxide mediated polymerization is also limited in many respects. For instance, in order to induce thermal cleavage of the alkoxyamine, high temperatures (100-145°C) are typically required, and the reaction rates are slow, lasting 1-3 days to achieve high conversions. Moreover, dispersion reaction processes are typically

more complicated since they require a pressurized environment to prevent evaporation of solvents and water at those high temperatures.

1.3.2.2. Reversible Addition Fragmentation Chain Transfer (RAFT)

Another technique greatly responsible for the revival of living radical polymerization is reversible addition fragmentation chain transfer (RAFT). Although RAFT polymerization is the youngest of the new techniques, some of the integral reaction components in the RAFT mechanism (xanthate esters) have been used for quite some time now for the deoxygenation of alcohols.[31] When xanthate esters are employed as chain transfer agents the acronym MADIX (macromolecular design by interchange of xanthate) is typically used to describe the RAFT process. Zard and coworkers (1988) first proposed work involving xanthate esters and reversible chain transfer agents as an effective tool in generating alkyl and acyl radicals.[32] Ten years later the first reported publication of using thiocarbonylthio compounds as RAFT agents occurred in 1998 by the CSIRO group.[33] Figure 1.3 provides an overview of the typical structures of the chain transfer agents employed in RAFT polymerizations.

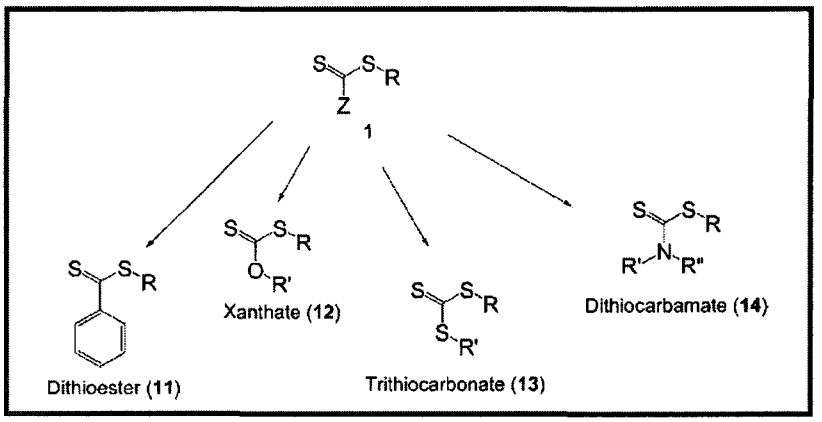

Figure 1.3: General structures of RAFT Agents[34]

The RAFT mechanism is demonstrated in Scheme 1.6. Similarily to conventional free radical polymerizations, the RAFT process is initiated via thermally sensitive azo, or peroxide type initiators. The radicals (I·) that are produced from the decomposition of these free radical initiators react with monomer molecules to produce a polymer chain with length m (P_m·). Newly formed polymeric radicals then react with dithioesters (chain transfer agents) which leads to the formation of a dynamic exchange process consisting of an addition step to produce an immediate radical and the subsequent fragmentation step. The addition/fragmentation process is reversible and occurs when the active polymeric radical (P_m·) reacts with the chain transfer agent, the dithioester, at the S=C bond forming intermediate radical as shown in section (II). If the reaction shifts to the right, fragmentation will occur thus leading to the formation of a new radical specie (R·) from the R leaving group as well as a dormant polymer chain [P_m-S-(Z)C=S] (section (II) Scheme 1.6) . The newly formed (R·) can then undergo propagation with monomer to form a polymer chain with length n (P_n·) as shown in section (III) of Scheme 1.6. The

polymeric chain ($P_n^{\cdot}$) can then react with a virgin chain transfer agent or with an existing dithioester capped dormant specie [P_m-S-(Z)C=S]. Undergoing an addition reaction with an existing dormant chain, as in the case depicted in Scheme 1.6 (section IV), results in the formation of a immediate radical [P_n-S-(Z)C$^{\cdot}$-S-P_m)]. Subsequently, fragmentation to the right results in the release of the R group ($P_m^{\cdot}$) and once again the generation of a stable dormant chain. The active radical population is thus minimized through the rapid exchange process between propagating radicals and dormant chains which consequently ensures equal growth probability for all chains.

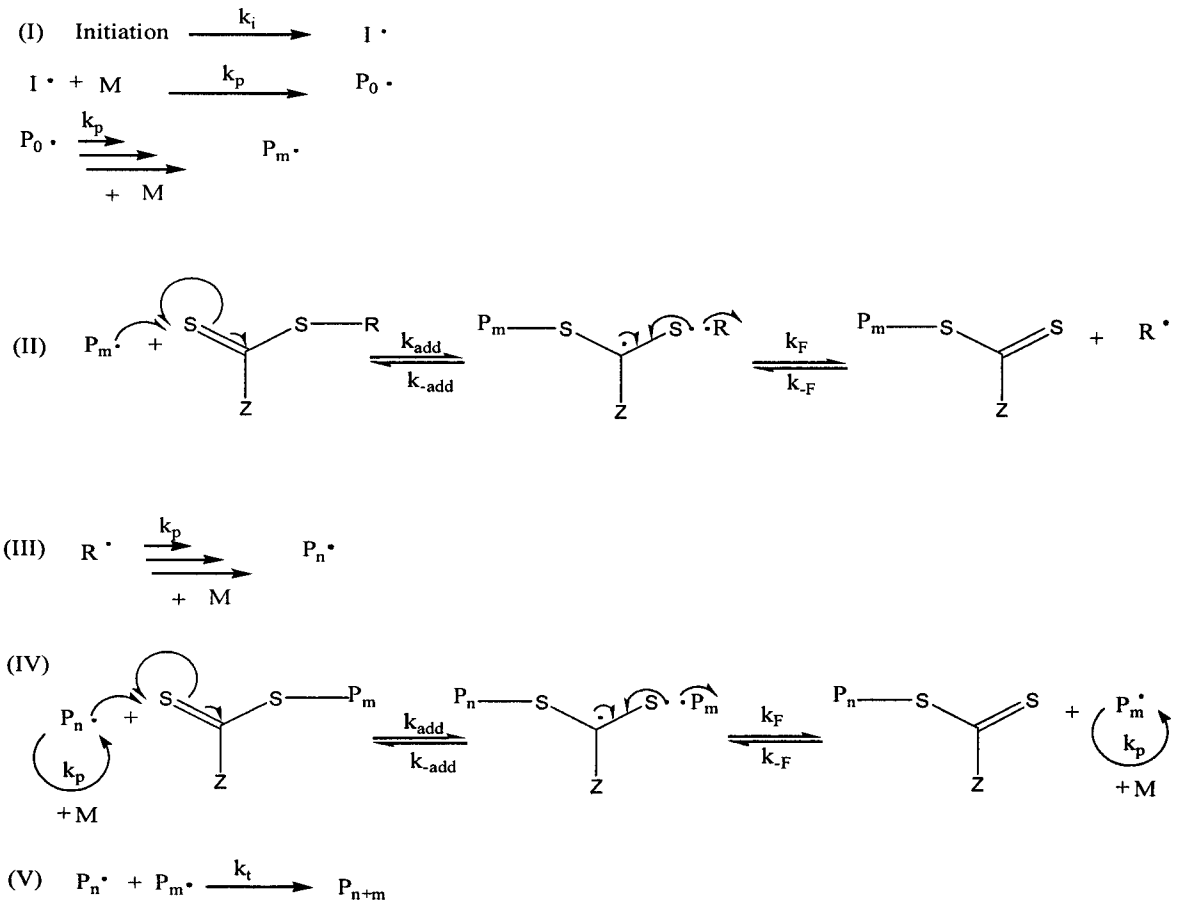

Scheme 1.6: RAFT Mechanism

RAFT polymerization is a robust and versatile process. Many diverse monomer types, including styrene, methacrylates, acrylates, acrylamides, and even the highly reactive vinyl acetate, have been polymerized using RAFT process. Different chain transfer agents can be matched up for a given monomer type making this process very conducive to a very broad range of monomers. Analogous to free radical polymerization, RAFT polymerizations are also tolerant to a wide range of reaction conditions, and solvents. Moreover, RAFT polymerizations have been performed successfully with a variety of different reaction processes such as in bulk, solution, emulsion, and suspension.

1.3.2.3. Atom transfer radical polymerization (ATRP)

Atom transfer radical polymerization is a controlled/living polymerization method used to synthesize polymers with tailored molecular weights and narrow polymer distribution. It has received considerable interest from industry and academia alike since its discovery in 1995,[22, 23] and has been used to develop a wide assortment of products with specialized macromolecular architectures.[35-37] ATRP is a catalytic process and is shown in Scheme 1.7. It relies on a reversible reaction between the alkyl halide (RX) initiator and a ligated metal salt (Mt^nY/Ligand) to form a radical ($R\cdot$) which can go on to propagate with a monomer unit, terminate through reactions with impurities or other radicals. The radical ($R\cdot$) can also be deactivated with an oxidized catalyst (X-$Mt^{n+1}Y$/Ligand) to form dormant polymer chains (R_n-X) and the reduced form of the catalyst (Mt^nY/Ligand). The dormant polymer chains (R_n-X) can be reversibly reactivated and deactivated via the same process. Termination is minimized due to an equilibrium

that favours the deactivation of the radicals forming dormant alkyl halide species (R_n-X). During this equilibrium period polymeric chains grow, in the quasi absence of termination, in a living manner. That is, with polymer molecular weights proportional to monomer conversions and narrow polymer molecular weight distributions.

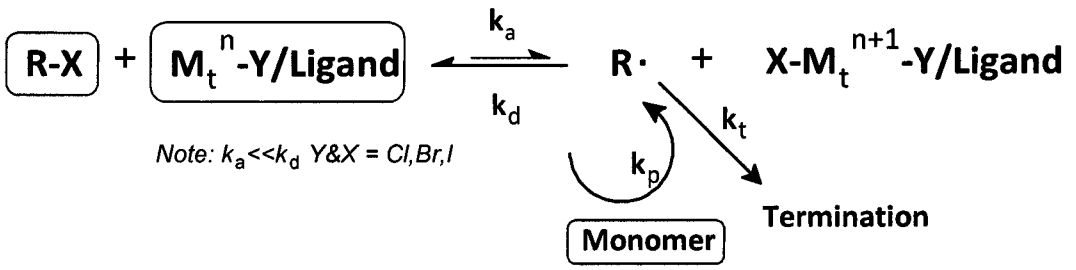

Scheme 1.7: ATRP Mechanism, rectangular boxes represent the reagents initially charged in the reacting vessel

For ATRP the theoretical degree of polymerization is defined by Equation 1.10, and determined by the ratio between the initial monomer and initiator concentration (assuming negligible termination). The degree of polymerization increases linearly as a function of monomer conversion. The polydispersity index is shown in Equation 1.11, and is dependent on the rate of deactivation (k_d[X-Mt^{n+1}Y/Ligand]). Polydispersities that are less than 1.11 are considered to be well controlled in ATRP.[35] Higher polydispersities are usually obtained for acrylate type systems because of their higher propagation rate constants in comparison to styrene, and methacrylate type monomers.

$$DP_n = \frac{[M]_0 \cdot \times}{[RX]_0} \qquad (1.10)$$

$$PDI = \frac{M_w}{M_n} = 1 + \left(\frac{[RX]_0 k_p}{k_d[\mathrm{Mt}^{n+1}]}\right)\left(\frac{2}{x} - 1\right) \qquad (1.11)$$

The rate of polymerization (R_p) in ATRP is governed by Equation 1.12, where the ATRP equilibrium rate constant (K_{ATRP}) is defined by the ratio between the activation and deactivation rate constant ($K_{ATRP}=k_a/k_d$). The apparent rate constant (k_{app}) can be obtained by generating a first order rate plot with respect to the monomer. These relationships presented in Equations 1.10-1.12 can be useful in the design of a successful ATRP. Increasing the polymerization rate for instance, can be achieved by several means. One way is to have an increase in K_{ATRP} (i.e. a decrease in k_d) or an increase in the reduced catalyst concentration ($[Mt^n]$). The catalyst concentration has an effect on the molecular weight distribution (Equation 1.11), the radical concentration and invariably on the rate of polymerization. The catalyst concentration however, does not have an effect of the degree of polymerization (Equation 1.10). Increasing the reaction rate in ATRP can also be attained through increasing the initiator concentration, although it will also result in an increase in the polydispersity and a decrease in the degree of polymerization.

$$R_p = k_p[M][R\cdot] = k_p k_{ATRP}[RX]_0 \frac{[Mt^n]}{[Mt^{n+1}]}[M] = k_{app}[M] \qquad (1.12)$$

The widespread popularity of ATRP in academia is not unfounded. ATRP is a robust technique that has been proven to be effective in many different processes, including heterogeneous and homogenous systems. ATRP has been performed successfully in emulsion, bulk, solution and suspension and with a considerable tolerance to a variety of solvent types such as organic, water, supercritical CO_2 and ionic liquids. Additionally, ATRP has been performed effectively on an assortment of monomers, some which include methacrylates,[38] styrenes,[39] acrylates,[40] acrylonitrile,[41] (metha)crylic acids as well as various other monomers.[42]

1.3.2.3.1. Reverse Atom Transfer Radical Polymerization (RATRP)

In conventional ATRPs the initiation system involves the loading of the alkyl halide initiator (R_n-X) as well as the reduced metal halide (Mt^nY/Ligand) to generate free radicals and an oxidized catalyst. Reverse ATRP was developed to enter the ATRP process using the oxidized metal halide catalyst. This facilitates the handling of the catalyst. In reverse ATRP the products are fed into the reactor initially, as shown by the mechanism in Scheme 1.8. A free radical initiator is loaded which generates radicals ($R\cdot$) upon thermal decomposition of the initiator. These radicals reduce the loaded catalyst (X-$Mt^{n+1}Y$/Ligand) to generate the activating catalyst (Mt^nY/Ligand) and a dormant polymer chain (R_n-X). The same cycle is repeated where the deactivated polymer chain (R_n-X) is reversibly re-activated and deactivated via the dynamic ATRP equilibrium.

RATRP is distinct from other ATRP initiation systems employing a second radical source (ICAR ATRP & SR&NI ATRP) since no alkyl halide initiator is initially charged in the reactor. A necessary criterion for living systems with controlled molecular

weight distribution is that all chains be initiated early on in the polymerization in order to ensure equal opportunity for propagation between all the growing chains. To fulfil this condition in RATRP, the free radical initiator must decompose rapidly, readily reacting with deactivators to produce activating species and dormant polymeric chains thus initiating the ATRP equilibrium. High reaction temperatures are typically administered as a means of accelerating the decomposition of the initiation as well as shortening the induction period. The catalyst concentration must be fed in at nearly equal molar loadings relative to the initiator. A limitation of this technique is its inability to form clean block copolymers as illustrated in Scheme 1.9. Additionally, the use of a free radical initiator source also hinders the ability to add functionality to the polymer end groups (on the initiator side). For RATRP systems the degree of polymerization is governed by Equation 1.13 where f is the initiator efficiency. The evolution of chain length growth is dependent on the amount of free radical initiator that has been consumed by the system at a certain time.

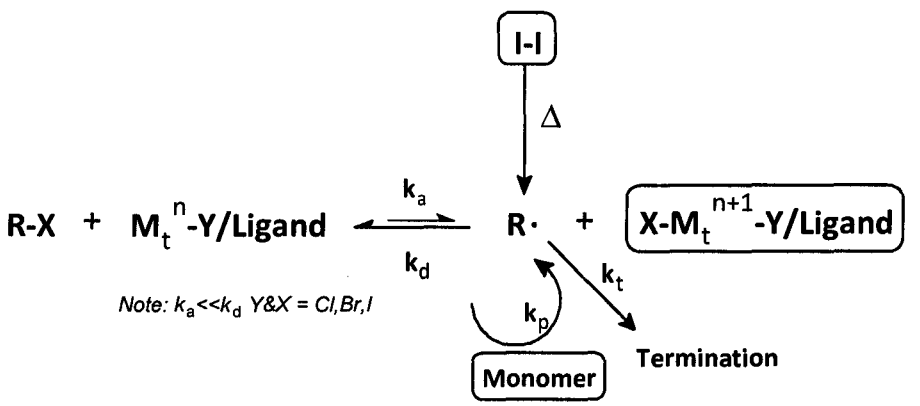

Scheme 1.8: Reverse ATRP mechanism, rectangular boxes represent the reagents initially charged in the reacting vessel

$$DP_n = \frac{[M]_0 \cdot \times}{2f([AIBN]_0 - [AIBN]_t)} \qquad (1.13)$$

The advantages of utilizing the reverse initiation technique is that it enables the handing of the less sensitive form of the catalyst in the presence of oxygen during the preparation stage thus making it more attractive for scaled up commercial processes. In addition, from a cost perspective the initiators used in RATRP are relatively inexpensive compared to the alkyl halide species used in conventional ATRP systems.

RATRP has been employed in many different processes including emulsion,[43, 44] bulk and solution in both heterogeneous and homogenous catalytic systems. The most commonly used initiators for RATRP have been diethyl 2,3-dicyano-2,3-diphenylsuccinate(DCDPS),[45-48] 1,1,2,2-tetraphenyl-1,2-ethanediol (TPED) [49] and AIBN.[43, 50-52] Narrowly distributed polymer (PDI =1.06), with high initiator efficiency (96%) has been produced using AIBN in conjunction with $CuBr_2$/pyridinimine catalysts systems.[43] Initiating systems employing microwave irradiation have also been used to polymerize MMA [53-55] and styrene.[56] For example, the introduction of microwaves for the RATRP of MMA in DMF with a $FeCl_3/PPh_3$ catalytic system resulted in an over 10 fold increase in the rate as compared to conventional heating processes at lower temperatures (69°C). However, the initiator efficiency was low since the experimental molecular weight did not follow the theoretical values closely, and the polymer distribution was broad with PDI of approximately 1.50.[54]

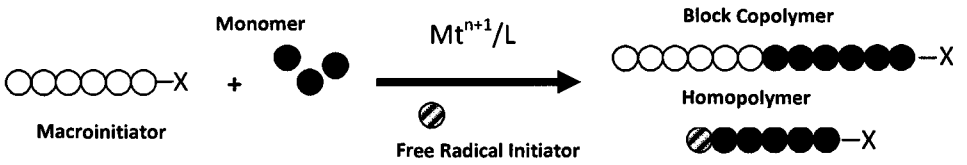

Scheme 1.9: Formation of Block Copolymers

1.3.2.3.2. Simultaneous Reverse and Normal Initiation (SR&NI)

SR&NI was developed to overcome the inability of RATRP to introduce functionality to the living polymer, a limitation preventing the creation of more complex macromolecular architectures. Similarly to RATRP, a SR&NI process utilizes the radicals generated from the decomposition of the free radical initiation to convert the oxidized metal salt to form activating species as well as dormant polymer as shown in Scheme 1.10. SR&NI is a particularly effective method in processes where highly active catalytic systems are used and easily contaminated in the presence of oxygen. This method differs from RATRP as an alkyl halide initiator is also added to the reaction and the majority of the polymeric chains generate from this initiator. The degree of polymerization is expressed in Equation 1.14 and is controlled by the initial concentration of alkyl halide initiator. In these systems the concentration of free radical initiator (AIBN) is usually kept low at 10% of the molar concentration of the alkyl halide initiator and does not have a considerable influence on the molecular weight. This technique has been used to yield well defined polymers with molecular weights of 40 000 g/mol and low polydispersity (<1.10). This reaction was conducted using a bulk process for styrene and butyl acrylate in the presence of both a heterogeneous and homogeneous catalytic system.[57] SR&NI has

also been performed successfully in other reaction processes such as mini emulsion for the formation of block, and gradient copolymers.[58]

$$DP_n = \frac{[M]_0 \cdot \times}{[RX]_0 + (2f([AIBN]_0 - [AIBN]_t))} \quad (1.14)$$

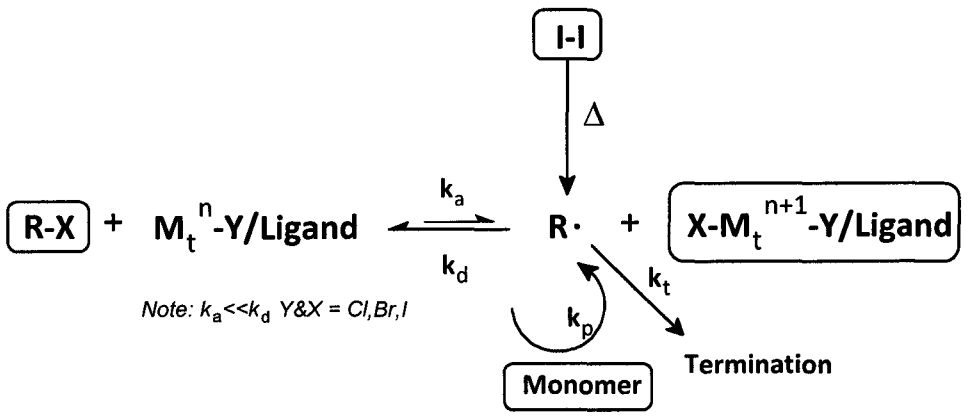

Scheme 1.10: Simultaneous reverse and normal initiation (SR&NI) mechanism, rectangular boxes represent the reagents initially charged in the reacting vessel

1.3.2.3.3. Initiators for Continuous Activator Regeneration (ICAR) ATRP

Recently, new techniques have been developed to overcome the use of high catalyst loadings in ATRP. Initiators for continuous activator regeneration ATRP was developed in 2006 with an emphasis on using the generation of free radicals to continuously produce activators (Mt^nY/Ligand) from the accumulated oxidated catalyst (X-Mt^{n+1}Y/Ligand).[59] The oxidated catalyst species accumulate in all ATRP systems due to radical termination reactions, however, in most ATRP systems the initial catalyst concentration is high and thus there are sufficient activating agents present to facilitate the reaction. In ICAR-ATRP low catalyst loadings are used and thus a thermal initiator is needed to reduce the oxidized ATRP copper catalyst (X-Mt^{n+1}-Y/L) to its activating state

(Mt^n-Y/Ligand). The reduced catalyst can then generate propagating radicals from an alkyl-halide initiator through halide abstraction and this in turn leads to the ATRP process. This is nearly identical to SR&NI method; however, it differs with respect to the amount of catalyst loaded. In ICAR systems the catalyst concentration is less than 50 ppm compared to 1000 ppm typically employed in SR&NI reactions. Moreover, the reaction rate here is dictated by the free radical initiator not the ATRP rate law.

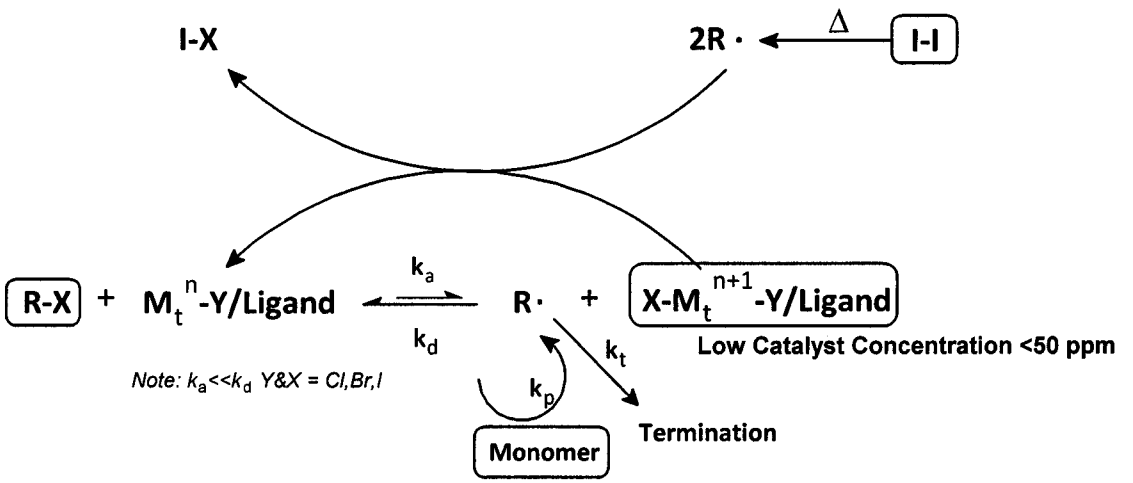

Scheme 1.11: ICAR ATRP mechanism, rectangular boxes represent the reagents initially charged in the reacting vessel

1.3.2.3.4. Activators Generated by Electron Transfer (AGET) ATRP

Similar to SR&NI ATRP, AGET ATRP utilizes alkyl halide initiating species as well as the oxidized form of the catalyst. In this mechanism however, a free radical initiator is replaced by a reduction agent. The reducing agent serves the purpose of driving the stable catalyst precursor to the left to form the reduced metal halide. The main difference is that the reducing agent does not create new radicals capable of forming new active centers for the reaction. The advantage of this method is that it allows for the

construction of very complex macromolecular structures. Pure block copolymers can be produced, free of homopolymer entities as shown in Scheme 1.12. AGET ATRP has been employed to develop various macromolecular architectures.[60] Another advantage of this method is that excess reducing agent can be loaded and used to remove dissolved oxygen and other impurities from the reaction making it a versatile process requiring less stringent preparation procedures.

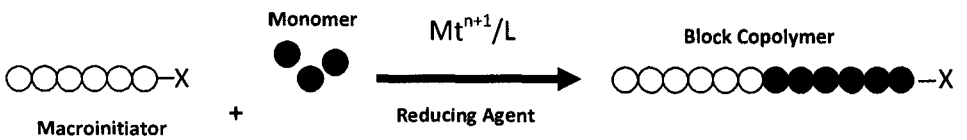

Scheme 1.12: Formation of Pure Block Copolymers

1.3.2.3.5. Activator Regenerated Electron Transfer (ARGET) ATRP

More recently, the scientific community has focussed its attention on a new mechanism, ARGET. AGET and ARGET are identical from a mechanistic view point but differ in the amount of the oxidized catalyst complex (X-Mt^{n+1}Y/Ligand) and reducing agent initially charged in the reactor. Contrary to most AGET ATRPs, ARGET ATRP systems are run with an excess amount of reducing agent in order to effectively regenerate activating species (Mt^{n}Y/Ligand) from low the concentration of oxidized catalyst (X-Mt^{n+1}Y/Ligand) as well as to remove any dissolved oxygen in the system. The ARGET ATRP of styrene was performed with only 10 ppm of the catalyst system $CuCl_2$/Me_6TREN, obtaining an experimental molecular weight of 63 000 (Mn_{theo} = 64

000) and PDI of 1.17 [61]. More recently, ARGET has been employed to construct a wide array of products using more environmentally friendly reducing agents. For example ascorbic acid (vitamin C) was used as a reducing agent for the ARGET ATRP of MMA, MA, BA and styrene. With 25 ppm Cu, a molecular weight of 30 700 (Mn_{theo} = 23 260) and polydispersity of 1.27 was obtained for the PMMA case.[62] The reaction rates for ARGET systems are slow. For the polymerization of MMA using ascorbic acid, the reaction achieved 59% conversion in 18 hours[62].

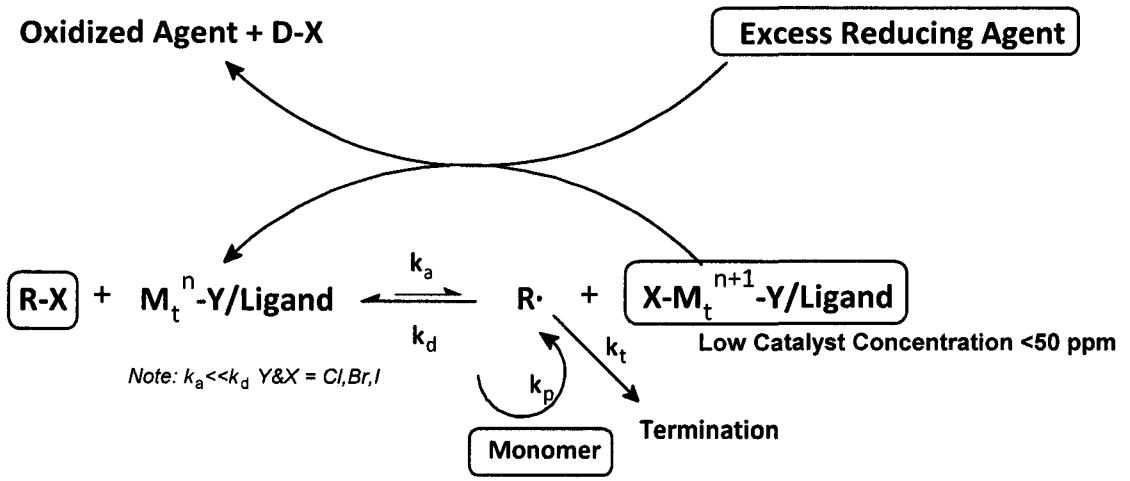

Scheme 1.13: ARGET ATRP Mechanism, rectangular boxes represent the reagents initially charged in the reacting vessel

1.4. Comparison of NMP, ATRP, and RAFT

The most promising and successful controlled living radical polymerization techniques are NMP, RAFT and ATRP. They can all be employed in a wide range of reaction processes (bulk, solution, suspension, emulsion), and are tolerant to water and small amounts of oxygen. Therefore, these methods do not necessitate tedious pre-

polymerization purification procedures and strict reaction conditions. ATRP is the most tolerant to oxygen impurities out of these three systems, especially when modified initiation methods are used and the oxidized form of the ATRP catalyst in initially loaded. Overall these techniques are robust and are relatively versatile, in particular ATRP and RAFT where a wide range of temperatures can be utilized. NMP is limited in this regard however, as the reaction conditions necessitate high temperatures to >100°C in order for the alkoxyamine to be effective.

The applicability of these methods with various monomer types is also unique for each method. RAFT and ATRP can be most widely applied to a vast range of monomer families including, methacrylates, acrylates, styrenes, acylamides and acylonitrile. NMP on the other hand is limited, and mostly applicable for the polymerization of styrenes and its derivatives, although some newly developed alkoxyamines have been used to produce well defined methacrylate [30] and acrylate polymers.[63]

All three methods utilize different capping agents, for instance, nitroxides for NMP, dithioesters for RAFT and alkyl halides with transition metal catalysts for ATRP. In NMP the availability of nitroxides have been severely limited, until recently, and are generally expensive and difficult to synthesize. Recently, the focal point of the NMP research community has been on the development of new nitroxides that are more conducive for polymerizations with methacrylates and acrylates as well as on finding new more efficient synthesis routes to produce them. The chain transfer agents used in RAFT are not immune to the lack of commercial availability of these capping agents. They also require tedious organic synthesis methods to produce the chain transfer agents required in

RAFT polymerizations. ATRP is thus the exception of the three methods. The reactant components including intiators (alkyl halides), catalyst (metal-salt) and ligands used in ATRP are widely commercially available and relatively inexpensive. There has also been significant investment to increase the capacity to produce more of the complex ligands (Me_6TREN) employed in some ATRP to make them more readily available. Overall the widespread commercial availability of reaction components as well as the lack of pre-polymerization synthesis and purification makes ATRP an attractive method.

One of the most appealing characteristics of ATRP is the fact that it is a catalytic process and depending on the activity of the catalyst species, minute amounts of catalyst can be sufficient enough to mediate the growth of many polymeric chains. This is in stark contrast to the other methods where for every growing polymeric chain they require an equal-molar concentration of either a chain transfer agent for RAFT or nitroxide for NMP. From a cost prospective the efficient catalytic approach further amplifies the cost disparity between the three methods.

In all of these living radical polymerization systems, the mediators that are used remain in the final product and can affect their properties. This predicament is obvious when conducting an ATRP with a copper catalyst for example, as the final product becomes discoloured, restricting its use in most applications. The same problems are existent for NMP and RAFT, especially since higher concentrations of the mediating species are loaded to ensure a 1:1 molar ratio with the growing chains. For instance, the chain transfer agent in RAFT polymerization contains dithioesters which are known to exude unpleasant odours as well as discolour the final product. Consequently, these

impurities remaining in the final product require post polymerization purification steps that hinder its widespread applicability at the industrial level.

Overall, ATRP in our opinion appears to that have the most commercial potential, compared to its living radical polymerization counterparts. ATRP has been applied to a wide range of monomers, temperatures, reaction processes and is tolerant to water and oxygen impurities. Moreover, the reaction components are all widely available which thus eliminates the need to perform tedious organic synthesis reactions and pre-polymerization purification steps. The ATRP catalytic process is the most attractive feature of this reaction where depending on the activity of the catalyst, minute amounts of mediator can be utilized to mediate the growth of many active chains.

1.5. Challenges of ATRP

The tremendous efforts of those working on ATRP have increasingly enhanced the potential wide scale commercialization of this method. However, there are still some major obstacles which have restricted the leap into full scale industrialization. One major challenge is the slow reaction kinetics of ATRP as compared to conventional free radical processes. While free radical polymerizations typically achieve high conversions within a few hours, the time scales of most ATRP systems are an order of magnitude higher. These slow reaction kinetics have been typically overcome through the use of high and costly catalyst loadings to augment reaction rates. [38] This strategy however leads to high levels of catalyst contamination in the final product. For most end uses, the product will

thus require further post-polymerization purification steps which increase the cost of production.

Another approach taken to increase ATRP rates has been to develop new catalysts with higher ATRP equilibrium constants. This approach is not trivial since the catalyst's equilibrium point must be matched to the type of monomer to be polymerized. For example, Cu(I)/Me_6TREN catalyzes the rapid ATRP of butyl-acrylate but does not lead to the fast and efficient catalysis of methyl-methacrylate (MMA) or styrene.[64] Great efforts have been made in the ATRP community to develop and discover new, more active catalysts, where only a minute catalyst concentration will be necessary to mediate the polymerization.[65-67]

A wide range of studies have investigated the use of various catalyst concentrations in ATRP systems with MMA. These are summarized in Table 1.1a and 1.1b.

Table 1.1a: ATRPs of MMA at Various Catalyst Concentrations (M_t)

			Catalyst							Molar Ratios					
entry	**I**	**R-X**	**Mt**	**Ligand**	**T(°C)**	**I_{eff}**	**PDI**	**Mt(ppm)**	**k_{app} (s^{-1})**	**[MMA]**	**[RX]**	**[L]**	**[Mt]**	**[I]**	**Ref**
1	n/a	MBP	CuBr	HMTETA	90	88	1.13	21	2.3×10^{-5}	100	1	1	0.01	n/a	68
2	AIBN	EtBrPA	$CuCl_2$	TPMA	60	0.91	1.23	50	?	200	1	0.01	0.01	0.1	59
3a	n/a	**2**	$CuCl_2$	2,2-dipyridyl	80	0.61	1.33	70	?	100	1	0.063	0.021	n/a	69
4a	DMPA	n/a	**6**	n/a	25	0.81	1.4	125	9.14×10^{-6}	2000	n/a	1	1	1	70
5	n/a	MBP	CuBr	HMTETA	90	0.82	1.11	210	6.7×10^{-5}	100	1	1	0.1	n/a	68
6b	n/a	n/a	CuCl	PMDETA	69	1.68	1.75	220	7.6×10^{-5}	3000	1	2	1	n/a	71
7	n/a	n/a	CuBr	**3**	100	0.5	1.2	270	2.8×10^{-6}	200	1	0.75	0.25	n/a	72
8[a]	n/a	**2**	CuCl	2,2-dipyridyl	80	0.95	1.25	327	7.48×10^{-5}	100	1	0.3	0.1	n/a	69
9	AIBN	n/a	$CuBr_2$	TMEDA	80	0.77	1.11	334	1.02×10^{-4}	604	n/a	2	1	1.9	73
10	AIBN	n/a	$CuBr_2$	PDMETA	80	0.58	1.26	334	1.57×10^{-4}	604	n/a	2	1	1.9	73
11	AIBN	n/a	$CuBr_2$	dNbpy	80	0.91	1.08	334	5.46×10^{-5}	604	n/a	2	1	1.9	73
12	n/a	n/a	CuBr	dNBpy	90	n/a	n/a	340	5.0×10^{-5}	200	1	0.46	0.23	n/a	74
13[b]	n/a	DCIX	CuCl	PMDETA	72	0.43	1.65	394	4.44×10^{-4}	400	1	0.75	0.25	n/a	75
14	n/a	n/a	CuCl	PMDETA	69	0.92	1.2	540	9.3×10^{-6}	2400	1	2	2	n/a	71
15	**7**	n/a	$CuCl_2$	Bipy	85	0.43	1.13	631	2.91×10^{-6}	1000	n/a	2	1	0.5	47
16	n/a	n/a	CuBr	dNBpy	90	1.08	1.1	660	8.3×10^{-5}	222	1	1	0.5	n/a	38
17	n/a	n/a	CuCl	PMDETA	90	0.75	1.3	690	1.2×10^{-4}	800	1	2	1	n/a	76
18	AIBN	n/a	$CuBr_2$	PMDETA	69	0.21	1.4	784	2.03×10^{-4}	600	n/a	1	1	3	50
19	AIBN	n/a	$FeCl_3$	PPh_3	85	0.35	1.26	881	1.40×10^{-4}	2455	n/a	12	4	1	51
20	AIBN	n/a	$FeCl_3$	Isophthalic Acid	110	0.7	1.43	1100	2.56×10^{-5}	500	n/a	4	2	1	77
21[b]	AIBN	n/a	$CuBr_2$	TMEDA	69	0.43	1.53	1117	8.19×10^{-5}	1680	n/a	16.8	4	1	53
22	n/a	n/a	CuBr	^{n}Bu-1	90	n/a	n/a	1120	4.5×10^{-5}	100	1	1.07	0.36	n/a	78
23	n/a	n/a	$FeCl_2$	I.Acid	90	0.82	1.4	1120	6.3×10^{-5}	500	1	4	2	n/a	79
24	n/a	TCX	CuCl	PMDETA	80	1.05	1.17	1175	7.78×10^{-5}	400	1	3	1	n/a	80
25	n/a	TCX	CuCl	PMDETA	90	1.04	1.17	1175	1.37×10^{-4}	400	1	3	1	n/a	80

Table 1.1b: ATRPs of MMA at Various Catalyst Concentrations (M_t)

			Catalyst							Molar Ratios					
entry	I	R-X	Mt	Ligand	T(°C)	I_{eff}	PDI	Mt(ppm)	k_{app} (s^{-1})	[MMA]	[RX]	[L]	[Mt]	[I]	Ref
26b	n/a	n/a	$FeCl_3 \cdot 6H_2O$	PPh_3	69	0.92	1.33	1229	4.4×10^{-4}	1600	n/a	8	4	2	54
27b	AIBN	n/a	$FeCl_3 \cdot 6H_2O$	PPh_3	69	0.88	1.53	1229	8.27×10^{-4}	1600	n/a	8	4	2.5	54
28	TPM	n/a	$CuCl_2 \cdot 2H_2O$	PMDETA	90	0.3	1.32	1255	1.66×10^{-4}	250	n/a	1	1	1	81
29	AIBN	n/a	$CuBr_2$	dNbpy	90	0.89	1.2	1451	6.57×10^{-5}	425	n/a	4	2	1	82
30	n/a	n/a	CuBr	TMEDA	90	0.94	1.38	1510	1.4×10^{-4}	200	1	2	1	n/a	83
31	n/a	n/a	CuBr	PMDETA	90	0.79	1.15	1510	5.6×10^{-5}	200	1	1	1	n/a	83
32	n/a	n/a	CuBr	HMTETA	90	0.79	1.12	1510	6.9×10^{-5}	200	1	1	1	n/a	83
33b	n/a	DCIX	CuCl	PMDETA	72	0.65	1.5	1556	7.33×10^{-5}	400	1	3	1	n/a	75
34	n/a	n/a	CuCl	Me_6TREN	60	0.35	2.2	1590	3.8×10^{-5}	200	1	1	1	n/a	64
35	AIBN	n/a	$CuBr_2$	**1**	100	0.88	1.06	1684	1.94×10^{-4}	90	n/a	2	1	0.75	43
36	n/a	n/a	CuBr	HHTETA	75	0.75	1.2	2120	1.1×10^{-4}	300	1	1	1	n/a	84
37	n/a	n/a	CuBr	HMTETA	90	0.57	1.23	2130	8.9×10^{-5}	100	1	1	1	n/a	68
38	n/a	BrEB	CuCl	Bipy	40	0.97	1.17	2240	1.19×10^{-4}	100	1	2	1	n/a	85
39	n/a	BrEB	CuCl	Bipy	80	0.58	1.22	2240	?	100	1	2	1	n/a	85
40	n/a	BrEB	CuCl	Bipy	80	0.96	1.21	2240	5.06×10^{-4}	100	1	2	1	n/a	85
41	n/a	BrEB	CuBr	Bipy	80	0.63	1.34	2240	?	100	1	2	1	n/a	85
42	n/a	TCX	CuCl	PMDETA	80	0.93	1.25	2311	1.4×10^{-4}	400	1	6	2	n/a	80
43	n/a	n/a	CuCl	Bpy	130	n/a	n/a	2580	5.6×10^{-4}	246	1	3	1	n/a	23
44b	AIBN	n/a	$CuBr_2$	TMEDA	69	0.51	1.54	2909	1.94×10^{-4}	560	n/a	16.8	4	1	53
45	n/a	Me_3SiCl	CuCl	PMDETA	90	0.006	1.42	3047	1.85×10^{-6}	100	1	1.5	1	n/a	86
46	n/a	n/a	CuBr	Et-1	90	0.8	1.2	3300	1.7×10^{-4}	100	1	2	1	n/a	78
47b	n/a	DCIX	CuCl	PMDETA	72	0.67	1.5	4530	1.25×10^{-3}	400	1	9	3	n/a	75
48	n/a	EBiB	$FeCl_2 \cdot 4H_2O$	HMPA	90	0.94	1.15	6154	1.48×10^{-4}	200	1	1	1	n/a	87
49	n/a	n/a	CuBr	NHPHI	90	n/a	n/a	6830	1.3×10^{-4}	30	1	3	1	n/a	88
50	AIBN	n/a	$FeCl_3$	PPh_3	85	0.85	1.29	n/a	6.62×10^{-5}	2460	n/a	12	4	1	51

Abbreviations: HMPA, hexamethylphosphoric triamide; PMDETA, N,N,N',N",N"-pentamethyldiethylenetriamine: HMTETA, Hexamethyltriethylenetetramine; TMEDA, tetramethylethylenediamine; NHPMI, N-(n-hexyl)pyridylmethanimine; Bpy, 2,2'-bipyridine; dNBpy, 4,4'-di(5-nonyl)-2,2'-bipyridine; Et-1, N-ethyl-2-pyridylmethanimine; n-Bu-1, N-(n-butyl)-2-pyridylmethanimine; I.acid, Isophthalic Acid; Me6TREN, tris[2-(dimethylamino)ethyl]amine; **1**, N,n-octadecyl-2-pyridylmethanimine; **2**, 2,2-dichloroacetophenone; **3**, 2-pyridinecarbaldehyde, **4**, α,α,α',α'-tetrachloroxylene; **5**, α,α'-Dichloroxylene; **6**, Ferric dithiocarbamate

1.6. Objective and Outline of This Thesis

We propose here a practical approach to enhance the reaction rate of ATRP through the addition of an external radical source. More specifically, ATRP in the presence of a high loading of free radical initiator and low catalyst concentrations is investigated in this work. The scientific community has not yet explored the use of high free radical initiator loadings with ATRP as a means of enhancing polymerization rates. This results primarily from a lack of knowledge relating polymer macromolecular structure to end use material properties. It is expected that the effect of adding a second radical source, in this case a thermally activated free radical initiator, would cause unwanted broadening of the polymer weight distribution. Thermally activated free radical initiators have been combined with ATRP in the past but only at low concentrations to avoid this unwanted effect. In these systems this small concentration of thermally activated free radical initiator is used for the sole purpose of continuously regenerating the activating catalyst (M_t^n/L) from its oxidized counterpart (M_t^{n+1}/L) (ICAR ATRP).[59] This strategy thus allows lower catalyst concentrations to be used since deactivation of the catalyst by side reactions (termination, contamination) is countered. No studies to date, however, have investigated the use of a hybrid system incorporating high free radical initiator loadings on ATRP as a means of enhancing reaction kinetics and what "control/livingness" penalty must one pay for this added benefit.

The second objective of this work is to utilize this hybrid ATRP system containing various concentrations of free radical initiator as a means of determining termination rate parameters. In addition, the development of a composite map

incorporating the coupling effects of conversion and chain length on the termination rate coefficient will be investigated. A study of this nature is of considerable interest because of the need for accurate and reliable rate parameters for ATRP and other radical polymerizations.

Chapter 1 reported on the recent activities in the literature with respect to controlled/living radical polymerization including NMP, RAFT and ATRP. In addition, an overview of the techniques used to determine rate parameters has been discussed.

Chapter 2 describes the methodology and materials used to carry out the experiments and analyze data. More specifically a detailed procedure describing the polymerization preparation and reaction conditions are outlined. The characterization methods employed are discussed including gel permeation chromatography (GPC) and nuclear magnetic resonance (NMR).

Chapter 3 will discuss the experimental results and analysis of the studies involving rate enhanced ATRP at high free radical loadings. Additionally, results of the determination of termination rate coefficient study will also be discussed in great detail. Finally, in Chapter 4, conclusions are offered and recommendations about future work are discussed.

CHAPTER 2

EXPERIMENTAL MATERIALS & METHODOLOGY

2.1. Materials

Methyl methacrylate (MMA) (99.9%, Aldrich) was used in all of the polymerizations. It was dried over CaH_2 and distilled under vacuum to remove any impurities as well as the inhibitor and then stored in the freezer before use. *N,N,N',N'',N''*-Pentamethyldiethylenetriamine (PMDETA, 99%) and methyl α-bromophenylacetate (MBP, 97%) were used as received from Aldrich. Toluene was distilled from CaH_2. 2,2'-Azobis(isobutyronitrile) (AIBN) was recrystallized using the following procedure. AIBN was dissolved in an Erlenmeyer flask containing methanol at 50°C. Once dissolved completely, the flask was put in an ice bath for approximately 25 minutes until AIBN crystallites were formed. The solid/liquid mixture was then poured into a hirsch funnel lined with filter paper where the solid cake (AIBN) was removed and dried prior to use. The structures of these aforementioned chemicals are described below in Figure 2.1.

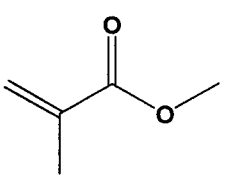

Methyl Methacrylate

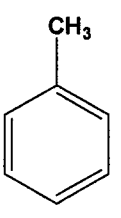

Toluene

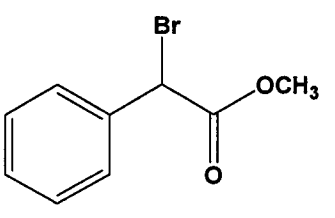

Methyl α-bromophenylacetate

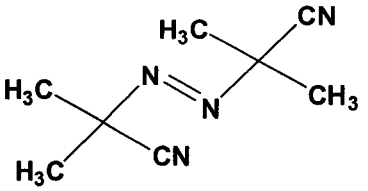

Azobisisobutyronitrile

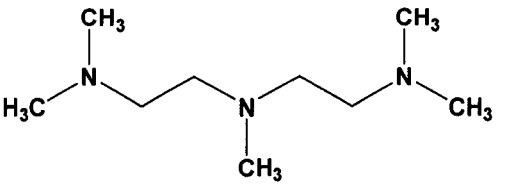

N,N,N',N'',N''-Pentamethyldiethylenetriamine

Figure 2.1: Chemical structures of the reagents and solvent used in the experiments

2.2. Experimental Procedures

2.2.1. Polymerization Procedures

Separate glass vessels filled with toluene, MMA, MBP and PMDETA were sealed with a rubber septum and secured with copper wire. These vessels were purged with N_2 for 40 min. In a 100 mL Schlenk flask, various ratios of AIBN and $CuBr_2$ were added along with a magnetic stirrer. The flask was then sealed with a rubber septum and further secured with copper wire, Parafilm, and PVC tape to prevent the potential ingress of air in the reactor. Four vacuum-nitrogen cycles were applied to the vessel containing the AIBN and $CuBr_2$ and then purged with N_2 for an additional 15 min. The toluene, MMA, MBP and PMDETA from their respective purged vessels were then transferred to the Schlenk flask containing the metal salt and AIBN via nitrogen purged stainless steel needles. The resulting mixture was heterogeneous. In a typical polymerization run for 78 ppm Cu, the ratios utilized were as follows: MMA (20 g, 200 mmol), MBP (0.229g, 1 mmol) AIBN (1.64g, 10 mmol), PMDETA (10 μL, 0.05 mmol), $CuBr_2$ (0.0111g,0.05mmol), and toluene (18.4 g). MMA and toluene were used in a volumetric ratio of 1:1 for all of the polymerizations. The flask containing all of the reacting species was then put in an oil bath operated at 70°C with stirring. Samples were taken at various time intervals with

nitrogen purged syringes and transferred to vials, then put in the freezer and used for gel permeation chromatography (GPC) and nuclear magnetic resonance (NMR) spectroscopy analysis.

2.2.1.1 Synthesis of Poly (methyl methacrylate) Macroinitiator

The macroinitiator was synthesized using the procedure described above in Section 2.2.1. More specifically the following recipe was used, MMA (20 g, 200 mmol), MBP (0.229g, 1 mmol), AIBN (0.82g, 5 mmol), PMDETA (10 μL, 0.05 mmol), $CuBr_2$ (0.0111g,0.05mmol), and toluene (18.4 g). MMA and toluene were used in a volumetric ratio of 1:1 at a reaction temperature of 70°C. In addition, the polymerization was carried out to a conversion of ~50%, to ensure that the majority of the living chains were viable. The reacting solution containing residual MMA, PMMA, Toluene, AIBN and the copper catalyst was placed in methanol to precipitate the PMMA out of solution. The PMMA was then decanted, filtered and dried before being re-dissolved in THF. Once re-dissolved the mixture was passed through a column with basic alumina to remove any remaining impurities. The THF/PMMA mixture was reintroduced to a vessel containing methanol to precipitate PMMA out of solution and then subsequently dried.

2.2.1.2 PMMA Chain Extension

Chain extension from the synthesized macroinitiator was performed using the same procedure outlined in Section 2.2.1 but with the following recipe, MMA (29 g, 200 mmol), PMMA macroinitiator (10g, 1mmol), AIBN (1.2 g, 5 mmol), PMDETA (15 μL, 0.05 mmol), $CuBr_2$ (0.0162g,0.05 mmol), and toluene (40 g). MMA and toluene were used in a volumetric ratio of 40:60 at a reaction temperature of 70°C.

2.2.2 Characterization

^{1}H NMR spectra were recorded on a Bruker ARX-200 spectrometer at 200MHz. Samples were diluted in $CDCl_3$ where the chemical shifts were reported downfield from 0.00 ppm using the residual $CHCl_3$ signal at 7.26 ppm as an internal reference. The monomer conversion was determined from the intensity ratio of OCH_3 signals from the polymer and monomer at 3.60 and 3.75 ppm respectively. Polymer molecular weights and polydispersity were determined by GPC. Narrow polystyrene standards were used to calibrate the instrument. A Waters 710 Autoinjector, 410 RI detector, 600 pump system as well as three linear columns in series (Waters Styragel HR 5E, 2 x Shodex KF-804L) were used to perform the experiments. Tetrahydrafuran (THF, HPLC grade) was used as the mobile phase and was pumped through the system at 1mL/min. The temperature of the columns and detector were 35°C and 40°C respectively. The Waters Millennium software package was used to record and analyze the data.

2.3. Procedure for k_t Determination

2.3.1. Estimate k_t from NMR Measurements

Polymerizations were carried out in the manner described in the above section. Monomer conversion was determined by NMR for a series of samples at different time intervals, typically at least 11 data points were collected for each run. A 5th order polynomial function was fitted to the corresponding conversion versus time curve. The rate of polymerization was then determined from this data.

$$\frac{d[R_r\cdot]}{dt} = 2fk_{di}[I]_0 e^{-kd\cdot t} + k_a[Cu^I][P_rX] - k_d[Cu^{II}][R_r\cdot] - 2k_t[R_r\cdot]^2 \quad (2.1)$$

The magnitude of the activation and deactivation rates was assumed to be the same. Therefore Equation 2.1 can be reduced to Equation 2.2. Solving for the termination rate coefficient k_t in Equation 2.2 yields Equation 2.3, where the radical concentration $[R_r\cdot]$ is written in terms of the rate of polymerization.

$$\frac{d[R_r\cdot]}{dt} = 2fk_{di}[I]_0 e^{-kd\cdot t} - 2k_t[R_r\cdot]^2 \qquad (2.2)$$

$$k_t(t) = \frac{2fk_d[I]_0 e^{-k_d t} - \dfrac{d\left(\dfrac{R_p(t)}{k_p([M]_0 - \int_0^t R_p(t)dt)}\right)}{dt}}{2\left(\dfrac{R_p(t)}{k_p([M]_0 - \int_0^t R_p(t)dt)}\right)^2} \qquad (2.3)$$

The initiation parameters used in this study were based on well known literature values for AIBN. An initiator efficiency of 0.70 [20] and the decomposition rate coefficient of 4.01 x $10^{-5}s^{-1}$ were used for AIBN at 70°C.[3] The propagation rate coefficient of 1050 $L\cdot mol^{-1}s^{-1}$ was used for MMA at 70°C.[89]

The corresponding monodisperse chain length was determined using Equation 2.4. In this equation $[RX]_0$, and $[M]_0$ represent the concentrations of ATRP initiator and monomer at t = 0, respectively. Moreover, X is the monomer conversion and [AIBN] represents the free radical initiator concentration. Consequently, the termination rate

coefficient can be effectively determined as a function of the corresponding chain length and conversion data.

$$i(t) = \frac{[M]_0 \cdot X}{[RX]_0 + 2f([AIBN]_0 - [AIBN]_t)} \qquad (2.4)$$

In order to generate an effective plot illustrating these coupling effects on the termination rate coefficient (k_t), the software package Table Curve 3D was employed. The set of data containing k_t, chain length and conversion data were imported into Table Curve 3D software. This data was then fit with a three dimensional Chebyshev function (r^2=1.0), to construct a composite mesh corresponding to the data input range.

2.4. Rate Enhanced ATRP in the Presence of High Free Radical Initiator Experiments

2.4.1 Analysis of GPC Curves

The polymerizations performed in this section follow the same batch procedure described above. Moreover, the characterization tools utilized are common with the other core experimental objective. In this study, the gel permeation chromatography data was used to extract information pertaining to the living characteristics for several polymerizations. The methodology involved taking the data collected from the Millennium software of the GPC and fitting a function that mirrored the left side of data mean. The regions of the GPC curve that were overlapped with the fitted function would be characteristic of polymer chains that grew directly from the ATRP initiator at t = 0 and are represented by the shaded regions in Figure 2.2. In order to quantify the percentage of

these regions, the relative area differences were calculated using a trapezoidal integration technique. It was assumed that the area on the left side of the mean was equal for both the GPC data and the generated function.

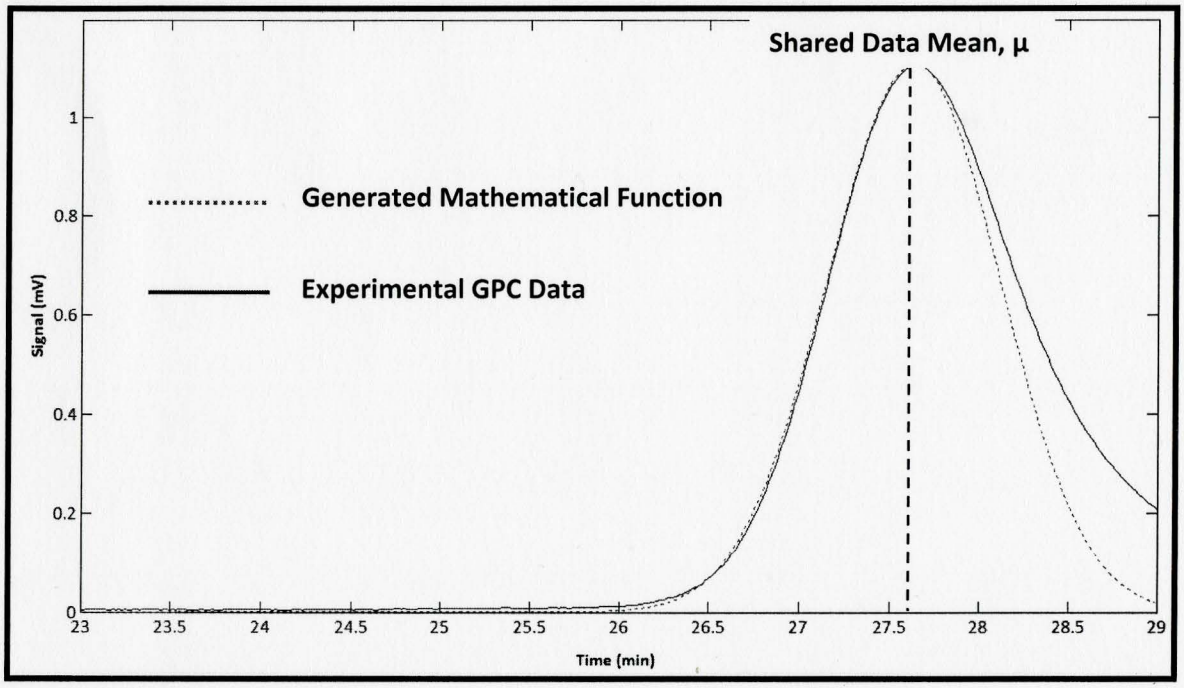

Figure 2.2: Analysis of Gel Permeation Chromatography (GPC) Data

The area representative of the chains derived from the free radical initiator can be determined quantitatively by taking the difference in area on the right side of the mean for the GPC and model function data respectively then dividing it by the total area under the curve. A Matlab program was developed to fit the generated function on the GPC curves and calculate the difference in the areas under the curve, the program is summarized in Appendix A.

2.5. Modelling ATRP Process with a Second Radical Source

A model that takes into account the addition of a second radical source in ATRP was developed. The purpose of this model was to gain further insight into the evolution of molecular weight, polydispersity and reaction kinetics for a system (Scheme 1.11) that has not been studied to date.

2.5.1. Mass Balance Equations

The mass balance equations (2.5-2.12) for a batch reaction are shown below for the living, dormant and dead chains. In this model, M, P_rX, R_r,C, and XC are the monomer, dormant chain, living chain, catalyst, and oxidized catalyst.

Living Chains:

$$\frac{d[R_r]}{dt} = 2fk_{di}[I] + k_p[R_{r-1}][M] - k_p[R_r][M] - k_d[R_r][XC] + k_a[P_rX][C] - k_t\sum_{r=0}^{r=\infty}[R_r][R_r] - k_{tr}[R_r] \quad (2.5)$$

Dormant Chains:

$$\frac{d[P_r]}{dt} = k_d[R_r][XC] - k_a[P_rX][C] \quad (2.6)$$

Monomer:

$$\frac{d[M]}{dt} = -k_p[M]\left(\sum_{r=0}^{r=\infty}[R_r]\right) \quad (2.7)$$

Oxidized Catalyst:

$$\frac{d[XC]}{dt} = k_a[C]\left(\sum_{r=0}^{r=\infty}[P_rX]\right) - k_d[XC]\left(\sum_{r=0}^{r=\infty}[R_r]\right) \quad (2.8)$$

Reduced Catalyst:

$$\frac{d[C]}{dt} = k_d[XC]\left(\sum_{r=0}^{r=\infty}[R_r]\right) - k_a[C]\left(\sum_{r=0}^{r=\infty}[P_rX]\right) \tag{2.9}$$

Termination via Disproportionation:

$$\frac{d[TD_r]}{dt} = k_{td}\left[\sum_{r=0}^{r=\infty}R_r\right]\left[\sum_{r=0}^{r=\infty}R_r\right] + k_{tr}\left[\sum_{r=0}^{r=\infty}R_r\right] \tag{2.10}$$

Termination via Combination:

$$\frac{d[TC_r]}{dt} = \frac{k_{tc}}{2}\left(\sum_{r=0}^{r=\infty}[R_r]\right)\left(\sum_{r=0}^{r=\infty}[R_r]\right) \tag{2.11}$$

Free Radical Initiator:

$$\frac{d[I]}{dt} = -k_{decomp}[I] \tag{2.12}$$

2.5.2 Method of Moments

To follow the development of the number- and weight-average molecular weights, the method of moments was used. The moments of radical, dormant, and terminated chains are defined by Equation 2.13.

$$\begin{aligned} Y_i &= \sum_{r=0}^{\infty} r^i[R_r] \\ Q_i &= \sum_{r=0}^{\infty} r^i[P_r] \\ X_i &= \sum_{r=0}^{\infty} r^i[TC_r] \\ Z_i &= \sum_{r=0}^{\infty} r^i[TD_r] \end{aligned} \tag{2.13}$$

Zero Order:

$$\frac{dY_0}{dt} = 2fk_{decomp}[I] + k_a[C]Q_0 - k_d[XC]Y_0 - k_tY_0Y_0 - k_{tr}Y_0 \quad (2.14)$$

$$\frac{dQ_0}{dt} = k_d[XC]Y_0 - k_a[C]Q_0 \quad (2.15)$$

$$\frac{dX_0}{dt} = \frac{k_{tc}}{2}Y_0Y_0 \quad (2.16)$$

$$\frac{dZ_0}{dt} = k_{td}Y_0Y_0 + k_{tr}Y_0 \quad (2.17)$$

First Order :

$$\frac{dY_1}{dt} = k_p[M]Y_0 - k_a[C]Q_1 - k_d[XC]Y_1 - k_tY_0Y_1 - k_{tr}Y_1 \quad (2.18)$$

$$\frac{dQ_1}{dt} = k_d[XC]Y_1 - k_a[C]Q_1 \quad (2.19)$$

$$\frac{dX_1}{dt} = k_{tc}Y_1Y_0 \quad (2.20)$$

$$\frac{dZ_1}{dt} = k_{td}Y_1Y_0 + k_{tr}Y_1 \quad (2.21)$$

Second Order:

$$\frac{dY_2}{dt} = 2k_p[M]Y_1 + k_p[M]Y_0 + k_a[C]Q_2 - k_d[XC]Y_2 - k_tY_0Y_2 - k_{tr}Y_2 \quad (2.22)$$

$$\frac{dQ_2}{dt} = k_d[XC]Y_2 - k_a[C]Q_2 \quad (2.23)$$

$$\frac{dX_2}{dt} = k_{tc}(Y_0 Y_2 + Y_1 Y_1) \tag{2.24}$$

$$\frac{dZ_2}{dt} = k_{td} Y_2 Y_0 + k_{tr} Y_2 \tag{2.25}$$

2.5.3. Matlab Program: ATRP with a Second Radical Source

The differential equations with the corresponding Matlab declaration variables:

$$\frac{dY_0}{dt} = V_1 \qquad \frac{dY_1}{dt} = V_3 \qquad \frac{dY_2}{dt} = V_5 \qquad \frac{d[M]}{dt} = V_7$$

$$\frac{dQ_0}{dt} = V_2 \qquad \frac{dQ_1}{dt} = V_4 \qquad \frac{dQ_2}{dt} = V_6 \qquad \frac{d[XC]}{dt} = V_8$$

$$\frac{dX_0}{dt} = V_{10} \qquad \frac{dX_1}{dt} = V_{11} \qquad \frac{dX_2}{dt} = V_{12} \qquad \frac{d[I]}{dt} = V_9$$

$$\frac{dZ_0}{dt} = V_{13} \qquad \frac{dz_1}{dt} = V_{14} \qquad \frac{dZ_2}{dt} = V_{15}$$

The corresponding the Matlab program is shown in Appendix B.

CHAPTER 3

RESULTS AND DISCUSSION

3.1. Enhancing Reaction Kinetics in ATRP at Low Catalyst Concentrations

One of the core objectives of this project was to increase the reaction kinetics of ATRP through the addition of an external radical source. The idea is to design a hybrid reaction system incorporating the fast reaction rates associated with free radical polymerization while combining it with the controllability features of ATRP. The development of such a system is of considerable interest from an industrial perspective, as the reaction kinetics of most ATRPs are much slower than current free radical processes. Very few studies to date have addressed this key issue of practicality, which is the main motivation behind this work.

3.1.1. Simulated Experimental Results for a Rate Enhanced ATRP at Low Catalyst Concentrations

Table 3.1: Parameters and Initial Conditions for the ATRP of MMA in Solution

Parameter	Value	Reference or Comments
k_{di} (s^{-1})	4.01×10^{-5}	25
k_d ($L \cdot mol^{-1} \cdot s^{-1}$)	5.40×10^{7}	59
k_a ($L \cdot mol^{-1} \cdot s^{-1}$)	2.70	65
k_{tc} ($L \cdot mol^{-1} \cdot s^{-1}$)	7.25×10^{6}	3
k_{td} ($L \cdot mol^{-1} \cdot s^{-1}$)	2.175×10^{7}	3
k_t ($L \cdot mol^{-1} \cdot s^{-1}$)	2.90×10^{7}	90
k_p ($L \cdot mol^{-1} \cdot s^{-1}$)	1050	89
k_{tr} (s^{-1})	0.048	91
F	0.70	16
T(°C)	70	
$[M]_0$ ($mol \cdot L^{-1}$)	4.67	
$[R\text{-}X]_0$ ($mol \cdot L^{-1}$)	0.0234	

The development of a mathematical model describing the reaction conditions for an ATRP of MMA with a second radical source was particularly important since it provided much needed insight into the reaction kinetics and molecular weight behaviour of such systems. Firstly, a series of simulations elucidating the effects of increasing free radical initiator concentrations was generated and is shown in Figure 3.1. At low free radical initiator loadings (0.00234M), the model predicts a long induction time of nearly 2 hours corresponding to the slow deactivation of Cu^{II} to its activation state (Cu^{I}). The predicted reaction rate is slow, achieving 90% conversion in approximately 19 hours. Increasing the free radical initiator concentration by a factor of 10 (0.0234 M) results in a

considerable increase in the reaction rate such that high conversions can be reached in 3-4 hours. A further increase in free radical initiator concentration by a factor of 5 and 10 resulted in even faster reaction kinetics where 90% monomer conversion can be achieved in 2 hours.

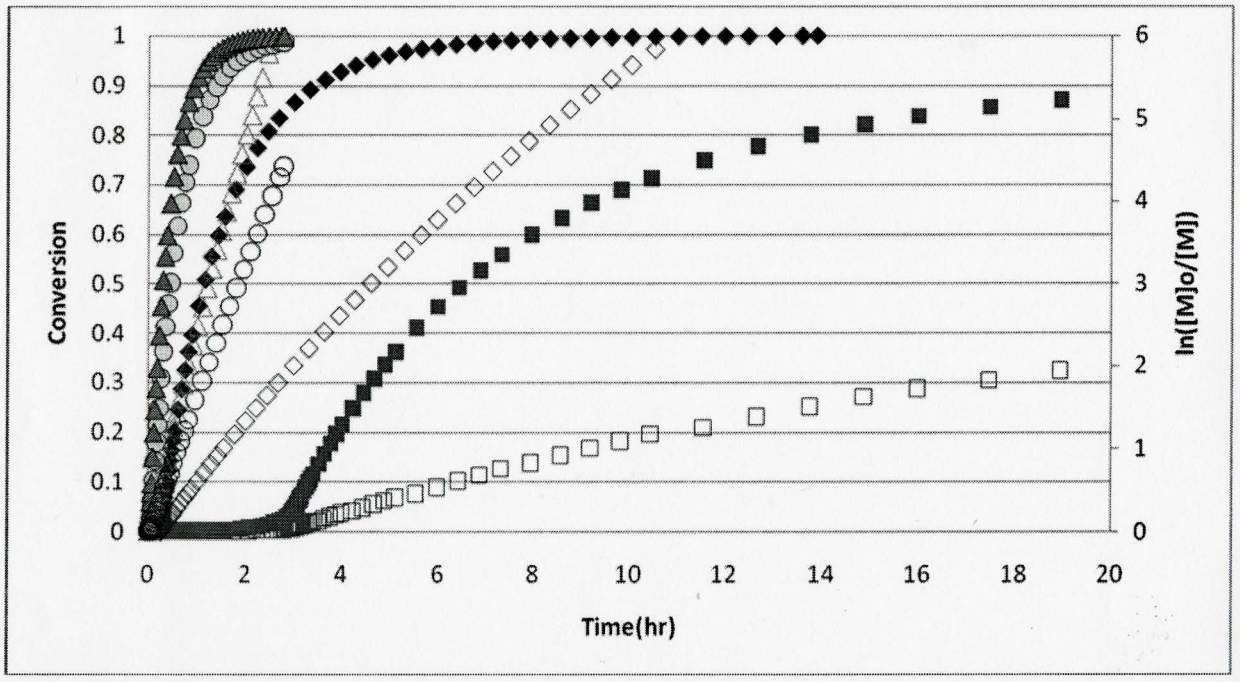

Figure 3.1. Simulated monomer conversion vs. time and First Order Rate Plot for the ATRP of MMA with Varying Free Radical Initiator Concentrations: [MMA]:[MBP]:[AIBN]:[$CuBr_2$]:[PMDETA]=(4.67:0.0234:n:0.00117: 0.00117M), n=0.00234M (□,■), n=0.0234M(◇,◆), n=0.117 M(○,●), n=0.234M (△,▲), 50% Toluene(v/v), T=70˚C, Closed Symbols Boxes Represent Conversion Axis, Open Symbols Represent (ln[M]o/[M]) Axis

The addition of a second radical source has a significant effect on the molecular weight and the polydispersity as shown in Figure 3.2. The model predictions demonstrate that increasing the free radical initiator concentration as expected would result in an overall decrease in the average molecular weight. When the simulations are run with a low concentration of free radical initiator (0.00234M) the polymerization is projected to

be well controlled with a low polydispersity of 1.05. In addition, the evolution of the molecular weight is characteristic of living systems growing linearly as a function of conversion. Increasing the free radical initiator concentration 10 fold (0.0234M) yields a molecular weight function that increases in a linear fashion with conversion before exhibiting a noticeable decrease in the average molecular weight at high conversions (85%). The decrease in the molecular weight can be attributed to the growing influence of continuously generated free radicals which are acting as new active sites. The model predicts that the polydispersity in this case will remain relatively low at 1.30. When higher free radical initiator loadings are modeled the molecular weight grows in a living manner for the majority of the conversion regime however, it experiences a downward trend again at higher conversions. High polydispersities (>1.50) are predicted by the model when high free radical initiator concentrations are employed.

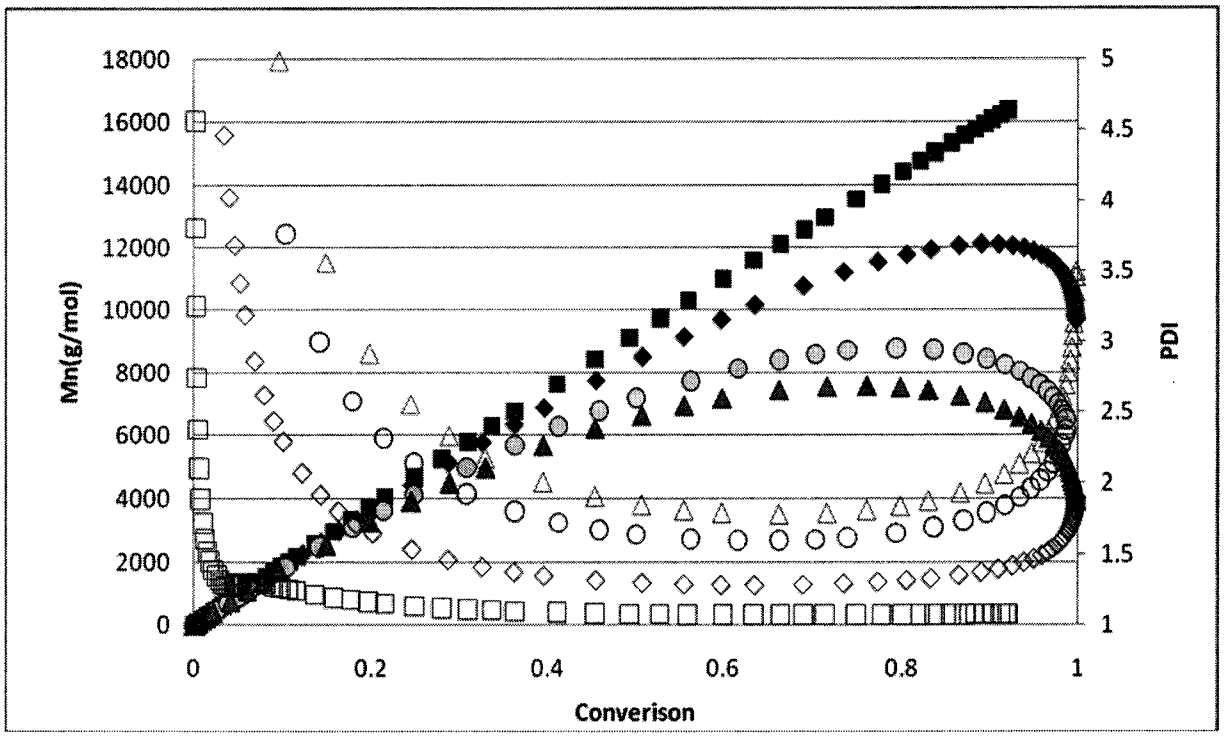

Figure 3.2: Simulated Number Average Molecular Weight and PDI vs. Conversion at various Free Radical Initiator Concentrations [MMA]:[MBP]:[AIBN]:[$CuBr_2$]:[PMDETA]=(4.67:0.0234:n:0.00117: 0.00117M), n=0.00234M (□,■), n=0.0234M(◇,◆), n=0.117 M(○,●), n=0.234M (△,▲), 50% Toluene(v/v), T=70°C, Closed Symbols Boxes Represent Mn Axis, Open Symbols Represent PDI Axis

Additional simulations were performed to obtain greater insight into the projected reaction behaviour of an ATRP system, with a fixed high free radical initiator loading (0.234M) at various copper concentrations. The modelled reaction kinetics of such a system are shown below in Figure 3.3. When high catalyst concentrations (4.67mM) are employed in the simulation, the reaction rate is projected to be slightly slower than when lower catalyst concentrations are used. The high concentration of deactivating species (Cu^{II}) initially present hinders the rate of reaction momentarily until sufficient amounts of activating agents (Cu^{I}) are generated. A reduction in the catalyst concentration by a

factor of 4, 20 and 200 has no apparent influence on the rate of polymerization. In fact, the rate of polymerization at low catalyst loadings is solely governed by the free radical initiator concentration and its corresponding reaction parameters.

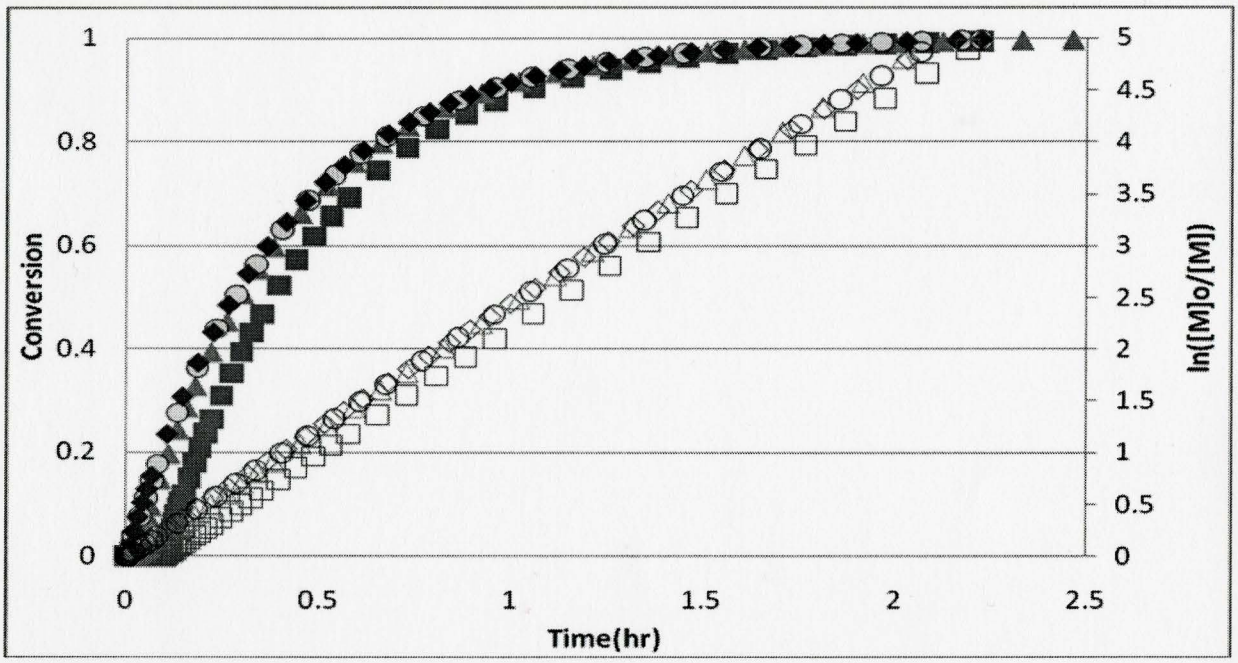

Figure 3.3: Simulated monomer conversion vs. time and First Order Rate Plot for the ATRP of MMA with Varying Catalyst Concentrations: [MMA]:[MBP]:[AIBN]:[$CuBr_2$]:[PMDETA]=(4.67:0.0234:0.234:n: 0.00117M), n=4.67mM (□,■), n=1.17mM(△,▲), n=0.234m M(○,●), n=0.0234mM (◇,◆), 50% Toluene(v/v), T=70°C, Closed Symbols Boxes Represent Conversion Axis, Open Symbols Represent (ln[M]o/[M]) Axis

Reductions in the catalyst concentration do not have a considerable effect on the reaction rate, however, the same cannot be said in regards to the molecular weight and polymer molecular weight distribution as demonstrated in Figure 3.4. The polymer molecular weight distribution becomes narrower with increasing catalyst loadings. For instance, at the lowest catalyst loading of 0.0234mM the model projects a polydispersity value greater than 4, while a high catalyst loading of 4.67 mM yields a PDI of ~1.40.

Molecular weight development of the various cases are similar, however, when higher catalyst concentrations are used (0.234mM & 0.0234mM) molecular weights are slightly lower. This is attributed to the slower reaction kinetics initially experienced at higher catalyst loadings. That is at a given conversion the number of active sites present is slightly greater thus causing the average molecular weight to be lower. The mathematical modelling demonstrated in this section provides greater insight into the projected reaction behaviour for ATRP systems with a second radical source. Experimental studies investigating the reaction conditions simulated in this section were performed and are discussed in the following sections.

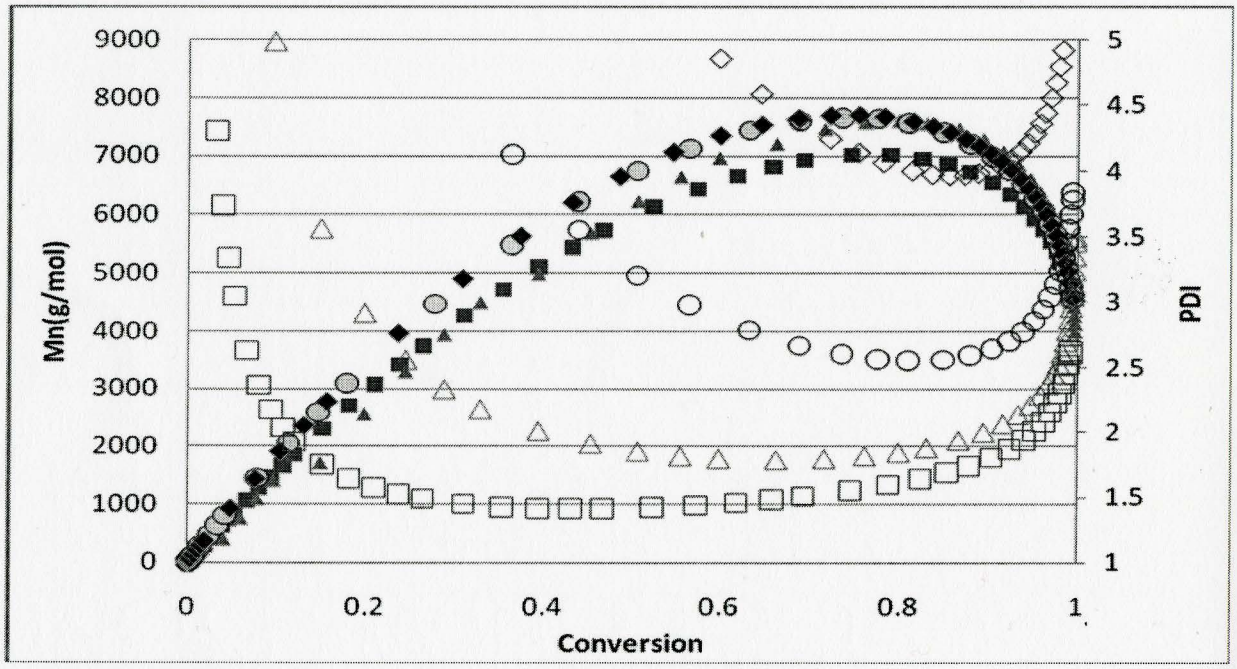

Figure 3.4: Simulated Number Average Molecular Weight and PDI vs. Conversion at various Catalyst Concentrations
[MMA]:[MBP]:[AIBN]:[$CuBr_2$]:[PMDETA]=(4.67:0.0234:0.234:n: 0.00117M), n=4.67mM (□,■), n=1.17mM(△,▲), n=0.234m M(○,●), n=0.0234mM (◇,◆), 50% Toluene(v/v), T=70°C, Closed Symbols Boxes Represent Mn Axis, Open Symbols Represent PDI Axis

3.1.2. Experimental Reaction Kinetics

Increasing the free radical initiator concentration in concert with ATRP was investigated through a series of batch experiments that are shown in Table 3.2. The free radical initiator concentration had a considerable effect on the apparent rate constant (k_{app}) defined by Equation 3.1. For example, Entry 1 in Table 3.2 represents the case where the lowest concentration of AIBN was used at a 0.1 molar ratio (0.00234M). This low free radical initiator concentration (0.00234 M) is the amount that is typically administered in ICAR ATRP systems, and this results in slow reaction kinetics reaching 48% conversion in just over 8 hours ($k_{app} = 2.5 \times 10^{-5}\ s^{-1}$). Furthermore, this particular reaction reached 70% conversion in about 22 hours. The reaction rate decreased significantly once the free radical initiator was completely consumed after 10 hours. Consequently, the polymerization began to accumulate a larger amount of persistent radicals (deactivators) that reduced the reaction rate as there was a deficiency in activating species to drive the polymerization.

$$R_p = k_p[R\cdot][M] = k_{app}[M] \qquad (3.1)$$

When the free radical initiator concentration was increased by a factor of 10 (Entry 2, Table 3.2) to a concentration of 0.0234 M, there was an increase in the apparent rate constant ($k_{app} = 7.8 \times 10^{-5} s^{-1}$) and the reaction achieved 76% conversion in over 5 hours. Increasing the free radical concentration further by a factor of 5 and 10 (Entries 3, 4, Table 3.2) resulted in conversions of 81% ($k_{app} = 2.6 \times 10^{-4}$) and 91% ($k_{app} = 3.6 \times 10^{-4}$) respectively in just over two hours. These high free radical initiator concentrations of

0.117 M (Entry 3, Table 3.2) and 0.234 M (Entry 4, Table 3.2) resulted in reaction rates that are more than an order of magnitude greater than the reaction kinetics obtained for the ICAR ATRP case (Entry 1, Table 3.2). The first order rate plots of the cases described in Table 3.2 are shown in Figure 3.5. It should be noted that reaction rates obtained in this study are amongst the fastest in the literature. Moreover, the data presented also yielded another interesting finding that unlike SR&NI ATRP and other ATRP processes, the reaction rate here was governed by the free radical initiation parameters. This finding is highly advantageous because it allows for a great deal of versatility in the design of the polymerization system since the reaction rates can then be identical to those experienced in free radical polymerization while harnessing the attractive features of ATRP.

Table 3.2: Effect of increased initiator concentration on ATRP

						Molar Ratios				
Entry	**t(min)**	**PDI**	**X**	**$Mt_{(ppm)}$**	**κ_{app} (1/s)**	**[MMA]**	**[RX]**	**[L]**	**[M_t]**	**[I]**
1	495	1.05	0.48	80	2.5×10^{-5}	200	1	0.05	0.05	0.1
2	310	1.14	0.76	80	7.8×10^{-5}	200	1	0.05	0.05	1
3	120	1.22	0.81	78	2.6×10^{-4}	200	1	0.05	0.05	5
4	120	1.29	0.93	78	3.5×10^{-4}	200	1	0.05	0.05	10

Reaction conditions: Methyl methacrylate (MMA); RX = Methyl α-bromophenylacetate; L = . *N,N,N',N'',N''*-Pentamethyldiethylenetriamine; $M_t = CuBr_2$; I = 2,2'-azobis(isobutyronitrile); 50% Toluene (v/v) ; T = 70°C;

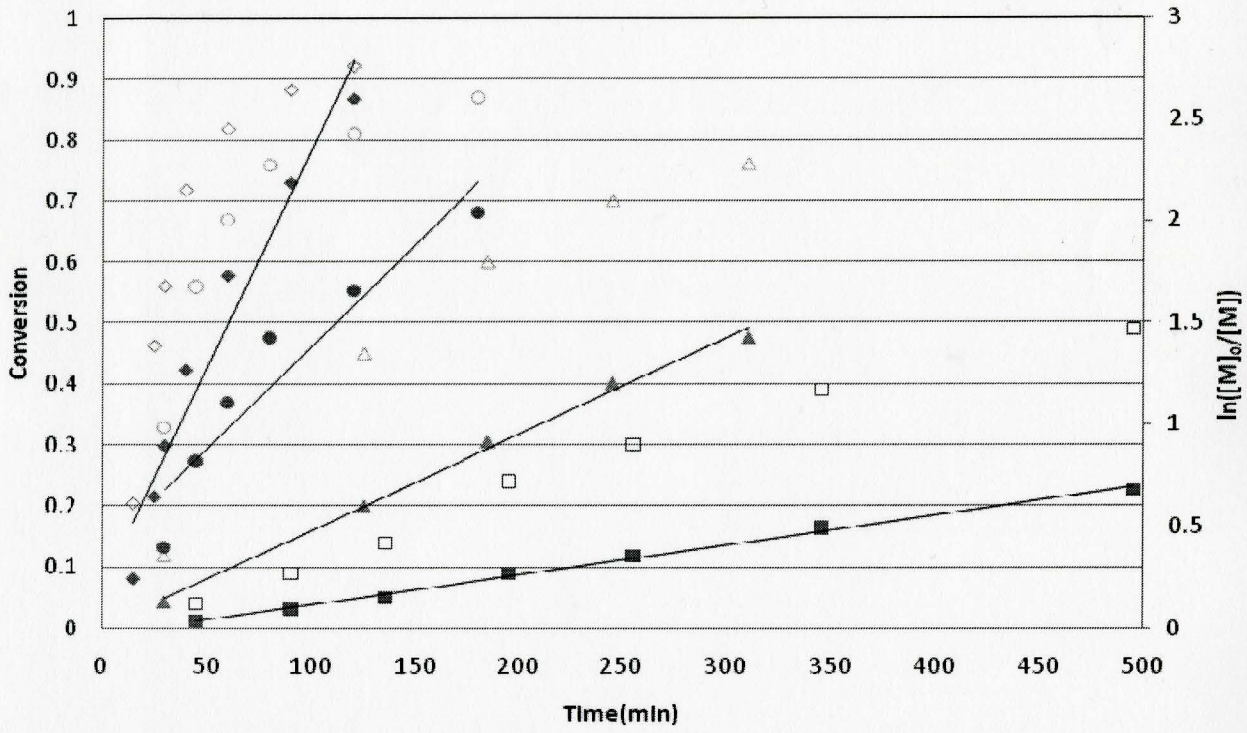

Figure 3.5: Monomer conversion vs. time and first order rate plot for the ATRP of MMA with varying free radical initiator concentrations: [MMA]:[MBP]:[AIBN]:[$CuBr_2$]:[PMDETA]=(4.67:0.0234:n:0.00117: 0.00117M), n=0.00234M (□,■), n=0.0234M(△,▲), n=0.117 M(○,●), n=0.234M (◇,◆), 50% Toluene(v/v), T=70˚C; open symbols represent conversion axis & closed symbols represent the $\ln([M]_0/[M])$axis.

3.1.3. Experimental Molecular Weight Results

The effect of the free radical initiator concentration on the molecular weight and polymer distribution was investigated. When low free radical initiator loadings were administered (0.00234 M), the polymerization was well controlled, as shown in Figure 3.6. The experimental molecular weight grew linearly as a function of conversion, very closely following the theoretical molecular weight curve that is defined in Equation 3.2.

$$Mn_{Theo} = \frac{[M]_0}{([R-X]_0 + 2f([AIBN]_0 - [AIBN]_t))} \cdot MW_{MMA} \times X \qquad (3.2)$$

Additionally, the polymer MW distribution was considerably narrow with a PDI of 1.05. Increasing the initiator concentration 10 fold (0.0234 M) resulted in a decrease in the average molecular weight, but the polymer grew in a linear fashion with respect to increasing monomer conversion. The theoretical molecular weight values were also followed closely by the experimental data, and the polydispersity remained low at 1.15. Increasing the free radical initiator concentration by a further factor of 5 (0.117 M) and 10 (0.234 M), resulted in polymerizations that exhibited living characteristics with molecular weight growing linearly with conversion however, at the expense of the molecular weight distribution polydispersity which increased slightly to 1.22 and 1.30 respectively. Interestingly, in these two extreme cases with high initiator loadings, the theoretical molecular weight curve did not agree well with the experimental data. We believe this behaviour results from a false assumption that the initiator efficiency is constant. It is probable, however, that as the reaction becomes diffusion controlled at higher conversions the initiator efficiency decreases on account of the lower mobility of the primary radicals which are less likely to diffuse outside the solvent cage and participate in the propagation step. Moreover, at high conversions the monomer was less concentrated in the solution thus making the probability of radical recombination even more favourable.

Despite the increased free radical initiator concentration and particularly fast reaction kinetics, the polymerizations continued to demonstrate controlled/living characteristics while achieving relatively narrow molecular weight distributions.

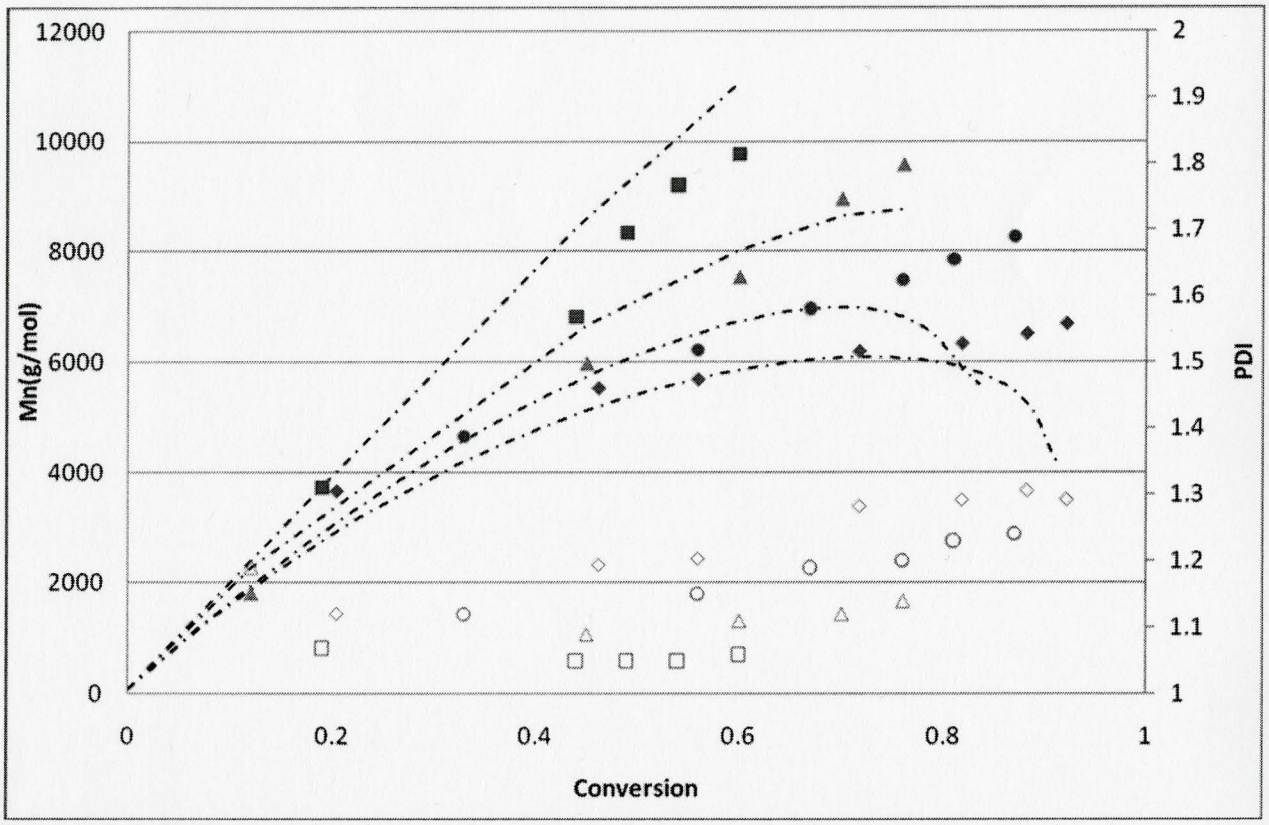

Figure 3.6. PMMA Molecular weight and polydispersity as a function of conversion for varying free radical initiator concentrations: [MMA]:[MBP]:[AIBN]:[$CuBr_2$]:[PMDETA]=4.67:0.0234:**n**:0.00117: 0.00117M, n =0.00234M (□,■), n =0.0234M(△,▲), n =0.117 M(○,●), n=0.234M (◇,◆),Mn_{Theo}(---), f= 0.70, 50% Toluene (v/v), T=70˚C; open symbols Mn axis & closed symbols represent the PDI axis.

3.1.4 Analysis of GPC Curves

In order to characterize and assess quantitatively the amount of polymer chains that were derived from the ATRP initiator at t = 0, and trace their overall influence over the course of the reaction, a unique GPC analysis method was employed. GPC data from a series of different time intervals were obtained for a given polymerization, and were then fit with a mathematical function. The model function would share the same mean value as the GPC data while mirroring the GPC data curve on the left side of the mean.

The total area of the GPC data mirrored by the model function would represent the contribution of the molecular weight that was derived from the ATRP initiator and correspond to the shaded regions in Figures 3.7-3.10, while the non-overlapping region would emulate the fraction of polymer chains that grew from radicals generated from the free radical initiator and denoted as the white area in Figures 3.7-3.10. The plot shown in Figure 3.7 is representative of a sample taken at 46% conversion for a system employing a free radical initiator concentration of 0.0234 M. It is evident from this plot that the majority of the curve is overlapped by the model function which correlates to a high contribution of ATRP initiated polymer chains on the overall molecular weight. Quantifying this region translated into an overall area of nearly 95% as indicated by Figure 3.11A. As the reaction proceeded to 76% conversion in Figure 3.8, it appears that the region correlating with the ATRP initiated polymer chains remained relatively similar. In fact, computing the difference in the two areas under the GPC curve indicate that there was only a slight decrease in the contribution of polymer chains derived from the ATRP initiator on the total molecular weight as the representative region under the GPC curve remained high at 90% (Figure 3.11B).

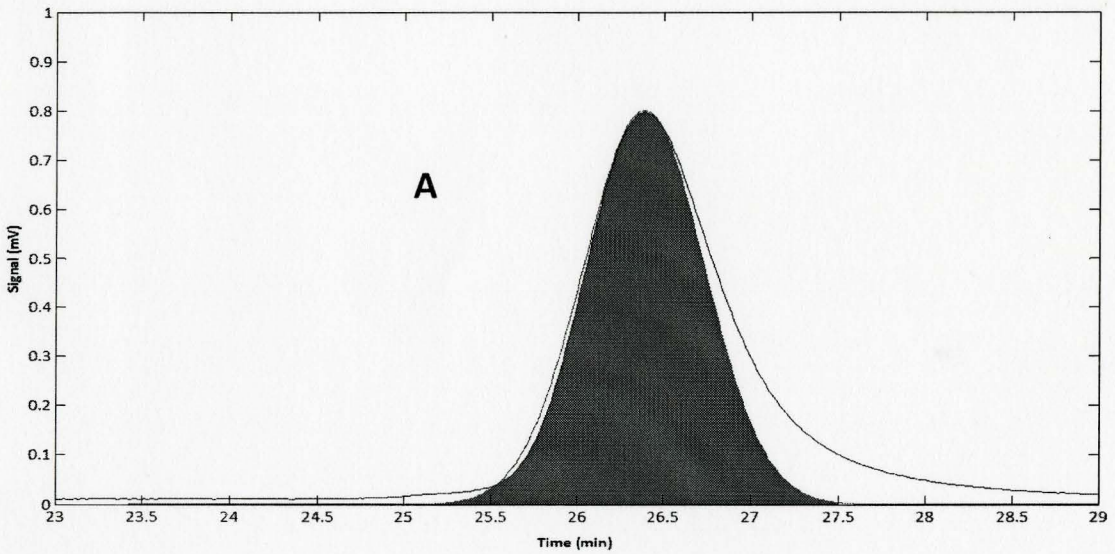

Figure 3.7. Gel Permeation Chromatography (GPC) Plot at 45% monomer conversion, [MMA]:[MBP]:[AIBN]:[$CuBr_2$]:[PMDETA]= (4.67:0.0234:**0.0234**:0.00117: 0.00117M), A model function was fit on an experimental GPC curve to represent the molecular weight contribution of polymer chains derived from the ATRP initiator at t = 0 (dark region) of a the data set. The molecular weight contribution from growing polymer chains from the free radical initiator is represented by the white region.

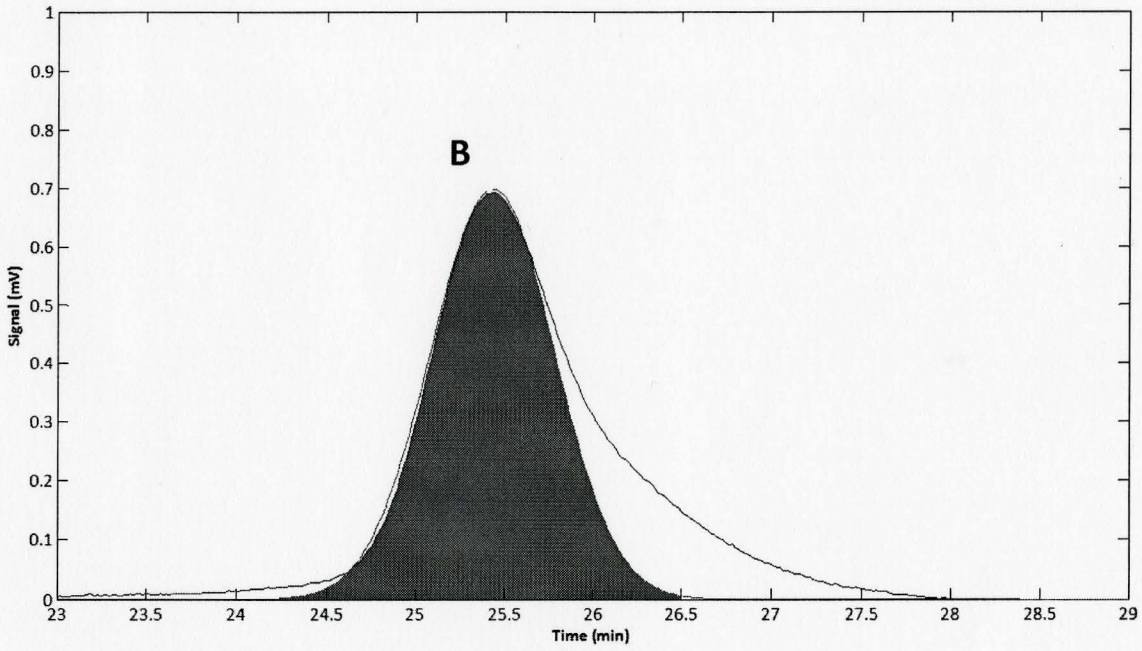

Figure 3.8: Gel Permeation Chromatography (GPC) Plot at 76% monomer conversion, [MMA]:[MBP]:[AIBN]:[$CuBr_2$]:[PMDETA]= (4.67:0.0234:**0.0234**:0.00117: 0.00117M), A model function was fit on an experimental GPC curve to represent the molecular weight contribution of polymer chains derived from the ATRP initiator at t = 0 (dark region) of a the data set. The molecular weight contribution from growing polymer chains from the free radical initiator is represented by the white region.

Increasing the free radical initiator significantly appeared to have a more influential effect on the contribution of the free radical initiated polymer chains on the total molecular weight. For example, Figure 3.9 is representative of the case where extremely high free radical initiator concentrations were administered (0.234 M). At the early stages of the polymerization (21% conversion), the molecular weight is primarily influenced by polymer chains derived from ATRP initiated sites as shown in Figure 3.11C which translated into a total area of 90%.

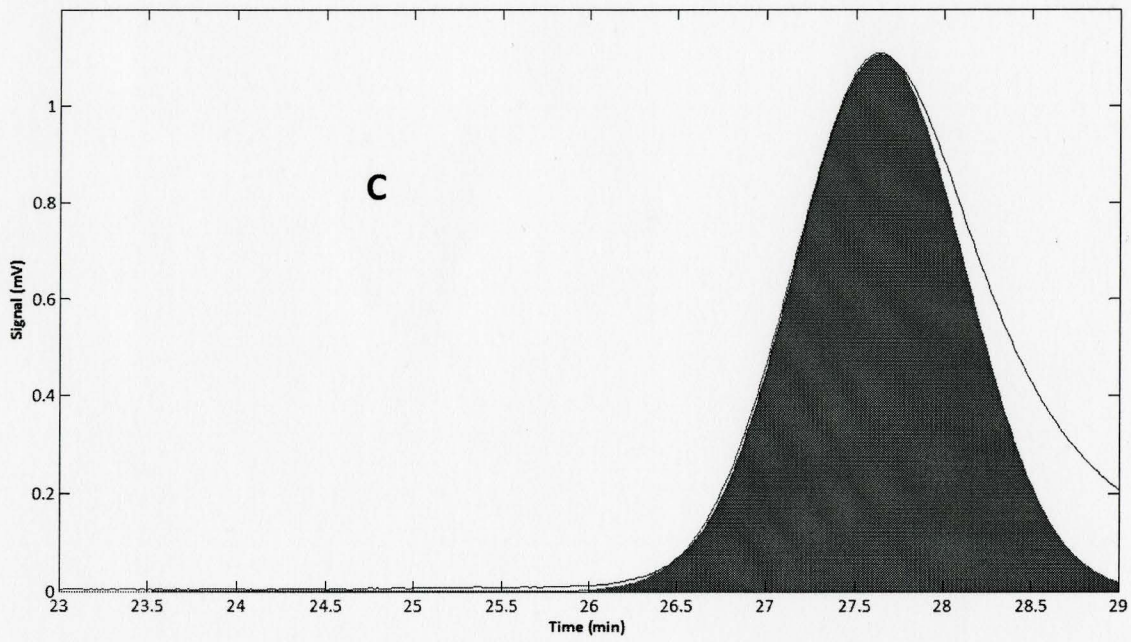

Figure 3.9: Gel Permeation Chromatography (GPC) Plot at 21% monomer conversion, [MMA]:[MBP]:[AIBN]:[$CuBr_2$]:[PMDETA]= (4.67:0.0234:**0.234**:0.00117: 0.00117M), A model function was fit on an experimental GPC curve to represent the molecular weight contribution of polymer chains derived from the ATRP initiator at t = 0 (dark region) of a the data set. The molecular weight contribution from growing polymer chains from the free radical initiator is represented by the white region.

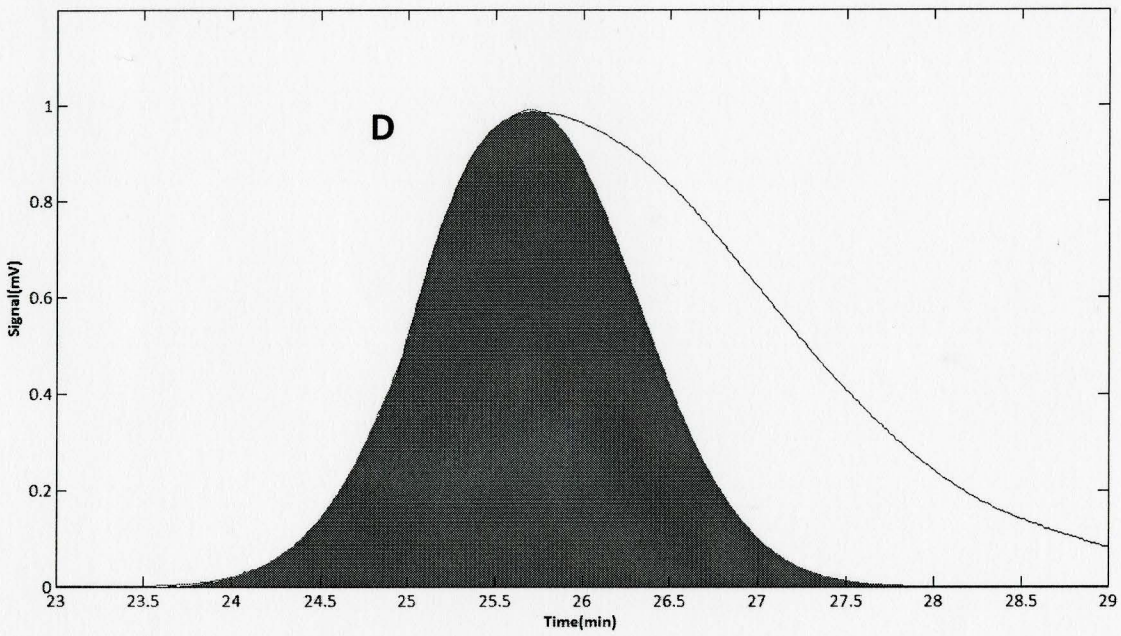

Figure 3.10: Gel Permeation Chromatography (GPC) Plot at 92% monomer conversion, [MMA]:[MBP]:[AIBN]:[$CuBr_2$]:[PMDETA]= (4.67:0.0234:**0.234**:0.00117: 0.00117M), A model function was fit on an experimental GPC curve to represent the molecular weight contribution of polymer chains derived from the ATRP initiator at t = 0 (dark region) of a the data set. The molecular weight contribution from growing polymer chains from the free radical initiator is represented by the white region.

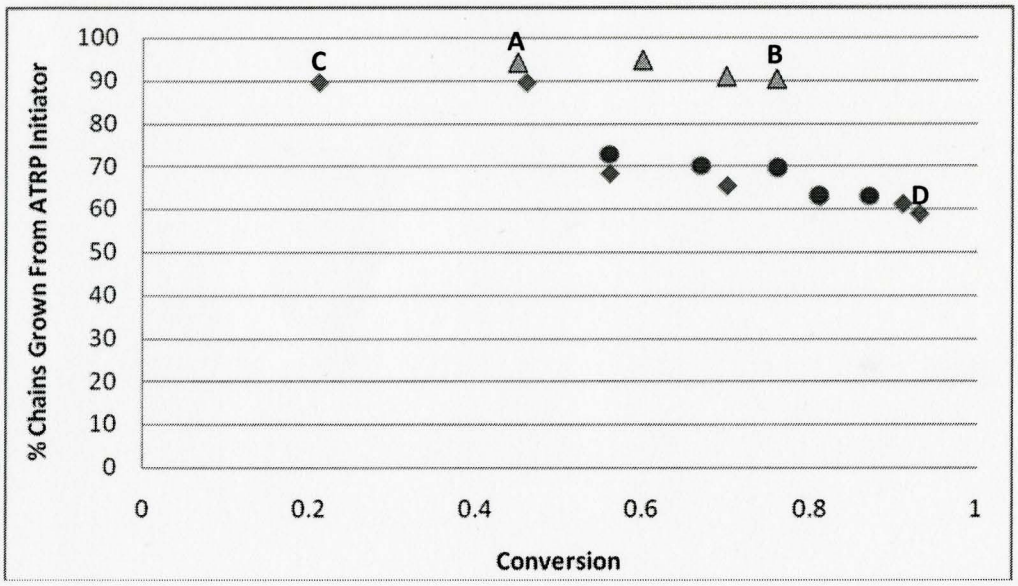

Figure 3.11: Percentage of polymer chains derived from the ATRP Initiator (Figures 3.5,3.6) as function of monomer conversion for the ATRP of MMA with varying free radical initiator concentrations:
[MMA]:[MBP]:[AIBN]:[$CuBr_2$]:[PMDETA]=(4.67:0.0234:n:0.00117: 0.00117 M), n = 23.4 mM(△,▲), n =117 mM(○,●), n = 234 mM (◇,◆), 50 %(v/v) Toluene, T=70˚C

However, as the reaction proceeded to high conversions (92%) as demonstrated in Figure 3.10, there was a clear decrease in the total contribution of ATRP initiated polymer chains on the total molecular weight from ~90% to ~60% (Figure 3.11D). Upon further examination of Figure 3.10 it is apparent that there was an increase in smaller dead chains which contributed to a broader tail end of the GPC curve. This result can also be attributed to the continuous decomposition of free radical initiator throughout the course of the polymerization. The early stages of the polymerization are dominated by growth from the alkyl halide initiator. However, as the reaction proceeds and more radicals are generated from the free radical initiator which results in an increase in the number of new active sites and thus the formation of smaller polymer chains. Model simulations were used to confirm this hypothesis. The kinetic chain length is defined as

the ratio of propagation to termination as expressed in Equation 3.3, where ν is the kinetic chain length and, k_p and k_t are the propagation and termination rate constants.

$$\nu = \frac{k_p[M]}{2k_t[R]} \qquad (3.3)$$

In the model simulations described in Figure 3.12, there was a downward shift in the kinetic chain length with increasing monomer conversion. This trend was more significant however, when high free radical initiator loadings were used. In the most extreme case where 0.234 M (n=10) was administered, the kinetic chain length at 21% conversion was around 110 repeat monomer units, while at 92% conversions the chain length decreased considerably to less than 20. The simulations further reiterated the fact that there was an apparent decrease in kinetic chain length which helps explain the formation of smaller chains and broadening of the GPC curve at higher conversions.

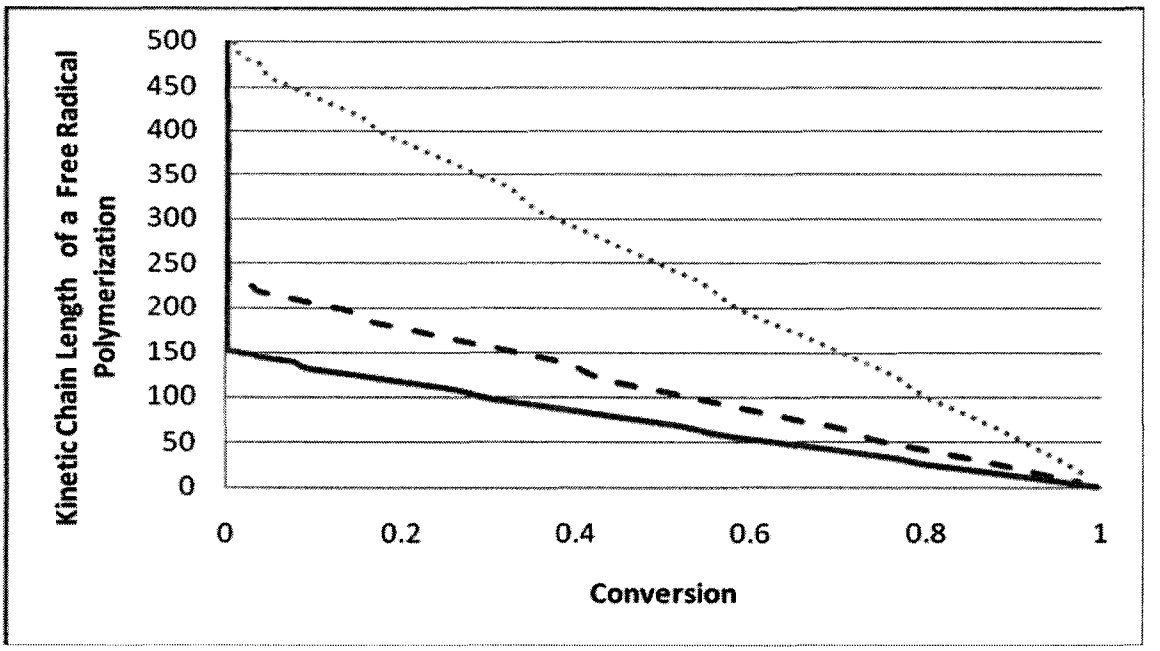

Figure 3.12: Simulated Kinetic Chain Length of Free Radical Polymerization vs. Conversion : ATRP of MMA
[MMA]:[MBP]:[AIBN]:[$CuBr_2$]:[PMDETA]=(200:1:n:0.05:0.05) n = 10 (—) , n = 5 (– –) , n= 1 (····)

3.1.5 Chain Extension from PMMA Macroinitiator

Another key feature of ATRP is the ability to construct complex macromolecular architectures. Chain extension studies are typically used to illustrate the feasibility of fabricating these well defined structures through polymeric growth from a pre-existing living polymer. In this study, a PMMA macroinitiator was synthesized using ATRP in concert with high free radical initiator loadings. The synthesis of the macroinitiator involved a 45 minute polymerization of MMA where the reaction was halted at ~50% conversion to ensure a high percentage of living chains, as previously discussed above in Figure 3.11. The contents from the reacting vessel were placed in methanol where PMMA was precipitated out of solution and filtered. Subsequently, the PMMA

macroinitiator was purified by passing it through a column with basic alumina to remove any impurities. With the macroinitiator prepared, a chain extension polymerization was performed using ATRP with high free radical initiator loadings. The successful chain extension of PMMA from the living macroinitiator was confirmed by GPC measurements and shown in Figure 3.13. The GPC data demonstrates the evolution of increasing molecular weight from the PMMA macroinitiator. For example, initially the macroinitiator has a molecular weight of 6900 g/mol and as the reaction progresses there is a controlled increase in polymeric growth as shown at 41% (M_n = 9700 g/mol) and 63% (M_n = 15300 g/mol) conversions respectively. The data presented in Figure 3.13 confirm the fact that the macroinitiator derived from a rate enhanced ATRP system is living and can thus be used to prepare well defined macromolecular structures.

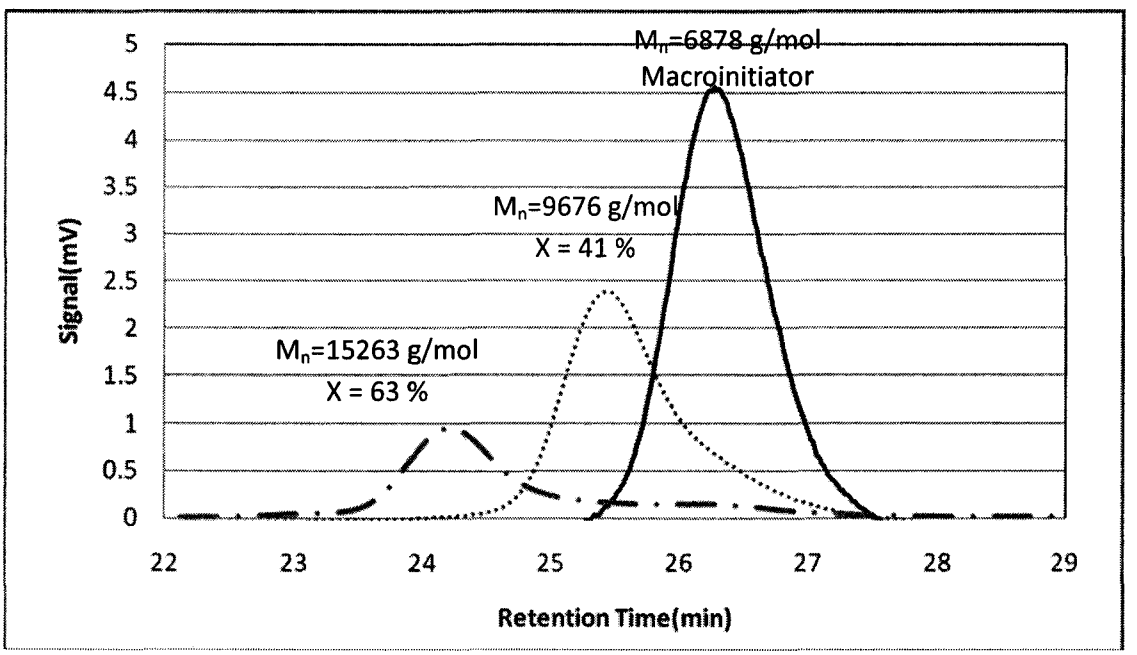

Figure 3.13: Gel Permeation Chromatography (GPC) data showing the molecular weight evolution from the PMMA chain extension, [MMA]:[MI]:[AIBN]:[$CuBr_2$]:[PMDETA]= (3.74:0.019:0.093:0.00093:0.00093M), 60 %(v/v) in Toluene, T=70°C

Once again the GPC data from the chain extension experiments can be used to quantify the portion of polymer chains that have evolved from the prepared macroinitiator throughout the course of the polymerization. For instance, Figure 3.14 and 3.15 shows the molecular weight evolution of the chain extended PMMA at two different conversions. At nearly 41% conversion, the area representative of polymer chains derived from the macroinitiator was approximately 80%.

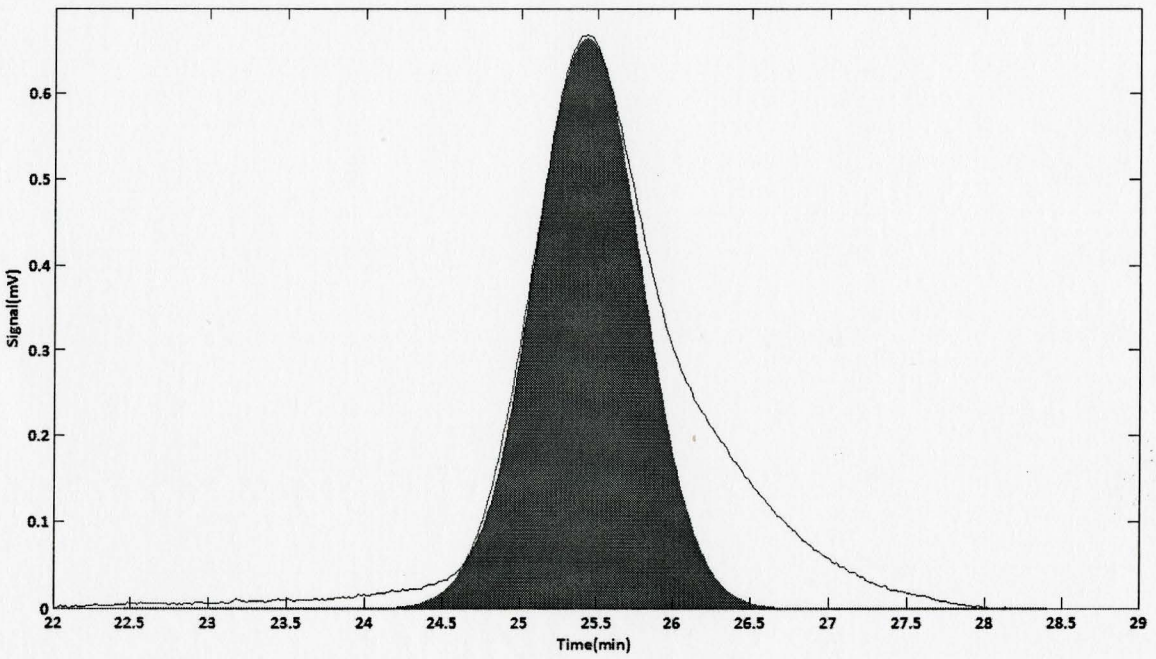

Figure 3.14: Gel Permeation Chromatography (GPC) Plot at 41 % monomer conversion, [MMA]:[MBP]:[AIBN]:[$CuBr_2$]:[PMDETA]= (3.74:0.019:0.093:0.00093:0.00093M A model function was fit on an experimental GPC curve to represent the molecular weight contribution of polymer chains derived from the ATRP initiator at t = 0 (dark region) of a the data set. The molecular weight contribution from growing polymer chains from the free radical initiator is represented by the white region.

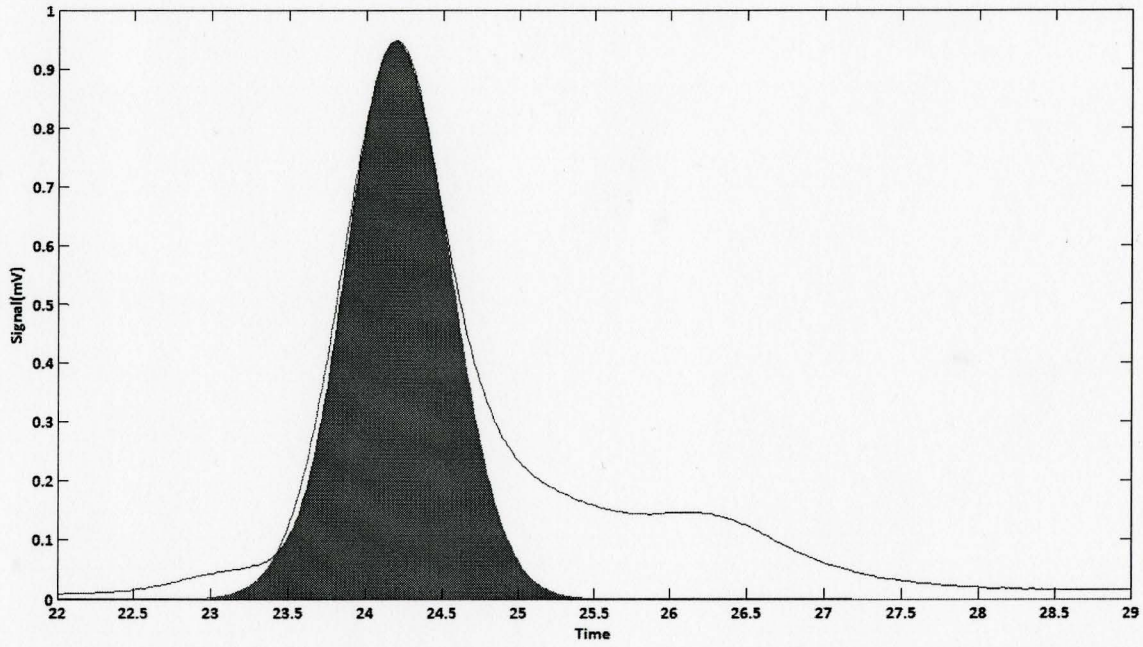

Figure 3.15 Gel Permeation Chromatography (GPC) Plot at 63% monomer conversion, [MMA]:[MBP]:[AIBN]:[$CuBr_2$]:[PMDETA]= (3.74:0.019:0.093:0.00093:0.00093M), A model function was fit on an experimental GPC curve to represent the molecular weight contribution of polymer chains derived from the ATRP initiator at t = 0 (dark region) of a the data set. The molecular weight contribution from growing polymer chains from the free radical initiator is represented by the white region.

As the polymerization progressed further and reached a conversion of 63% (Figure 3.15), one can observe the development of a low molecular tail which can be attributed to the growing influence of the free radical initiator. Under these conditions the kinetic chain length is calculated to be in the range of ~100 to 55 repeat units. The overall contribution however, of polymer chains born from the free radical initiator relative to the total area was 30% indicating that a significant portion of the polymer distribution is continuing to grow from the prepared macroinitiator.

The analysis of these GPC curves provides good insight into the degree of living character that is sacrificed as a result of increasing reaction rates. Ultimately there is a balance here between rate and control. Compromising control for a faster polymerization may be more desirable depending on the application. This method provides an optimization blueprint for the design of ATRP systems in the presence of free radical initiator.

3.1.6. Effect of Catalyst Concentration

Another issue which has slowed the widespread use and applicability of ATRP at the industrial level is the high catalyst loadings that are typically administered to achieve appreciable reaction rates. Consequently, this approach results in costly separation processes to remove the residual catalyst from the final polymer product, which inherently increases the cost of production. The approach we have used in this study reduces catalyst concentrations and possibly eliminates the need for post polymerization purification processes.

A series of experiments were conducted to elucidate the effects of carrying out ATRPs in the presence of free radical initiator at various catalyst concentrations. The results are summarized in Table 3.3.

Table 3.3: Effect of Metal Salt Concentration on an ATRP with a 2nd Radical Source

						Molar Ratios				
Entry	PDI	T (min)	X	$Mt_{(ppm)}$	κ_{app} (1/s)	[MMA]	[RX]	[L]	[Mt]	[I]
1	1.3	120	0.91	328	3.6×10^{-4}	200	1	0.2	0.2	10
2	1.3	120	0.93	78	3.5×10^{-4}	200	1	0.05	0.05	10
3	1.3	120	0.93	16	3.7×10^{-4}	200	1	0.01	0.01	10
4	2.1	60	0.8	2	n/a	200	1	0.001	0.001	10

Reaction conditions: Methyl methacrylate (MMA); RX = Methyl α-bromophenylacetate; L = . *N,N,N',N'',N''*-Pentamethyldiethylenetriamine; $M_t = CuBr_2$; I = 2,2'-azobis(isobutyronitrile); 50% Toluene (v/v) ; T = 70°C; Catalyst Concentration (M_t)ppm =(Mass of Cu/Total Mass of System) x 10^6

The preliminary experiment (Entry 1, Table 3.3) was performed with metal salt loadings characteristic of SR&NI ATRP which corresponds to a 328 ppm Cu concentration. The reaction conditions for the first entry yielded an apparent rate constant of 3.6×10^{-4} s^{-1}. Upon further reduction of the catalyst concentration it was evident that a significant reduction in the metal salt concentration resulted in no decline in the polymerization rate. This finding reiterates what was determined in section 3.1, that only the free radical initiator parameters influence the reaction rate. In fact, the use of 328 ppm of Cu (Entry 1, Table 3.3) resulted in nearly identical reaction kinetics to the polymerization that was carried out at a low metal salt concentration of 16 ppm (Entry 3, Table 3.3). A reduction in the metal salt concentration from 328 to 16 ppm resulted in no significant loss of control as the polydispersity remained constant at 1.30 for Entries 1-3 of Table 3.3. However, the copper concentration cannot be decreased indefinitely because the molecular weight distribution is believed to be governed by Equation 3.4. This is shown in Table 3.3 when the deactivator concentration was too low (2 ppm) and the reaction lost control with a PDI of 2.10. At this copper concentration the amount of effective deactivation sites are insufficient relative to the overall radical population.

$$PD = \frac{M_w}{M_n} = 1 + \frac{k_p [R-X]_0}{k_d [Cu^{II}]} \left(\frac{2}{x} - 1 \right) \qquad (3.4)$$

Another attractive feature of these hybrid ATRP systems is that the concentration of ligand utilized is also significantly low. The ligand is a bulky molecular specie which forms coordination bonds with the transition metal catalyst and acts to improve the solubility of the catalyst in various reaction media and to balance the atom transfer ability of the catalyst. In conventional ATRP systems the amount of ligand administered is nearly 100 times greater than the amount of ligand used in these experiments.[83] This is particularly important because the ligand is usually the most expensive reaction component used in ATRP.

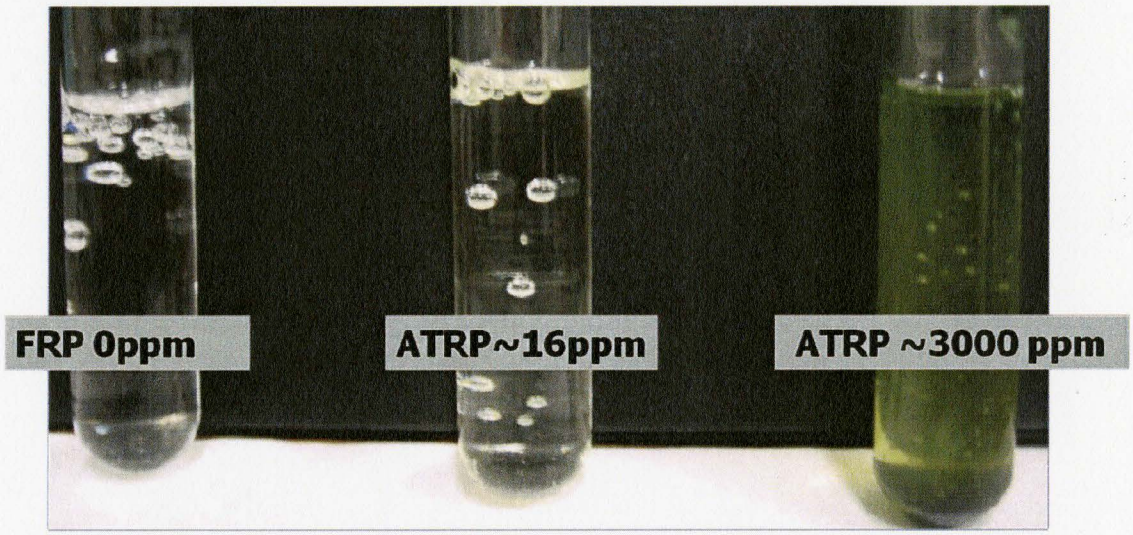

Figure 3.16: Image of post polymerization PMMA samples at different catalyst concentrations

The drastic reduction in the catalyst concentration and accelerated reaction rate experienced in this study is a significant finding. For instance, the reaction rate achieved

in this study with a low copper concentration of 16ppm is an order of magnitude faster than the next most rapid polymerization conducted with a similar diminutive copper concentration.[68] A visual interpretation of residual catalyst concentration remaining in the final product is shown in Figure 3.16. The test tube on the far right depicts the case that is common in most ATRP systems where high catalyst loadings are used. The discolouration of the sample is quite apparent and thus a post polymerization separation process will be necessary to purify the final product. The sample prepared by free radical polymerization on the far left is what the polymer should look like free of catalytic impurities. When the sample was prepared with the method outlined in this study at copper concentrations as low as 16 ppm, it is evident that the sample is nearly identical to that of the free radical polymerization case. In fact, the minute residual catalyst remaining in this sample does not necessitate any further purification steps for most applications, thus increasing the practicality and applicability of this method on a large scale. Therefore, ATRP in the presence of free radical initiator can be used to prepare well-controlled polymers with narrow molecular weight distribution at fast reaction rates without the need for costly separation processes.

3.2. Determination of k_t via NMR Technique

The second core objective of this project is to ascertain termination rate coefficient data from a hybrid ATRP experiment. The considerable interest expressed in the field of living radical polymerization has sparked the need for new reliable termination rate coefficient data to reflect the distinctiveness of these systems. In living systems termination occurs between macroradicals that are virtually the same chain length (i.e $k_t^{i,i}$), since the chain length distribution is nearly monodisperse. In this study we present the 1st NMR based technique to obtain termination rate coefficients using a hybrid ATRP system. A NMR method was used employed because it can track the rate of polymerization for systems with slower reaction kinetics. Other studies using differential scanning calorimetry (DSC) have been well documented, [9, 19, 20] however, they require polymerization systems with faster reaction kinetics, typically in bulk.

A series of ATRP batch polymerizations were carried out at 70°C for MMA in toluene. Samples from these experiments were frequently taken to construct a thorough data set. NMR spectroscopy was performed on each of these samples to obtain the monomer conversion as a function of time as shown in Figure 3.17. Our interest lies in the determination of k_t and its corresponding behaviour with respect to increasing chain length, and conversion. In order to effectively convey the rate of polymerization data for every time interval, a polynomial function was fit to existing data in Figure 3.17. As illustrated in Figure 3.17, the 5th order polynomial fits the data set well ($R^2 = 0.99$).

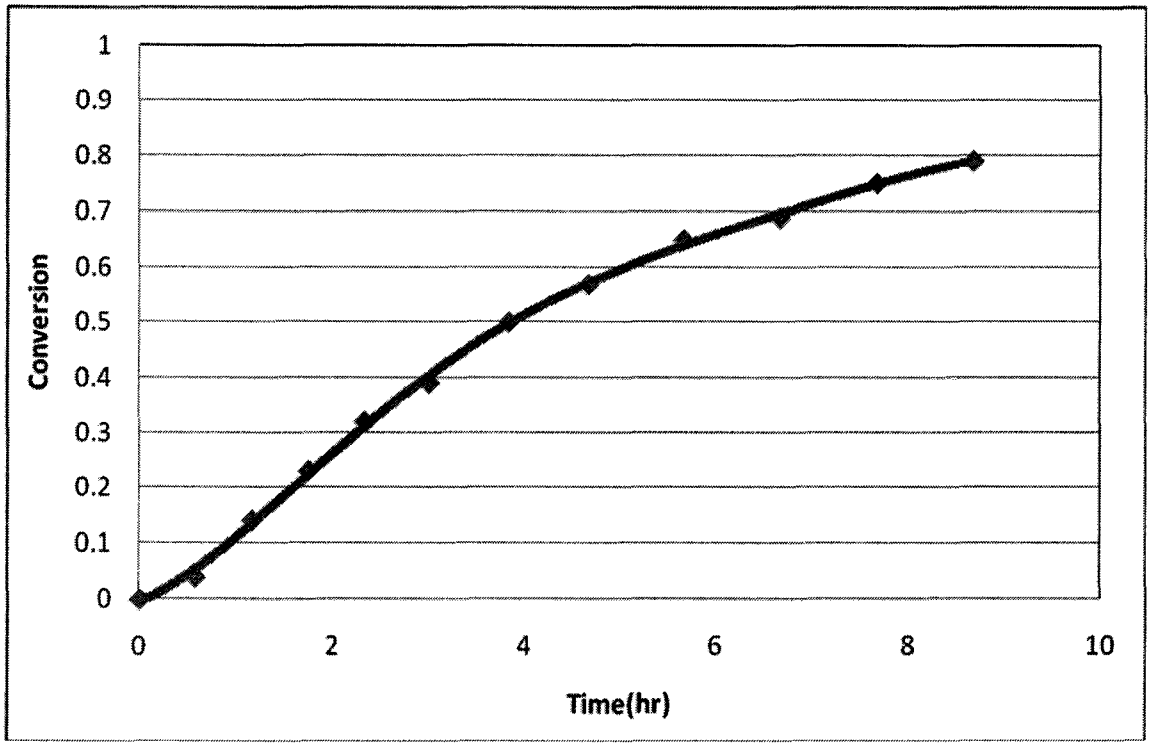

Figure 3.17: Conversion vs. Time plot for the ATRP of MMA in the presence of free radical initiator [MMA]:[MBP]:[AIBN]:[$CuBr_2$]:[PMDETA]=(200:1:0.5:0.05:0.05); experimental data (◆), fitted polynomial function (▬)

The termination rate coefficient and chain length data were then obtained using the methods outlined in Chapter 2. The termination rate coefficient could be obtained directly through the rearrangement of the radical mass balance equation expressed in equation 3.5.

$$k_t(t) = \frac{R_I - \frac{d[R\cdot]}{dt}}{2[R\cdot]^2} = \frac{2fk_d[I]_0 e^{-k_d t} - \frac{d\left(\frac{R_p(t)}{k_p([M]_0 - \int_0^t R_p(t)dt)}\right)}{dt}}{2\left(\frac{R_p(t)}{k_p([M]_0 - \int_0^t R_p(t)dt)}\right)^2} \quad (3.5)$$

The rate of initiation (R_I) terms in this equation are known from literature and the rate of polymerization data are obtained from the conversion vs. time data from the batch experiment (Figure 3.17). The corresponding polymer chain length for these studies was determined using theoretical molecular weight values obtained from Equation 3.6.

$$i(t) = \frac{[M]_0 \cdot X}{[RX]_0 + 2f([AIBN]_0 - [AIBN]_t)} \qquad (3.6)$$

The theoretical chain length was varied by altering the ATRP initiator (MBP) concentrations and keeping the free radical initiator concentration fixed, the subsequent plot is shown in Figure 3.18.

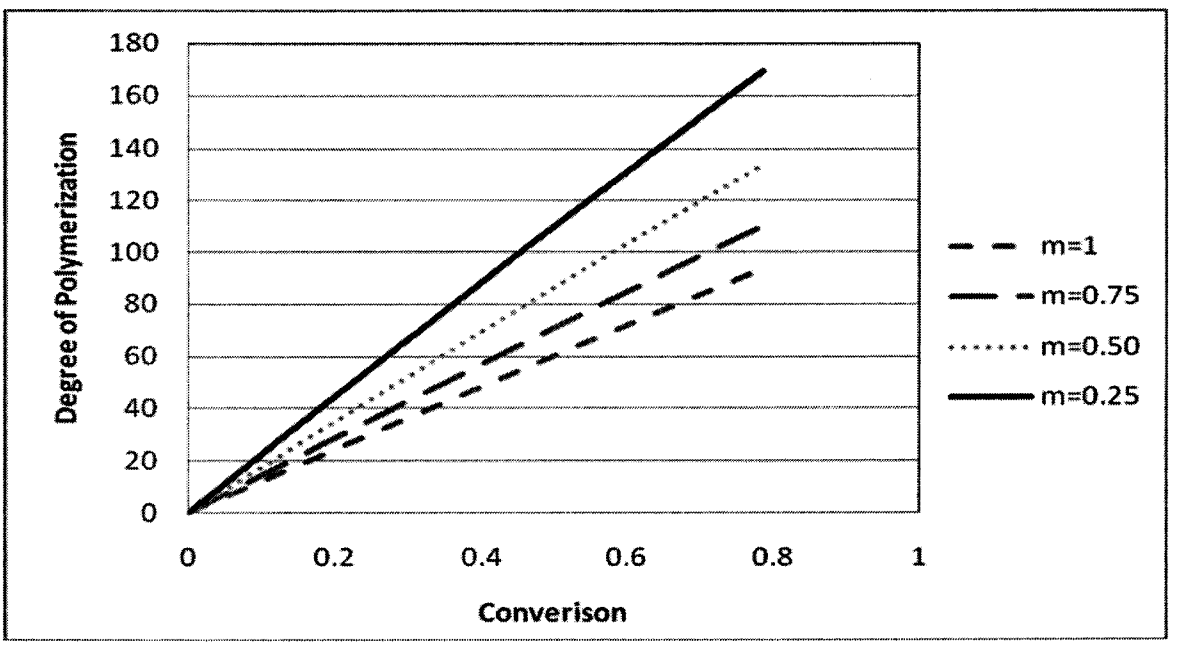

Figure 3.18: Theoretical Degree of Polymerization vs. Conversion plot for the ATRP of MMA in the presence of free radical initiator [MMA]:[MBP]:[AIBN]:[$CuBr_2$]:[PMDETA]=(200:m:0.5:0.05:0.05), Drawn over a conversion range where the initiator efficiency is known to constant (See section 3.1.3)

Recall from Chapter 1, the power law expression (Equation 3.7) which is commonly used to describe the chain length dependent bimolecular termination.

$$k_t^{i,i} = k_t^0 \cdot i^{-\alpha} \quad (3.7)$$

The experimental design of these polymerizations focused on producing polymers with targeted molecular weights associated with the short chain regime (i<100). Other studies of MMA in the short chain regime have yielded α values ranging from 0.50-0.65.[8, 92] The hybrid ATRP of MMA in solution was performed and the corresponding $k_t^{i,i}$ profile as a function of increasing chain length is demonstrated in Figure 3.19. This plot shows that increasing the ATRP initiator results in lower termination rate coefficients. This observed effect can be attributed to the increased viscosity when lower ATRP initiator concentrations are employed which consequently result in lower overall termination rate coefficients. The slope of a log $k_t^{i,i}$ versus log i plot yields $-\alpha$ and an intercept of k_t^0. At a chain length of i=1, the k_t^0 value is approximately ~6 x 10^8 L/mol·s. A distinct feature of this method is that the data pertaining to the first 10 chains of the polymerization can be extracted. Studies employing differential scanning calorimetry (DSC) measurements to obtain online rate of polymerization date are limited with respect to the first 10 polymeric chains since the first 5% conversion of these measurements are not reliable due the initial stabilization of the sample.[20] At higher chain lengths (i~100) the data begins to level off, indicating the transition from center of mass diffusion to segmental diffusion. The short chain regime (i < 100) profiled in this study yielded an average slope of 0.63 obtained from the log kt vs. log i plot and demonstrated in Figure 3.19. It appears to follow the

values that have been reported in the literature. This dependency value (0.63) suggests that the short chain regime of the rate-enhanced ATRP is dominated by the center of mass diffusion.

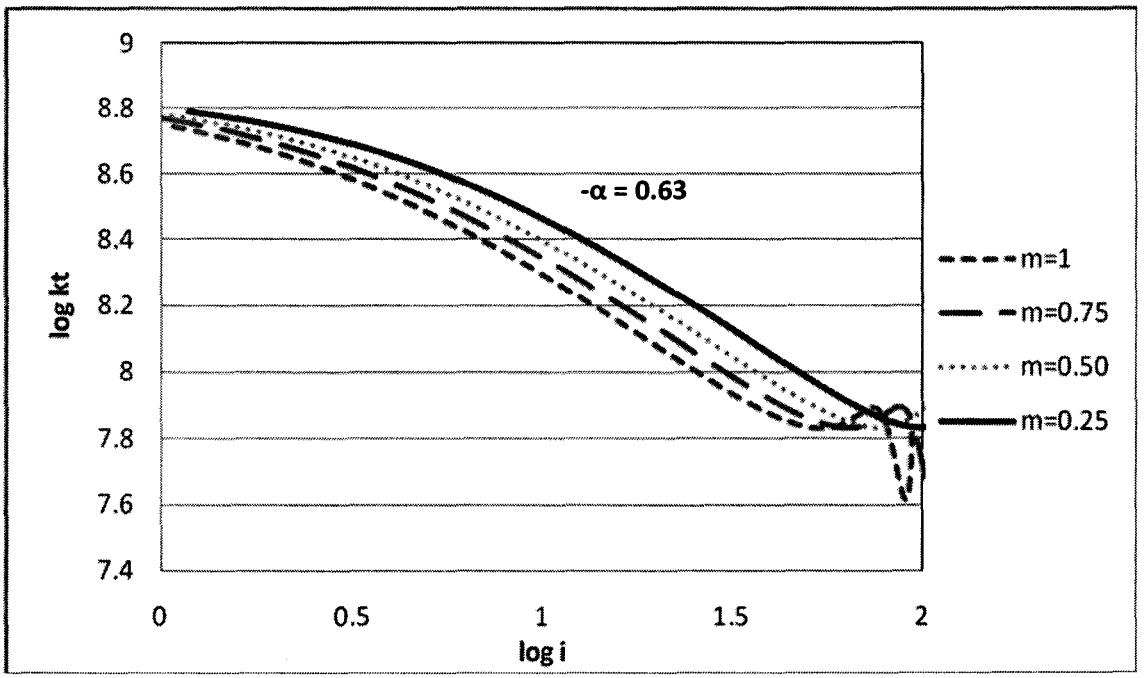

Figure 3.19: Log k_t vs. log chain length plot for the ATRP of MMA in the presence of free radical initiator [MMA]:[MBP]:[AIBN]:[$CuBr_2$]:[PMDETA]=(200:m:0.5:0.05:0.05)

The data presented in Figure 3.19 however, illustrates an irregular trend at higher chain lengths. That is the termination rate coefficient increases with increasing chain length. This observation appears to be purely an artefact from the polynomial fit used to construct the data set. In fact, Figure 3.20 demonstrates the raw experimental data fit with a line of best fit. The raw data shows an overall downward trend in log k_t for the region in question (log i =1.50-2.0), contrary to the generated polynomial functions in Figure 3.19.

The disparity between the raw data and the generated function might be attributed to the 5^{th} order function that may distort tiny inflection points into an artificial phenomenon.

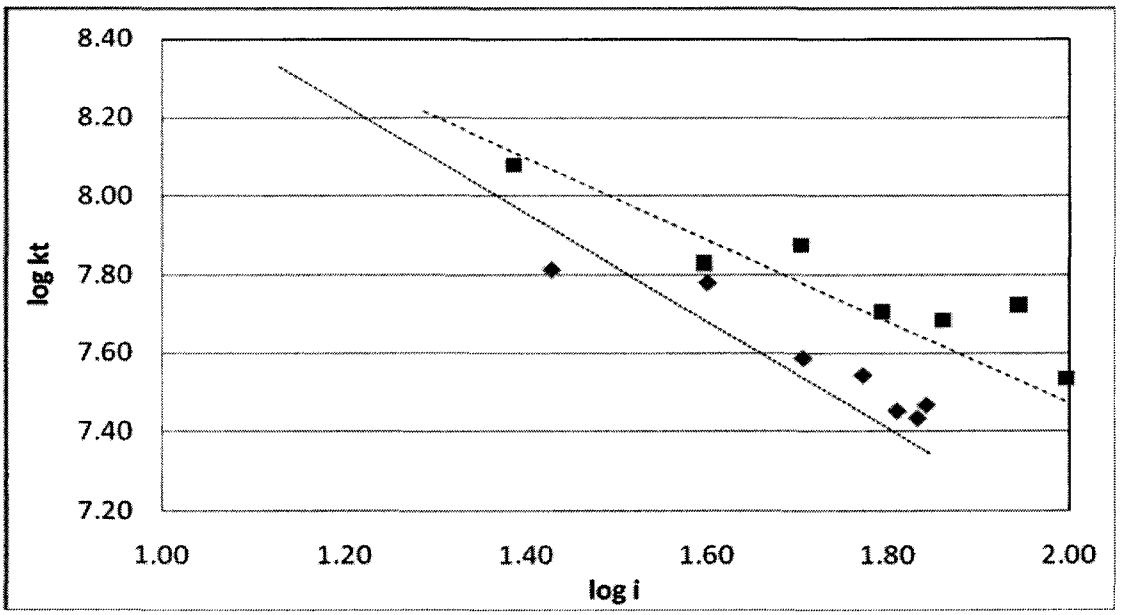

Figure 3.20: Log k_t vs. log chain length plot for the ATRP of MMA in the presence of free radical initiator with raw experimental data [MMA]:[MBP]:[AIBN]:[$CuBr_2$]:[PMDETA]=(200:1:n:0.05:0.05) , (n = 2, ····· , ◆), (n = 0.50, – – -, ■)

When the termination rate coefficient was plotted as a function of conversion using the data derived from the polynomial fit (data not shown) the same peculiar trend was observed. That is, the termination rate coefficient increased with increasing conversion. Once again this phenomenon is mostly likely a synthetic error caused by the polynomial fit. Plotting the raw data (Figure 3.21) however, demonstrates the expected trend where the termination rate coefficient experiences a downward trajectory with increasing monomer conversion.

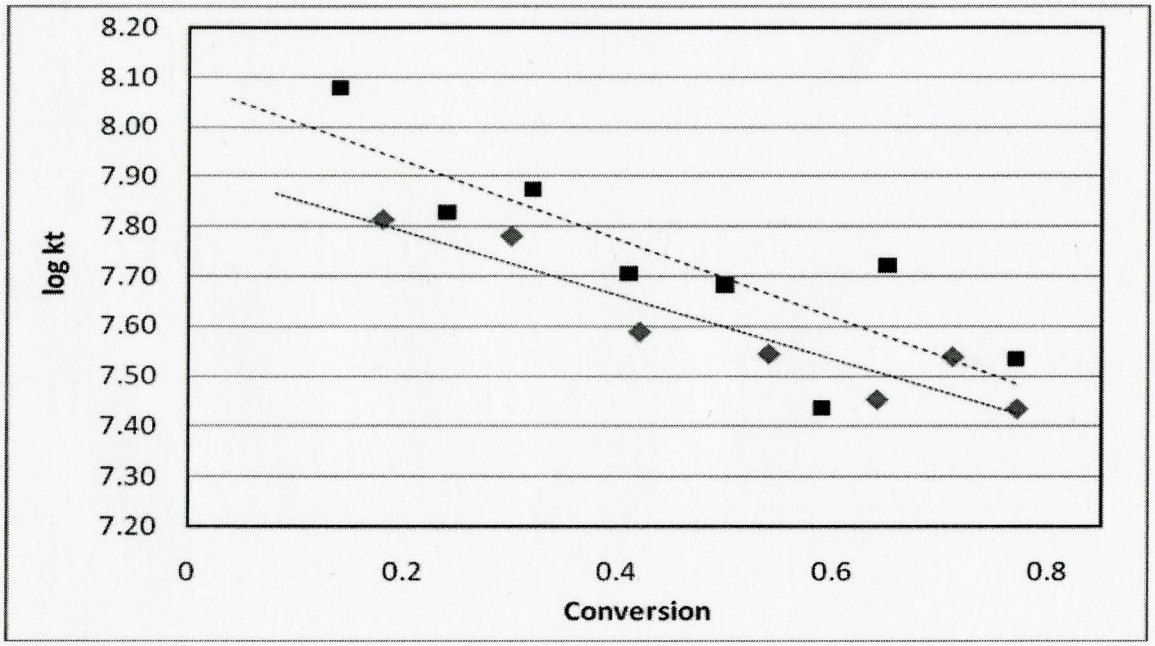

Figure 3.21: Log k_t vs. Conversion plot for the ATRP of MMA in the presence of free radical initiator with raw experimental data [MMA]:[MBP]:[AIBN]:[$CuBr_2$]:[PMDETA]=(200:1:n:0.05:0.05) (n = 2, ·····, ◆), (n = 0.50, - - - - , ■)

In order to assess the contribution of both conversion and chain length effects on the termination rate coefficient, a three dimensional plot was generated and shown in Figure 3.22. In Figure 3.22 the four data sets are representative of the experiments carried out in Figure 3.19. These experiments focused on studying the termination rate coefficient in the short chain regime (i<100), where low molecular weights were targeted.

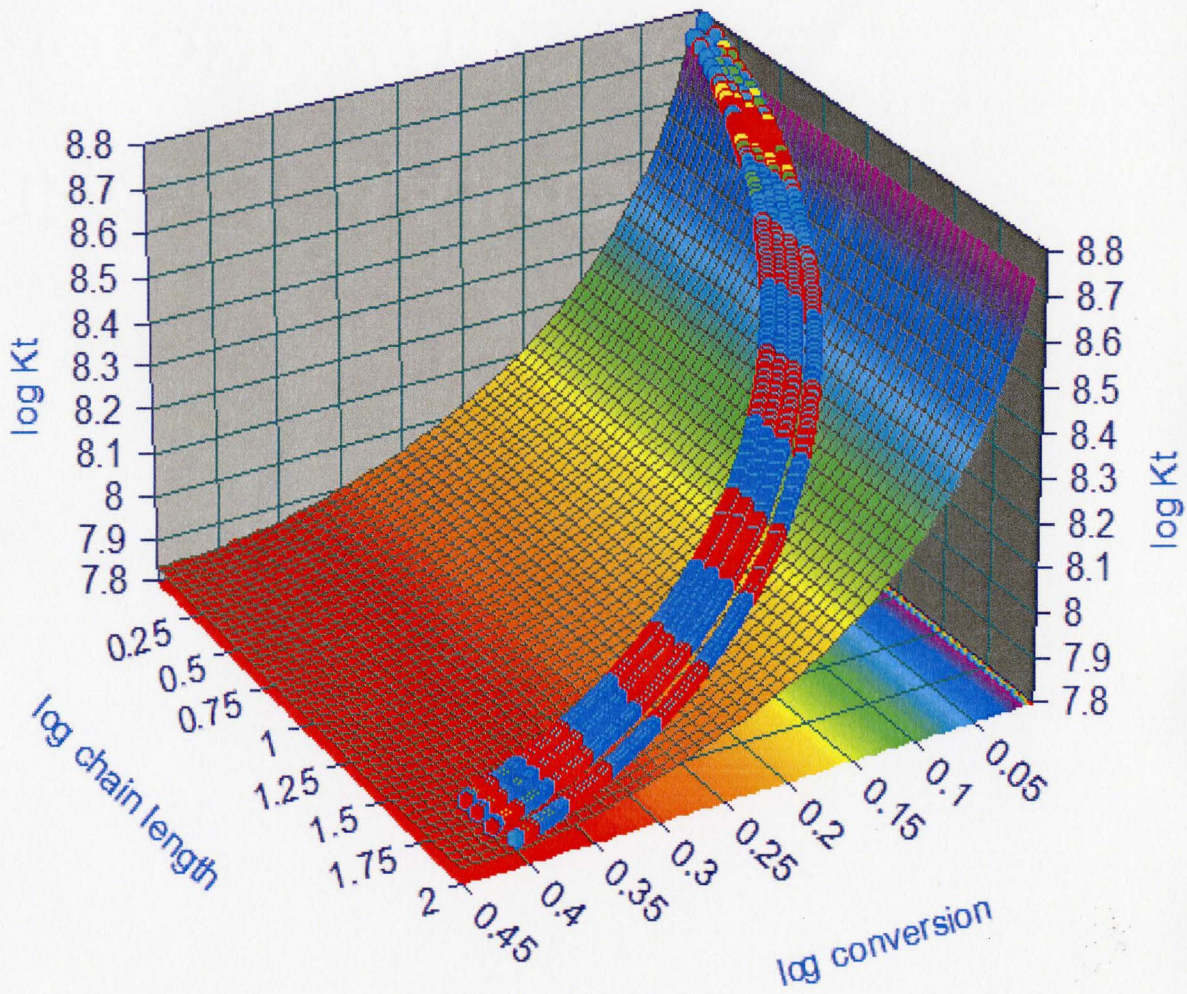

Figure 3.22. Three-dimensional plot of the termination rate coefficients for MMA at 70°C, at [AIBN] = 11.7 mM. The data was fit with a surface plot using the TableCurve 3D software., (r^2 =1.0)

A three dimensional function was fit to the four experimental data sets to construct a composite mesh for the data range. The plot shows that a greater chain length and conversion resulted in a lower $k_t^{i,i}$. Therefore an effective visual interpretation of the reaction system can be obtained using this method where a greater insight into the

coupling effects of conversion and chain length on the corresponding termination rate coefficient can be assessed.

CHAPTER 4

CONCLUSIONS AND RECOMMEDATIONS

4.1 Conclusions

A hybrid ATRP system was used as a means of promoting fast reaction kinetics at low catalyst concentrations. Increasing the free radical initiator concentration from 0.00234 M, a concentration that is typically administered for ICAR ATRP systems, to 0.117 M resulted in over an order of magnitude increase in the reaction rate. This translates to the rapid formation of polymer achieving 81% conversion in 120 minutes of reaction time. Increasing the free radical concentration further by a factor of 2 (0.234 M) resulted in considerably fast reaction rates attaining 91% conversion in 120 minutes. The reaction rate was found to be governed solely by the free radical initiation parameters and not by the ATRP rate law.

For the same increase in free radical initiator loadings (0.00234M to 0.117 M) the reaction exhibited living characteristics with molecular weight increasing linearly as a function of conversion and the distribution remained narrow, increasing slightly from 1.05 to 1.22. Even in the most extreme case where a very high free radical concentration was used (0.234 M), the reaction demonstrated living character and a low polydispersity of 1.30.

The polymerization was performed with various catalyst concentrations. It was found that the copper catalyst concentrations as low (16 ppm) were able to mediate the growth of over 100 growing polymer chains while at the same time not necessitating post

polymerization purification. In addition, the expensive ligand cost could be reduced dramatically since the ligand concentrations used in these experiments are nearly 100 times lower.

ATRP in the presence of free radical initiator was also used as a unique method to determine termination rate coefficients of MMA at 70°C as a function of the both the conversion and chain length. It was determined that in the short chain regime ($i<100$), the termination rate coefficient had an α value of 0.63, which is consistent with other literature values in this chain length regime. A three dimensional composite map was also developed to illustrate the coupling effects on the termination rate coefficient over the total range of the data which can be used for modelling systems of this nature.

4.2 Recommendations and Future Work

One frontier that needs to be explored further in this research is the development of well-defined macromolecular architectures using rate-enhanced ATRP. Some have suggested that this method is limited for the development of block copolymers because homopolymer moieties derived from the free radical initiator can be generated alongside the pure copolymer. However, despite the fact that the physical properties of pure block copolymers and hybrid derived copolymers may be different; both varieties of copolymer may be attractive for specific applications. There is still a lack of knowledge relating polymer macromolecular structure to end-use material properties. Further studies could utilize two dimensional GPC to relate the composition of homopolymer entities to the physical properties of the polymer product. The physical properties could be analyzed using differential scanning calorimeter to determine changes in the glass transition

temperature and to compare the dissimilarity between pure block copolymers and the hybrid copolymer.

Block copolymers could conceivably be derived in an efficient manner using rate enhanced ATRP. For example, a first block composed of MMA could be generated in less than one hour at a conversion where a high percentage of living chains is dominant. Next, the produced polymer can be precipitated out, purified and can act as the macromonomer for the generation of a well defined block copolymer. Further studies investigating the effects of ATRP in the presence of high free radical initiator loadings on other monomers including styrene and some acrylates would also provide more insight into these polymer systems.

Another recommendation for this project is to investigate the possibility of using online NMR measurements as a means of obtaining rate parameters. The advantage of this approach is it would yield a full data set range which would eliminate the need to use mathematical approximations to fit sparse reaction data. This improvement should provide more accurate values of rate parameter for an entire data range.

APPENDIX A:

MATLAB PROGRAM: ANALYSIS OF GPC CURVES

Matlab Program: Analysis of GPC Curves

```
load FFset.mat
close all
mindata = min(min(data));
data = data-2.41; %Subtracting baseline variation

%Calculate the time for significance.
noofpt = length(data(1,:));
for i = 1:noofpt
   for j = 1 : length(data)
      if data(j,i) > 1
         timestart(i) = time(j);
         break;
      end
   end
end

for i = 1:noofpt
   [peakval ind(i)]=max(data(1:1800,i));
   peaktime(i) = time(ind(i));
   areavec(i) = abs(trapz(time(1:ind(i)),data(1:ind(i),i)));
   data(:,i) = 0.5*data(:,i)/areavec(i);
   peakvalue(i) = peakval*0.5/areavec(i);
end

   temp = (time - peaktime(i));
   temp = temp.*temp;
   vardata = [0.25 0.25 0.25 0.25 0.25 0.25 0.25 0.25];
   htdata = [0.92 0.92 1.67 0.99 1.74 1.11 0.74 1.28];
   fitdata(:,i) = htdata(i)*(1/(2*pi*vardata(i)))*exp(-temp/(2*vardata(i)));
   figure, plot(time, fitdata(:,i),'r'); hold on; plot(time, data(:,i));
end

%Calculating the area difference
for i=1:noofpt %Original line
%for i = 1:1
```

```
    %tend = time(ind(i))+20*vardata(i);
    tend = 29;
    for j = 1:length(time)
        if time(j)>tend
            tend = j;
            break
        end
    end
    tstart = ind(i);
    area1(i) = trapz(time(tstart:tend),data(tstart:tend,i)) %This is area of GPC curve on
the right side of mean
    area2(i) = trapz(time(tstart:tend),fitdata(tstart:tend,i)) %This is area of normally
distribution curve on the right side of mean
    tgpc =  time(ind(i))-8*vardata(i);
    area3(i) = trapz(time(tgpc:tend),data(tgpc:tend,i))
    areadiff(i) = (area1(i)-area2(i))/(area3(i));
    figure, plot(time, fitdata(:,i),'r'); hold on; plot(time, data(:,i));
    xlabel('Time(min)');
    ylabel('Signal(mV)');
    hold on;
    %line([time(tend),time(tend)],[0 0.3],'LineStyle','--')
    %line([tgpc,tgpc],[0 0.3],'LineStyle','--')
    hold off
    tend
end
```

APPENDIX B

MATLAB PROGRAM: ATRP WITH A 2nd RADICAL SOURCE MODEL

Matlab Program: ATRP with a 2nd Radical Source Model

```
function dV = Icartotal(t,V)

%Reaction Description: A-ATRP of MMA in Soln at 70C Toluene 50%v/v
%Free Radical Constants Declaration

f=0.70; %Initiator Efficiency
kdecomp=4.01e-5; %Decomposition Coefficient of AIBN at 70°C
kt=2.9e7; %Total Termination rate coefficient
ktd=2.175e7; %Termination via Disportionation Rate Coefficient
ktc=7.25e6; %Termination via Combination Rate Coefficient
kp=1050; %Propagation Rate Coefficient [89]
ktr=0.046; %Chain Transfer Rate Coefficien[91]t

%ATRP Rate parameters
ka=2.7;% Activation Rate Constant [65]
kd=5.40e7;%Deactivation Rate Constant[59]
V80=0.001175;

%Differential Equations
dV(1)=2*f*kdecomp*V(9)+ka*(V80-V(8))*V(2)-kd*V(8)*V(1)-kt*V(1)*V(1)-ktr*V(1);
dV(2)= kd*V(8)*V(1)-ka*(V80-V(8))*V(2);
dV(3)= kp*V(7)*V(1)+ka*(V80-V(8))*V(4)-kd*V(8)*V(3)-kt*V(1)*V(3)-ktr*V(3);
dV(4)=kd*V(8)*V(3)-ka*(V80-V(8))*V(4);
dV(5)=2*kp*V(7)*V(3)+kp*V(7)*V(1)+ka*(V80-V(8))*V(6)-kd*V(8)*V(5)-
kt*V(1)*V(5)-ktr*V(5);
dV(6)=kd*V(8)*V(5)-ka*(V80-V(8))*V(6);
dV(7)=-kp*V(7)*V(1);
dV(8)=ka*(V80-V(8))*V(2)-kd*V(8)*V(1);
dV(9)=-kdecomp*V(9);
dV(10)=(ktc/2)*V(1)*V(1);
dV(11)=ktc*V(3)*V(1);
dV(12)=ktc*V(1)*V(5)+ktc*V(3)*V(3);
```

```
dV(13)=ktd*V(1)*V(1)+ktr*V(1);
dV(14)=ktd*V(3)*V(1)+ktr*V(3);
dV(15)=ktd*V(5)*V(1)+ktr*V(5);
dV=dV';

Main Run File:
close all
clc
Vinit = [0 0.0235 0 0 0 0 4.70 0.001175 0.0235 0 0 0 0 0 0]';
[t, V] = ode15s('Icartotal',[0,20000],Vinit);
for i = 2:length(V)
   Conv(i) = (V(i,3)+V(i, 4)+V(i,11)+V(i,14))/Vinit(7);
   Rn(i) = (V(i,3)+V(i, 4)+V(i,11)+V(i,14))/(V(i,1)+V(i, 2)+V(i,10)+V(i,13))
   Rw(i) = (V(i,5)+V(i, 6)+V(i,12)+V(i,15))/(V(i,14)+V(i, 11)+V(i,3)+V(i,4))
   PDI(i) = Rw(i)/Rn(i);
   if PDI(i)>5
      PDI(i) = NaN;
   End
```

REFERENCES

1. *Chemical Engineering News* **2005,** 83, (24), 67-76.

2. Matyjaszewski, K., Controlled/Living Radical Polymerization *Materials Today* **2005,** 8, (3), 26-33.

3. Matyjaszewski, K., Handbook of Radical Polymerization **2002.**

4. Mahabadi, H. K., EFFECTS OF CHAIN-LENGTH DEPENDENCE OF TERMINATION RATE-CONSTANT ON THE KINETICS OF FREE-RADICAL POLYMERIZATION .1. EVALUATION OF AN ANALYTICAL EXPRESSION RELATING THE APPARENT RATE-CONSTANT OF TERMINATION TO THE NUMBER-AVERAGE DEGREE OF POLYMERIZATION. *Macromolecules* **1985,** 18, (6), 1319-1324.

5. Mahabadi, H. K., EFFECT OF CHAIN-LENGTH DEPENDENCE OF TERMINATION RATE-CONSTANT ON THE KINETICS OF FREE-RADICAL POLYMERIZATION .2. EVALUATION OF AN ANALYTICAL EXPRESSION FOR THE RATE OF POLYMERIZATION. *Macromolecules* **1991,** 24, (2), 606-609.

6. Olaj, O. F.; Vana, P., Chain-length dependent termination in pulsed-laser polymerization, 6 - The evaluation of the rate coefficient of bimolecular termination k(t) for the reference system methyl methacrylate in bulk at 25 degrees C. *Macromolecular Rapid Communications* **1998,** 19, (10), 533-538.

7. Friedman, B.; Oshaughnessy, B., KINETICS OF INTERMOLECULAR REACTIONS IN DILUTE POLYMER-SOLUTIONS AND UNENTANGLED MELTS. *Macromolecules* **1993,** 26, (21), 5726-5739.

8. Olaj, O. F.; Kornherr, A.; Vana, P.; Zoder, M.; Zifferer, G., New aspects of chain-length dependent termination. *Macromolecular Symposia* **2002,** 182, 15-30.

9. Johnston-Hall, G.; Stenzel, M. H.; Davis, T. P.; Barner-Kowollik, C.; Monteiro, M. J., Chain length dependent termination rate coefficients of methyl methacrylate (MMA) in the gel regime: Accessing k(t)(i,i) using reversible addition-fragmentation chain transfer (RAFT) polymerization. *Macromolecules* **2007,** 40, (8), 2730-2736.

10. Olaj, O. F.; Bitai, I.; Hinkelmann, F., The Laser-Flash-Initiated Polymerization as a Tool of Evaluating (Individual) Kinetic Constants of Free-Radical Polymerization .2. The Direct Determination of the Rate-Constant of Chain Propagation. *Makromolekulare Chemie-Macromolecular Chemistry and Physics* **1987,** 188, (7), 1689-1702.

11. Le, T. T.; Hill, D. J. T., Simultaneous FT-NIR and ESR analyses to yield propagation rate coefficients for polymerization of methyl methacrylate based monomers. *Polymer International* **2003,** 52, (11), 1694-1700.

12. Zhu, S.; Tian, Y.; Hamielec, A. E.; Eaton, D. R., Radical Trapping and Termination in Free-Radical Polymerization of Mma. *Macromolecules* **1990,** 23, (4), 1144-1150.

13. Beuermann, S.; Buback, M.; Schmaltz, C., Termination rate coefficients of butyl acrylate free-radical homopolymerization in supercritical CO2 and in bulk. *Industrial & Engineering Chemistry Research* **1999,** 38, (9), 3338-3344.

14. Buback, M.; Kowollik, C., Termination kinetics of methyl methacrylate free-radical polymerization studied by time-resolved pulsed laser experiments. *Macromolecules* **1998,** 31, (10), 3211-3215.

15. Buback, M.; Kowollik, C., Termination kinetics in free-radical bulk copolymerization: The systems dodecyl acrylate dodecyl methacrylate and dodecyl acrylate methyl acrylate. *Macromolecules* **1999,** 32, (5), 1445-1452.

16. Vana, P.; Davis, T. R.; Barner-Kowollik, C., Easy access to chain-length-dependent termination rate coefficients using RAFT polymerization. *Macromolecular Rapid Communications* **2002,** 23, (16), 952-956.

17. Theis, A.; Davis, T. P.; Stenzel, M. H.; Barner-Kowollik, C., Mapping chain length and conversion dependent termination rate coefficients in methyl acrylate free radical polymerization. *Macromolecules* **2005,** 38, (24), 10323-10327.

18. Theis, A.; Feldermann, A.; Charton, N.; Stenzel, M. H.; Davis, T. P.; Barner-Kowollik, C., Access to chain length dependent termination rate coefficients of methyl acrylate via reversible addition-fragmentation chain transfer polymerization. *Macromolecules* **2005,** 38, (7), 2595-2605.

19. Johnston-Hall, G.; Monteiro, M. J., Kinetic modeling of "living" and conventional free radical polymerizations of methyl methacrylate in dilute and gel regimes. *Macromolecules* **2007,** 40, (20), 7171-7179.

20. Johnston-Hall, G.; Theis, A.; Monteiro, M. J.; Davis, T. P.; Stenzel, M. H.; Barner-Kowollik, C., Accessing chain length dependent termination rate coefficients of methyl methacrylate (MMA) via the reversible addition fragmentation chain transfer (RAFT) process. *Macromolecular Chemistry and Physics* **2005,** 206, (20), 2047-2053.

21. Szwarc, M., 'Living' Polymers. *Nature* **1956,** 178, 1168-1169.

22. Kato, M.; Kamigaito, M.; Sawamoto, M.; Higashimura, T., Polymerization of Methyl-Methacrylate with the Carbon-Tetrachloride Dichlorotris(Triphenylphosphine)Ruthenium(Ii) Methylaluminum Bis(2,6-Di-Tert-Butylphenoxide) Initiating System - Possibility of Living Radical Polymerization. *Macromolecules* **1995,** 28, (5), 1721-1723.

23. Wang, J. S.; Matyjaszewski, K., Controlled Living Radical Polymerization - Atom-Transfer Radical Polymerization in the Presence of Transition-Metal Complexes. *Journal of the American Chemical Society* **1995,** 117, (20), 5614-5615.

24. Georges, M. K.; Veregin, R. P. N.; Kazmaier, P. M.; Hamer, G. K., Narrow Molecular-Weight Resins by a Free-Radical Polymerization Process. *Macromolecules* **1993,** 26, (11), 2987-2988.

25. Odian, G., Principles of Polymerization Fourth Edition. **2004**.

26. Hawker, C. J., Architectural Control in Living Free-Radical Polymerizations - Preparation of Star and Graft Polymers. *Angewandte Chemie-International Edition in English* **1995,** 34, (13-14), 1456-1459.

27. Bohme, K.; Schmidt-Naake, G., A synthetic approach to star-like polymers of styrene and butyl acrylate by linking reactions using functionalized methacrylates. *Macromolecular Materials and Engineering* **2004,** 289, (3), 254-263.

28. Beil, J. B.; Zimmerman, S. C., Synthesis of nanosized "Cored" star polymers. *Macromolecules* **2004,** 37, (3), 778-787.

29. Parvole, J.; Laruelle, G.; Guimon, C.; Francois, J.; Billon, L., Initiator-grafted silica particles for controlled free radical polymerization: Influence of the initiator structure on the grafting density. *Macromolecular Rapid Communications* **2003,** 24, (18), 1074-1078.

30. Guillaneuf, Y.; Gigmes, D.; Marque, S. R. A.; Astolfi, P.; Greci, L.; Tordo, P.; Bertin, D., First effective nitroxide-mediated polymerization of methyl methacrylate. *Macromolecules* **2007,** 40, (9), 3108-3114.

31. Moad, G.; Rizzardo, E.; Thang, S. H., Living radical polymerization by the RAFT process. *Australian Journal of Chemistry* **2005,** 58, (6), 379-410.

32. Delduc, P.; Tailhan, C.; Zard, S. Z., A Convenient Source of Alkyl and Acyl Radicals. *Journal of the Chemical Society-Chemical Communications* **1988**, (4), 308-310.

33. Chiefari, J.; Chong, Y. K.; Ercole, F.; Krstina, J.; Jeffrey, J.; Le, T. P. T.; Mayadunne, R. T. A.; Meijs, G. F.; Moad, C.; Moad, G.; Rizzardo, E.; Thang, S. H.,

Moad, G. and et al. "Living Radical Polymerization by the RAFT Process". Australian Journal of Chemistry. 58, (2005) 379-410. *Macromolecules* **1998,** 31, 5559-5562.

34. Perrier, S.; Takolpuckdee, P., Macromolecular design via reversible addition-fragmentation chain transfer (RAFT)/Xanthates (MADIX) polymerization. *Journal of Polymer Science Part a-Polymer Chemistry* **2005,** 43, (22), 5347-5393.

35. Matyjaszewski, K.; Xia, J. H., Atom transfer radical polymerization. *Chemical Reviews* **2001,** 101, (9), 2921-2990.

36. Braunecker, W. A.; Matyjaszewski, K., Controlled/living radical polymerization: Features, developments, and perspectives. *Progress in Polymer Science* **2007,** 32, (1), 93-146.

37. Kamigaito, M.; Ando, T.; Sawamoto, M., Metal-catalyzed living radical polymerization. *Chemical Reviews* **2001,** 101, (12), 3689-3745.

38. Grimaud, T.; Matyjaszewski, K., Controlled/"living" radical polymerization of methyl methacrylate by atom transfer radical polymerization. *Macromolecules* **1997,** 30, (7), 2216-2218.

39. Percec, V.; Barboiu, B., Living Radical Polymerization of Styrene Initiated by Arenesulfonyl Chlorides and Cu-I(Bpy)(N)Cl. *Macromolecules* **1995,** 28, (23), 7970-7972.

40. Davis, K. A.; Paik, H. J.; Matyjaszewski, K., Kinetic investigation of the atom transfer radical polymerization of methyl acrylate. *Macromolecules* **1999,** 32, (6), 1767-1776.

41. Jo, S. M.; Gaynor, S. G.; Matyjaszewski, K., Homo and ABA block polymerizations of acrylonltrile, N-butyl acrylate, and 2-ethyl hexyl acrylate using ATRP. *Abstracts of Papers of the American Chemical Society* **1996,** 212, 91-Poly.

42. Xia, J. H.; Zhang, X.; Matyjaszewski, K., Atom transfer radical polymerization of 4-vinylpyridine. *Macromolecules* **1999,** 32, (10), 3531-3533.

43. Limer, A.; Haddleton, D. M., Reverse atom transfer radical polymerisation (RATRP) of methacrylates using copper(I)/pyridinimine catalysts in conjunction with AIBN. *European Polymer Journal* **2006,** 42, (1), 61-68.

44. Feng, H. K.; Dan, Y., The research of RATRP of styrene in the microemulsion. *Journal of Applied Polymer Science* **2006,** 99, (3), 1093-1099.

45. Hou, C.; Qu, R. J.; Ji, C. N.; Wang, C. H.; Wang, C. G., Synthesis of polyacrylonitrile via reverse atom transfer radical polymerization (ATRP) initiated by diethyl 2,3-dicyano-2,3-diphenylsuccinate, FeCl3, and triphenylphosphine. *Polymer International* **2006,** 55, (3), 326-329.

46. Hou, C.; Qu, R. J.; Liu, J. S.; Guo, Z. L.; Wang, C. H.; Ji, C. N.; Sun, C. M.; Wang, C. G., Reverse ATRP of acrylonitrile with diethyl 2,3-dicyano-2,3-diphenyl succinate/FeCl3/iminodiacetic acid. *Polymer* **2006,** 47, (5), 1505-1510.

47. Qin, D. Q.; Qin, S. H.; Qiu, K. Y., A copper-based reverse ATRP process for the living radical polymerization of methyl methacrylate. *Journal of Applied Polymer Science* **2001,** 81, (9), 2237-2245.

48. Hou, C.; Ji, C. N.; Wang, C. H.; Qu, R. J., A copper-based reverse atom-transfer radical polymerization process for the living radical polymerization of polyacrylonitrile. *Journal of Polymer Science Part a-Polymer Chemistry* **2006,** 44, (1), 226-231.

49. Chen, X. P.; Qiu, K. Y., Synthesis of well-defined poly(methyl methacrylate) by radical polymerization with a new initiation system TPED/FeCl3/PPh3. *Macromolecules* **1999,** 32, (26), 8711-8715.

50. Cheng, Z. O.; Zhu, X. L.; Zhang, L. F.; Zhou, N. C.; Chen, J. Y., Homogeneous solution reverse atom transfer radical polymerization of methyl methacrylate. *Journal of Macromolecular Science-Pure and Applied Chemistry* **2003,** A40, (4), 371-385.

51. Moineau, G.; Dubois, P.; Jerome, R.; Senninger, T.; Teyssie, P., Alternative atom transfer radical polymerization for MMA using FeCl3 and AIBN in the presence of triphenylphosphine: An easy way to well-controlled PMMA. *Macromolecules* **1998,** 31, (2), 545-547.

52. Chen, X. P.; Qiu, K. Y., 'Living' radical polymerization of styrene with AIBN/FeCl3/PPh3 initiating system via a reverse atom transfer radical polymerization process. *Polymer International* **2000,** 49, (11), 1529-1533.

53. Cheng, Z. P.; Zhu, X. L.; Chen, G. J.; Xu, W. J.; Lu, J. M., Reverse atom transfer radical solution polymerization of methyl methacrylate under pulsed microwave irradiation. *Journal of Polymer Science Part a-Polymer Chemistry* **2002,** 40, (21), 3823-3834.

54. Cheng, Z. P.; Zhu, X. L.; Zhang, L. F.; Zhou, N. C.; Xue, X. R., RATRP of MMA in AIBN/FeCl3/PPh3 initiation system under microwave irradiation. *Polymer Bulletin* **2003,** 49, (5), 363-369.

55. Chen, G. J.; Zhu, X. L.; Cheng, Z. P.; Xu, W. J.; Lu, J. M., Controlled/"living" radical polymerization of methyl methacrylate using AIBN as the initiator under microwave irradiation. *Radiation Physics and Chemistry* **2004,** 69, (2), 129-135.

56. Cheng, Z. P.; Zhu, X. L.; Zhou, N. C.; Zhu, J.; Zhang, Z. B., Atom transfer radical polymerization of styrene under pulsed microwave irradiation. *Radiation Physics and Chemistry* **2005,** 72, (6), 695-701.

57. Gromada, J.; Matyjaszewski, K., Simultaneous reverse and normal initiation in atom transfer radical polymerization. *Macromolecules* **2001,** 34, (22), 7664-7671.

58. Min, K.; Li, M.; Matyjaszewski, K., Preparation of gradient copolymers via ATRP using a simultaneous reverse and normal initiation process. I. Spontaneous gradient. *Journal of Polymer Science Part a-Polymer Chemistry* **2005,** 43, (16), 3616-3622.

59. Matyjaszewski, K.; Jakubowski, W.; Min, K.; Tang, W.; Huang, J. Y.; Braunecker, W. A.; Tsarevsky, N. V., Diminishing catalyst concentration in atom transfer radical polymerization with reducing agents. *Proceedings of the National Academy of Sciences of the United States of America* **2006,** 103, (42), 15309-15314.

60. Min, K.; Gao, H. F.; Matyjaszewski, K., Preparation of homopolymers and block copolymers in miniemulsion by ATRP using activators generated by electron transfer (AGET). *Journal of the American Chemical Society* **2005,** 127, (11), 3825-3830.

61. Jakubowski, W.; Min, K.; Matyjaszewski, K., Activators regenerated by electron transfer for atom transfer radical polymerization of styrene. *Macromolecules* **2006,** 39, (1), 39-45.

62. Min, K.; Gao, H. F.; Matyjaszewski, K., Use of ascorbic acid as reducing agent for synthesis of well-defined polymers by ARGET ATRP. *Macromolecules* **2007,** 40, (6), 1789-1791.

63. Benoit, D.; Grimaldi, S.; Robin, S.; Finet, J. P.; Tordo, P.; Gnanou, Y., Kinetics and mechanism of controlled free-radical polymerization of styrene and n-butyl acrylate in the presence of an acyclic beta-phosphonylated nitroxide. *Journal of the American Chemical Society* **2000,** 122, (25), 5929-5939.

64. Queffelec, J.; Gaynor, S. G.; Matyjaszewski, K., Optimization of atom transfer radical polymerization using Cu(I)/tris(2-(dimethylamino)ethyl)amine as a catalyst. *Macromolecules* **2000,** 33, (23), 8629-8639.

65. Tang, W.; Matyjaszewski, K., Effect of ligand structure on activation rate constants in ATRP. *Macromolecules* **2006,** 39, (15), 4953-4959.

66. Tang, H. D.; Arulsamy, N.; Radosz, M.; Shen, Y. Q.; Tsarevsky, N. V.; Braunecker, W. A.; Tang, W.; Matyjaszewski, K., Highly active copper-based catalyst for atom transfer radical polymerization. *Journal of the American Chemical Society* **2006,** 128, (50), 16277-16285.

67. Tsarevsky, N. V.; Braunecker, W. A.; Tang, W.; Brooks, S. J.; Matyjaszewski, K.; Weisman, G. R.; Wong, E. H., Copper-based ATRP catalysts of very high activity derived from dimethyl cross-bridged cyclam. *Journal of Molecular Catalysis a-Chemical* **2006,** 257, (1-2), 132-140.

68. Faucher, S.; Zhu, S. P., Heterogeneous atom transfer radical polymerization of methyl methacrylate at low metal salt concentrations. *Industrial & Engineering Chemistry Research* **2005,** 44, (4), 677-685.

69. Guan, Z. B.; Smart, B., A remarkable visible light effect on atom-transfer radical polymerization. *Macromolecules* **2000,** 33, (18), 6904-6906.

70. Qin, S. H.; Qin, D. Q.; Qiu, K. Y., A novel photo atom transfer radical polymerization of methyl methacrylate. *New Journal of Chemistry* **2001,** 25, (7), 893-895.

71. Cheng, Z. P.; Zhu, X. L.; Chen, M.; Chen, J. Y.; Zhang, L. F., Atom transfer radical polymerization of methyl methacrylate with low concentration of initiating system under microwave irradiation. *Polymer* **2003,** 44, (8), 2243-2247.

72. Haddleton, D. M.; Jasieczek, C. B.; Hannon, M. J.; Shooter, A. J., Atom transfer radical polymerization of methyl methacrylate initiated by alkyl bromide and 2-pyridinecarbaldehyde imine copper(I) complexes. *Macromolecules* **1997,** 30, (7), 2190-2193.

73. Pan, K.; Jiang, L.; Zhang, J.; Dan, Y., Copper-based reverse ATRP process for the controlled radical polymerization of methyl methacrylate. *Journal of Applied Polymer Science* **2007,** 105, (2), 521-526.

74. Wang, J. L.; Grimaud, T.; Matyjaszewski, K., Kinetic study of the homogeneous atom transfer radical polymerization of methyl methacrylate. *Macromolecules* **1997,** 30, (21), 6507-6512.

75. Li, X.; Zhu, X. L.; Cheng, Z. P.; Xu, W. J.; Chen, G. J., Atom-transfer radical polymerization of methyl methacrylate with alpha,alpha '-dichloroxylene/CuCl/N,N,N ',N ",N "-pentamethyldiethylenetriamine initiation system under microwave irradiation. *Journal of Applied Polymer Science* **2004,** 92, (4), 2189-2195.

76. Xue, L.; Agarwal, U. S.; Lemstra, P. J., High molecular weight PMMA by ATRP. *Macromolecules* **2002,** 35, (22), 8650-8652.

77. Zhu, S. M.; Yan, D. Y.; Zhang, G. S., Reverse atom transfer radical polymerization of methyl methacrylate with a new catalytic system, FeCl3/isophthalic acid. *Journal of Polymer Science Part a-Polymer Chemistry* **2001,** 39, (6), 765-774.

78. Haddleton, D. M.; Crossman, M. C.; Dana, B. H.; Duncalf, D. J.; Heming, A. M.; Kukulj, D.; Shooter, A. J., Atom transfer polymerization of methyl methacrylate mediated by alkylpyridylmethanimine type ligands, copper(I) bromide, and alkyl halides in hydrocarbon solution. *Macromolecules* **1999,** 32, (7), 2110-2119.

79. Zhu, S. M.; Yan, D. Y., Atom transfer radical polymerization of methyl methacrylate catalyzed by Iron(II) chloride/isophthalic acid system. *Macromolecules* **2000,** 33, (22), 8233-8238.

80. Li, X.; Zhu, X. L.; Cheng, Z. P.; Jian, Z.; Chen, G. J., Atom transfer radical polymerization of methyl methacrylate with alpha,alpha,alpha ',alpha '-tetrachloroxylene as an initiator. *Journal of Macromolecular Science Part a-Pure and Applied Chemistry* **2006,** 43, (9), 1445-1458.

81. Xu, Y. Q.; Xu, Q. F.; Lu, J. M.; Xia, X. W.; Wang, L. H., Reverse atom transfer radical polymerization of MMA initiated by triphenylmethane. *Polymer Bulletin* **2007,** 58, (5-6), 809-817.

82. Xia, J. H.; Matyjaszewski, K., Controlled/"living" radical polymerization. Homogeneous reverse atom transfer radical polymerization using AIBN as the initiator. *Macromolecules* **1997,** 30, (25), 7692-7696.

83. Xia, J. H.; Matyjaszewski, K., Controlled/"living" radical polymerization. Atom transfer radical polymerization using multidentate amine ligands. *Macromolecules* **1997,** 30, (25), 7697-7700.

84. Acar, M. H.; Bicak, N., Synthesis of hexylated triethylenetetramine: New ligand for homogeneous atom transfer radical polymerization. *Journal of Polymer Science Part a-Polymer Chemistry* **2003,** 41, (11), 1677-1680.

85. Wang, T. L.; Liu, Y. Z.; Jeng, B. C.; Cai, Y. C., The effect of initiators and reaction conditions on the polymer syntheses by atom transfer radical polymerization. *Journal of Polymer Research* **2005,** 12, (2), 67-75.

86. Li, H. Y.; Chen, S. T.; Zhang, X. F.; Lu, Y. Y.; Hu, Y. L., Study on the polymerizations of methyl methacrylate and styrene initiated with chlorotrimethylsilane and CuCl/N,N,N ', N ", N "-pentamethyldiethyltriamine. *European Polymer Journal* **2005,** 41, (12), 2874-2879.

87. Cao, J.; Chen, J.; Zhang, K. D.; Shen, Q.; Zhang, Y., A novel Fe catalyst FeCl2 center dot 4H(2)O/hexamethylphosphoric triamide for the ATRP of MMA. *Applied Catalysis a-General* **2006,** 311, 76-78.

88. Zhang, H. Q.; Klumperman, B.; Ming, W. H.; Fischer, H.; van der Linde, R., Effect of Cu(II) on the kinetics of the homogeneous atom transfer radical polymerization of methyl methacrylate. *Macromolecules* **2001,** 34, (18), 6169-6173.

89. Beuermann, S.; Buback, M.; Davis, T. P.; Gilbert, R. G.; Hutchinson, R. A.; Olaj, O. F.; Russell, G. T.; Schweer, J.; vanHerk, A. M., Critically evaluated rate coefficients for free-radical polymerization .2. Propagation rate coefficients for methyl methacrylate. *Macromolecular Chemistry and Physics* **1997,** 198, (5), 1545-1560.

90. Brandrup, J.; Immergut, E. H., Polymer Handbook. **1966**.

91. Delgadillo-Velazquez, O.; Vivaldo-Lima, E.; Quintero-Ortega, I. A.; Zhu, S. P., Effects of diffusion-controlled reactions on atom-transfer radical polymerization. *Aiche Journal* **2002,** 48, (11), 2597-2608.

92. Smith, G. B.; Russell, G. T.; Heuts, J. P. A., Termination in dilute-solution free-radical polymerization: A composite model. *Macromolecular Theory and Simulations* **2003,** 12, (5), 299-314.